00390
AISC E&R Library
7191

File: Semi-Rigid Connections
Type 2 Construction Frames

1069

STRUCTURAL RESEARCH STUDIES
Department of Civil Engineering

A PROCEDURE FOR THE PRELIMINARY DESIGN OF BUILDING STRUCTURES USING SEMI-RIGID BEAM-COLUMN CONNECTIONS

by
Pollyanna Stier Kimrey
&
J.B. Radziminski

sponsored by
AISC Educational Foundation
American Institute of Steel Construction, Inc.
Chicago, Illinois

UNIVERSITY OF SOUTH CAROLINA
COLUMBIA, SOUTH CAROLINA
JUNE, 1984

RR1069

7191

GK, DH, JAE

B301

UNIVERSITY OF SOUTH CAROLINA

COLUMBIA, S. C. 29208

COLLEGE OF ENGINEERING

September 4, 1984

Mr. Robert O. Disque
Assistant Director for Engineering and Research
American Institute of Steel Construction, Inc.
400 North Michigan Avenue
Chicago, Illinois 60611

Dear Bob:

Enclosed are two copies of the report, "A Procedure for the Preliminary Design of Building Structures Using Semi-Rigid Beam-Column Connections" by Penny Kimrey, completed as part of the fellowship award granted to her by AISC in 1982. I should mention that the empirical equation used to generate the moment-rotation curves on pp. 50-64 of Appendix A are currently being updated, as additional tests are completed under a continuing NSF grant, to include bolt diameter as one of the governing parameters (in addition to the five listed on p. 49.).

I believe that Penny has done a commendable job in this study, and has gained a lasting appreciation for the importance of connection flexibility on the behavior of framed structures, and for the complexities involved in the analysis of such systems. If you have any questions regarding the study, I will be glad to discuss them further with you.

I hope to see you at the ASCE Convention in San Fransisco this October.

Sincerely,

James B. Radziminski
Professor of Civil Engineering

cc: P. Kimrey
J.H. Bradburn

1 Copy - AISC Research Report
1 Copy - ROD Bookcase

00392

A PROCEDURE FOR THE PRELIMINARY DESIGN OF BUILDING STRUCTURES USING SEMI-RIGID BEAM-COLUMN CONNECTIONS

by

Pollyanna Stier Kimrey

Sponsored by
AISC Educational Foundation
American Institute of Steel Construction, Inc.
Chicago, Illinois

College of Engineering
University of South Carolina
Columbia, South Carolina
June 1984

00393

ABSTRACT

The purpose of the investigation has been to use the moment-rotation relationships developed from a study that has been undertaken at the University of South Carolina to formulate design aids which may be applicable to the direct utilization of semi-rigid connections in building systems. Several series of moment-rotation (M-Ø) curves have been generated herein for connections of varying stiffness, within reasonable limits of extrapolation beyond the connections studied experimentally.

A procedure has been demonstrated for the design of a beam which utilizes semi-rigid connections attached to non-rotating supports. The overload capacity of this beam was then compared to the overload capacity of a beam which utilized fully rigid connections. A procedure has also been developed for a preliminary selection of member and connection sizes for a single story, single bay frame utilizing semi-rigid connections. A comparison was made between this frame and a frame which contains fully rigid connections. Both frames consisted of the same members and same loading. Limit state analyses were performed for both frames to obtain a measure of the overload capacity associated with each frame.

As an alternative to using the complete M-Ø curve of a connection in determining the response of the beam and of the frame studied herein, an approach which utilized only the initial stiffness of the connection in the analyses was also considered.

00394

To predict the initial stiffness of the semi-rigid connections, a revised initial slope (RIS) for the M-Ø curves of the connections was developed. For the example beam, the connection moment predicted by the RIS was considerably greater than the connection moment predicted by the complete M-Ø curve. Conversely, for the example frame used in this paper, the RIS gives a very close approximation to the behavior of the connections predicted by the complete M-Ø curve, at least up to and including service load conditions.

80395

TABLE OF CONTENTS

00396

LIST OF TABLES

00397

LIST OF FIGURES

00398

00399

A PROCEDURE FOR THE PRELIMINARY DESIGN OF BUILDING STRUCTURES USING SEMI-RIGID BEAM-COLUMN CONNECTIONS

I. INTRODUCTION

The American Institute of Steel Construction endorses the use of Type 2 construction in building design. [1] The beam-column connections are considered, for design purposes, to behave flexibly under gravity loading, and are required to develop only enough moment capacity to provide resistance to lateral forces. It is evident, however, that such framing systems may be appropriately considered as being comprised of "semi-rigid" connections, which continuously transfer both shear and moment as loading progresses. Semi-rigid, or AISC Type 3 construction is not commonly used for design, however, because of the complexity of the non-linear frame analyses required of such systems, and the need to quantify the static and repeated- load behavior of the semi-rigid beam-column connections.

A program has been undertaken at the University of South Carolina, sponsored in part by the National Science Foundation, to investigate the static and cyclic moment-rotation characteristics of semi-rigid connections consisting of bolted top and bottom beam flange angles together with standard bolted web angles. The objectives of this investigation have been to experimentally determine the effect of varying the top and seat angle stiffness on the static response of the connections, and to obtain a measure of their hysteretic energy absorption under

controlled displacement cyclic loadings.

The results, to date, are presented in a report to the National Science Foundation. [2] To determine static moment-rotation behavior, eleven specimens, utilizing 8 in. and 14 in. deep beams and various sizes of flange and web angles, were subjected to static loading. Details of the test connections, and a schematic of the test setup are shown in Figs. 1.1-1.3 respectively. The tests enabled the identification of the significant material and geometric parameters required to formulate analytical models of the non-linear static connection response.

Several analytical models have been proposed to establish the initial stiffness of the type of semi-rigid connection considered in this investigation. Comparisons of the predicted stiffnesses with the experimental data from the static test investigation are presented in the NSF report. Further, using the results of the parametric study, a semi-empirical analytical model was developed to generate complete non-linear moment-rotation curves for the connections. This model has offered the greatest immediate promise as a practical means of describing the non-linear static response of the semi-rigid connections. Additionally, computer programs are available which apply the analytical moment-rotation descriptions of the semi-rigid connections to the analysis of complete structural frameworks.

00401

II. MOMENT-ROTATION CURVES AND PREDICTED INITIAL STIFFNESS FOR THE SEMI-RIGID CONNECTION

The object of the current investigation has been to use the moment-rotation relationships developed from the study described above to formulate design aids which may be applicable to the direct utilization of semi-rigid connections in building systems. Several series of moment-rotation curves have been generated for connections of varying stiffness, within reasonable limits of extrapolation beyond the connections studied experimentally, and used to frame beams of varying depth. Moment-rotation curves, for beams ranging in depth from 8 in. to 16 in., are presented in Appendix A. For each beam depth, curves are plotted for connections with flange angles of varying thickness and gage (in the leg of the angle mounted to the supporting column). This was completed for the 8 in., 10 in., 12 in., 14 in., and 16 in. deep beams, using flange angle gages of 2 in., 2-1/4 in., and 2-1/2 in., and angle thicknesses ranging from 5/16 in. to 7/8 in. For example, Fig. A10 of Appendix A shows the family of connection moment-rotation curves for a semi-rigid connection with a flange angle having a gage of 2-1/2 in. and with angle thicknesses ranging from 5/16 in. to 7/8 in., to be used to frame a beam with a depth of 14 inches.

To establish a procedure for the selection of connections of desired stiffness for a particular structural application, the following considerations were addressed first. Using the semi-empirical moment-rotation relationship which was developed

00402

in the NSF report, the static moment-rotation (M-Ø) curve for a specific connection was plotted. The initial stiffness of the semi-rigid connection (the initial slope of the semi-empirical moment-rotation curve) was then superimposed over the complete non-linear M-Ø curve. It must be pointed out that this initial slope is somewhat larger than the initial slope obtained from the actual test data. Further information on this can be obtained in the NSF report. For the 14 in. deep beams, a W14X38 section with a total length of 20 feet (the specimen examined in the experimental investigation) was considered. The standard beam line for the W14X38 section, using the 20 ft. test length and an allowable stress of 0.66 Fy (24 ksi), was then plotted over the M-Ø curve and initial stiffness line for the connection used to frame the beam to a stub column in the actual test. In this test, the top and seat angles were L6X4X3/8 X 0'-8", with a gage of 2-1/2 in. in the leg mounted to the stub column. It was found that the beam line intersected the non-linear M-Ø curve at a rotation considerably larger than the rotation predicted by the intersection of the beam line with the initial slope line. Similar results were obtained with the other member sizes and connection stiffnesses tested in the experimental investigation.

The above check was made to establish whether or not the initial slope line for a semi-rigid connection could be used in place of the full non-linear M-Ø curve in the design process. For the range of member sizes and connection stiffnesses used in this investigation, it was found that the initial stiffness

00403

provided unconservative predictions of the connection moment transfer capability and corresponding beam rotations at working load for a beam that is connected to fixed supports by these semi-rigid connections.

An additional, analytically predicted linear initial slope, developed in conjunction with the NSF sponsored study, was next considered.[3] This slope was generated by modeling the flange and web angles as segmental beams and computing their contributions to the initial connection stiffness. The assumption was made that elastic analysis is applicable. After computing the contribution of all elements, these were added, resulting in a revised prediction for the initial slope of the moment-rotation curve. This revised initial slope (RIS) closely predicts the initial slopes of the M-Ø curves obtained from the actual test data. Initial slopes obtained by this procedure have been calculated for each of the M-Ø curves that are shown in Appendix A. The values are tabulated in Table 2.1. A copy of the computer program which calculates the RIS and a list of its input variables are shown in Appendix B. A sample of the computer input and output data is also shown.

III. BEAM DESIGN EXAMPLE

3.1 Use of the Revised Initial Slope (RIS)

The next consideration was to design a beam that utilizes semi-rigid connections of the type that are examined in this

88404

study, and then to analyze this beam by use of the full M-Ø curve, and by the use of the RIS for the connections predicted behavior. Shown in Fig. 3.1a is a beam with semi-rigid connections attached to fixed supports. The beam was designed for a maximum moment of $wl^2/12$, the same as the design moment for a fully fixed-fixed beam, Fig. 3.1b. For this example the beam supports a uniform service loading of 2.25 k/ft over a span of 24 feet, resulting in a design moment ($wl^2/12$) of 1296^{in-k}. A W14X38 section of A36 steel, with an allowable moment (.66 Fy.Sx) of 1297.3^{in-k}, was selected for the beam. With the section thus selected, its beam line was thus defined. The intercept of the beam line on the moment axis corresponds to the fixed-end moment, $wl^2/12$, while the rotation axis intercept corresponds to the simple beam rotation of $wl^3/24EI$.[4]

The beam line was then used to select the semi-rigid connection that would develop a moment of $wl^2/24$ at the $2.25^{k}/ft$. service load. As seen in Fig. 3.1a, the connection moment of $wl^2/24$ corresponds to the beam midspan moment of $wl^2/12$. For the proper connection to be selected, the beam line was drawn through the family of semi-rigid M-Ø curves for the 14 in. beam depth. This procedure is shown in Fig. 3.2. For a 14 in. deep beam and a gage of 2-1/2 in. in the flange angles, a connection with a flange angle thickness of 1/2 in. was selected. As shown in the figure, this connection comes closest to developing a moment capacity of at least $wl^2/24$ (648^{in-k}) at service load. Note that the actual moment the

00405

connection will develop is 707 in-kips, corresponding to the intersection of the beam line with the M-Ø curve for that connection.

For the connection selected above, the revised initial slope (hereinafter designated "RIS") has a value of 328,700 in-kips/rad, as shown in Table 2.1. The connection moment which would be indicated if the RIS were used for the predicted behavior of the connection was compared to the connection moment predicted by the M-Ø curve. A graph of these two plots is shown in Fig. 3.3, where the beam line at service load is drawn over both plots. As shown in the figure, the connection moment predicted by the RIS is 1049 in-kips, which is a 48 percent increase in the moment predicted by the M-Ø curve, 707 in-kips.

The variation in the connection moment that is predicted by the RIS in a beam with semi-rigid connections attached to fixed supports suggests the limits within which the RIS can be used in the analysis of a frame. The beam that has just been analyzed is analagous to a beam that is connected to infinitely stiff columns in a frame. If this were indeed the case, then for this beam and loading the RIS predicts a moment that is 48 percent greater than the actual moment developed at the connection. However, the other extreme must also be considered. For example, a simply-supported beam would be analogous to a beam in a frame which is connected to columns that are very flexible; i.e., columns that have no stiffness. In this case the moment capacity at the connections would be zero. Therefore it does not make any

difference if the behavior of the semi-rigid connection is predicted by the RIS line or the M-Ø curve because the moment in the connection will essentially always be zero.

The above two examples of beams in a frame are not realistic because such members in actual frames are connected to columns which have a stiffness somewhere between the two extremes. However, it serves the purpose of suggesting bounds within which the RIS may be used in place of the full M-Ø curve to predict the behavior of semi-rigid connections in frames at working load. Later in this paper, an example frame which utilizes semi-rigid connections will be examined in greater detail, in which the connection moments predicted by the RIS will be compared to the moments predicted by the full M-Ø curve.

3.2 Overload Capacity

For the previous beam design example, utilizing semi-rigid connections of the type examined in this study, an estimate of the member "ultimate" or "over-load" capacity was determined. That is, the factor of safety with respect to collapse (based on a standard plastic hinging and collapse mechanism approach) was considered for the beam. From the experimentally determined M-Ø curves, it was found that the connection moment continued to increase well beyond the moment corresponding to working load conditions, as determined from the beam-line analysis described earlier. Because the connection M-Ø curves did not flatten to a horizontal slope, an iterative procedure was used to establish a

00407

conservative estimate of the plastic moment capacity of the connection. The approach used was as follows. A connection moment 20 percent larger than the working load moment was selected and used as the available moment at the connection at the formation of a collapse mechanism for the beam. From the corresponding collapse load, the beam line at ultimate load (assuming elastic behavior to prevail to the point of plastic hinge formation) was plotted over the M-Ø curve of the connection. If the intersection of this beam line with the M-Ø curve was within 1 or 2 percent of the assumed "plastic" moment of the connection (i.e., moment 20 percent larger than the working load moment), the calculated load was considered to be a reasonable estimate of the overload capacity of the beam. If the assumed and final moments were not close, the above procedure was repeated until coincidence was achieved.

For the beam in Fig. 3.1a, using the analysis technique described above, collapse is calculated to occur at an overload of 1.58 times the service load of 2.25 k/ft. The load was determined as follows. The fully plastic moment for the W14X38 section, Fy.Z, is 36 ksi X 61.5 in^3 = 2214 $^{in-k}$. The assumed connection capacity was taken as 1.2 X 707 $^{in-k}$, or 848.4 $^{in-k}$. Summing these values, the total static beam moment, $wl^2/8$, is 3062.4 $^{in-k}$ from which w=3.54 k/ft. The beam line at this estimated ultimate load was then drawn over the M-Ø curve of the connection, which predicted a connection moment of 860 $^{in-k}$. Because the assumed connection capacity of 848.4 $^{in-k}$ did not

00408

equal the capacity predicted by the beam line, an increased estimated connection capacity of 1.22 X 707^{in-k} or 864^{in-k} was used. This resulted in a ultimate load of 3.56 k/ft. The beam line at this load predicted a connection moment of 864^{in-k}. Thus collapse was calculated to occur at 3.56 k/ft. or 1.58 times the 2.25 k/ft service load.

The 3.56 k/ft estimated ultimate load was considered to be the full overload capacity of the member because the connection at this point had little reserve capacity, as shown in Fig. 3.4. (Also, the rotation of the connection would become exceedingly large upon further load application.) Fig. 3.4 shows the beam line at the estimated ultimate load together with the beam line at service load, both of which are plotted over the M-Ø curve of the connection. The beam line at ultimate load intersects the M-Ø curve on that portion of the curve which exhibits a very small slope (low connection stiffness). Note that in going from working load to ultimate load the moment in the connection increases about 22 percent, close to the 20 percent increase used to generate the trial ultimate load beam line.

The same analytical procedure was used to calculate the overload capacity for several of the beams and semi-rigid connections studied in the experimental investigation; the factors of safety with respect to collapse ranged from 1.5 to 1.55. (It should also be noted that, if it were assumed that the connection had no increase in capacity beyond that at working load, the corresponding factor of safety for the beams would

00409

decrease to approximately 1.47).

3.3 Comparison With Fully Fixed Beam

At this point it was thought appropriate to make a comparison between the example beam, which utilizes semi-rigid connections, and a beam which utilizes fully rigid connections at its ends (a fixed-fixed beam), shown in Fig. 3.1b. The same beam section (W14X38) with a length of 24 feet and a service load of 2.25 k/ft was used. A comparison between these two beams, showing the variation in connection moment with an increase in uniform gravity load, is shown in Fig. 3.5. As noted previously, and shown in the figure, the overload capacity for the beam with semi-rigid connections is 1.58. For the beam with rigid connections, first plastic hinge formation occurs at the ends of the beam at an overload ratio of 1.71. However, total collapse at this beam does not occur until a third plastic hinge forms at midspan of the beam, which occurs at a load 2.275 times the service load. Thus the factors of safety with respect to collapse for the beam with semi-rigid connections and the beam with rigid connections are 1.58 and 2.275, respectively.

IV. FRAME DESIGN EXAMPLE

4.1 Procedure for Frame Design

In this phase of the investigation, a procedure was developed for preliminary selection of member and connection

00410

sizes for a framed structure utilizing semi-rigid connections. A single story, single bay frame with a uniform gravity load was used. It was decided that, as a first trial, the beam would be designed for a maximum moment of $wl^2/10$, less than the $wl^2/8$ simple beam gravity load moment currently used in Type 2 construction. The reasoning for this selection was as follows. If the beam were framed to infinitely stiff columns, the same beam could be used with fully rigid connections (support moment = $wl^2/12$; mid-span moment = $wl^2/24$) or with semi-rigid connections that would develop $wl^2/24$ at working load (for which the beam mid-span moment would be $wl^2/12$). However, using such connections with columns of limited stiffness would result, at service load, in a transfer of moment from the ends to the mid-span of the beam, thereby increasing the moment at that point above $wl^2/12$ ($wl^2/10$ estimated).

After selecting a beam section of adequate capacity for the $wl^2/10$ moment, its standard beam line was defined. This beam line, combined with the estimated required connection stiffness, was used to select the appropriate connection details from the family of semi-rigid connection moment-rotation curves for that particular beam depth, as shown in Fig. 4.1. As noted above, the design moment for the selection of the connection was taken as $wl^2/24$, slightly less than one-half the allowable moment for the beam ($\sim wl^2/10$).

For a trial selection of the columns, the equivalent axial load design procedure was used, where the axial load of the

66411

column was taken to be wl/2 and the maximum moment in the column as $wl^2/24$.

The example frame that was studied is shown in Fig. 4.2. It consisted of a 24 ft. long W14X38 beam framed to 12 ft. long W8X28 columns. The beam was to carry a uniform service load of 1.88 k/ft. Normally, top and seat angles having a length of 6 inches would be used for framing into the W8X28 column flange. However, since the experimental program used 8-in. angles to generate the M-Ø curves for the W14X38 beam sections, it was felt that this combination would be most consistent with the test data. Further, it was found that the length of the top and seat angles had a relatively minor effect on connection stiffness compared to the angle thickness and gage. Therefore, the semi-rigid connections consisted of L6X4X3/8X0'-8" top and seat angles with a gage of 2-1/4 in. in the leg mounted to the column, and two L4 X 3 1/2 X 1/4 X 0'- 8 1/2" in. web angles. With all of the trial members and the details of the connection selected, the frame could now be analyzed. A program developed in conjunction with the NSF sponsored study was used for this analysis. [3] The program analyzes a plane frame by the stiffness method, incorporating the complete non-linear M-Ø relationship for the connections used. The program uses an iterative technique, the details of which are explained in the reference.

From this non-linear analysis, it was found that the actual moment carried by the connection at service load was less than

00412

the trial moment for which it was designed. As noted previously, the design moment for the selection of the semi-rigid connection was taken as $wl^2/24$, but the analysis showed that it only developed a moment of $wl^2/32.7$. Also, the analysis showed that the actual beam mid-span moment was $wl^2/10.6$ compared to the $wl^2/10$ originally assumed. Therefore, selecting a beam section for a capacity of $wl^2/10$ was a good approximation for the example chosen.

4.2 Comparison of Semi-Rigid Frame with Rigid Frame

4.2.1 Gravity Loading - AISC Specification Requirements

Using the non-linear analysis program, a comparison was made between the frame with semi-rigid connections and one utilizing fully rigid beam-column connections. (The frame which utilizes semi-rigid connections hereafter will be referred to simply as the "semi-rigid frame.") The rigid frame consisted of the same members and the same loading as the semi-rigid frame.

At service load the semi-rigid frame obviously developed smaller moments at the connection in comparison to the rigid frame, with its mid-span beam moment being correspondingly greater than that of the rigid frame. The results showed that, for the particular frames studied, the semi-rigid frame developed 84.9 percent of the 467.7 in-kips moment of the rigid frame at the connections, with its beam mid-span moment being 106 percent of that in the rigid frame (1152.2 in-kips). The complete bending moment diagrams at service load for the two frames are

80413

presented in Appendix C, pp. 70 to 73.

The columns and beams of each frame were then checked by the provisions of the AISC Specification. Both frames were unbraced in the plane of loading. For the design check only in-plane behavior was considered. That is, the beams and columns were assumed to be fully laterally supported so that the laterally unbraced length of the compression flange of the beams was taken to be zero, as was the slenderness ratio of the column about the minor axis ($k_y l/r_y$). Only in-plane behavior was considered to confine the analysis of each system to a comparison of the effects of the connection stiffness on the response of the frames in the plane of loading.

The rigid frame was checked by the standard procedure specified by AISC in Part 1. The column effective length factor, k, was found directly from the alignment chart in the AISC Commentary. For the semi-rigid frame, the AISC Specification was used, but adjustments to the k factor were made. [5] This adjustment takes into account the initial stiffness (RIS) of the semi-rigid connection. However, the unmodified alignment chart can usually be used directly for frames with semi-rigid connections because the flexibilities of such connections do not significantly reduce the effectiveness of the girder stiffness. The slight increase in the k factor usually has little effect on the allowable stress. For the frames in this study, the elastic k factors for the columns of the rigid frame and those in the frame with semi-rigid connections were 1.80 and 1.88,

00414

respectively. However, because the in-plane slenderness ratios, $k_x l/r_x$, of the semi-rigid frame and the rigid frame were both less than C_c the inelastic k values were used, as recommended by AISC.

The inelastic k factors for the columns in the rigid frame and the semi-rigid frame were calculated to be 1.75 and 1.82, respectively. Also, because only the in-plane behavior was considered, the allowable bending stress, F_{bx} for the beams and columns, which are compact sections, was taken as .66 Fy (24 ksi for the A36 steel). The coefficient, C_m, applied to the bending term in the interaction formula 1.6-1a of AISC Section 1.6, was taken as .85 for the columns, as specified for an unbraced frame.

From checks of the appropriate interaction formulas of Section 1.6, all members of both the rigid frame and the semi-rigid frame satisfied the requirements. These checks, and the bending moment diagrams for both frames under the uniform gravity service load are shown in Appendix C, pp. 70 to 73.

Both frames, having satisfied the provisions of the AISC Specification, Part 1, for service load conditions, were then checked in accordance with the strength requirements (factored load provisions) of Part 2 of the Specification. Both frames were subjected to a factored load equal to 1.7 times the service gravity load. The analyses were performed as before (i.e., using the complete non-linear moment-rotation curve to define the response of the semi-rigid frame), and the interaction formulas

00415

of Part 2 checked. Again, both the rigid frame and the semi-rigid frame passed the Specification requirements. C_m was taken conservatively as 1.0 for the beams of both frames in checking formula 2.4-2; for the columns, $C_m = 0.85$ was used as in the Part 1 checks. The specification checks, together with the bending moment diagrams for both frames at factored loads, are shown in Appendix C, pp. 74 to 75 .

4.2.2 Gravity Loading - Yield, Collapse Analyses

In this part of the study, the behavior of the rigid frame and of the semi-rigid frame was compared as the gravity loads were increased beyond the service load conditions. In the analyses, the condition of initial distress has been defined as the load at which either the column or the beam just begins to yield (based on an elastic analysis, and excluding residual stress consideration). In addition to establishing the load at first distress, limit state analyses were performed for the rigid and semi-rigid frames to obtain a measure of the overload capacity associated with each frame.

To determine the state of first distress and the limit state capacity of the two frames, only in-plane behavior was considered. The following set of equations was used to determine the load at first distress in a particular member of a frame:

$$\frac{P}{P_{crx}} + \left(\frac{Cm}{1-P/P_{EX}}\right) \frac{M^c}{My^c} \leq 1.0 \qquad [1]$$

0416

$$\frac{P}{P_y} + \frac{M^c}{M_y} \leq 1.0 \qquad [2]$$

$$\frac{M^b}{M_y^b} \leq 1.0 \qquad [3]$$

The equations used to estimate the ultimate load-carrying capacity for the members of each frame are as follows:

$$\frac{P}{P_{crx}} + \left(\frac{Cm}{1-P/P_{EX}}\right) \frac{M^c}{M_p^c} \leq 1.0 \qquad [4]$$

$$\frac{P}{Py} + \frac{M^c}{1.18\, M_p} \leq 1.0; \quad M^c \leq M_p^c \qquad [5]$$

$$\frac{M^b}{M_p^b} \leq 1.0 \qquad [6]$$

First distress, and the limit state strength along the length of the column are determined by Equations (1) and (4), respectively. First distress, and plastic hinge formation are determined by Equations (2) and (5), respectively, for the column cross-section, and by Equations (3) and (6), respectively for the beam cross-section. Note that Equations (3) and (6) do not include the axial load effects on the beam which, for the cases studied, are relatively small.

In Equations (1) through (6) above, P is the applied axial load in the column, M^c is the maximum moment in the column, and M^b is the maximum moment in the beam, all of which are directly related to the external loading. P_{crx} is the buckling load

00417

(inelastic) of the column; P_{EX} is the Euler buckling load of the column; M_y is the yield moment of the member cross-section; M_p is the fully plastic moment of the member cross-section; and P_y is the product of the yield stress and the nominal area of the column.

The term Cm requires further explanation as used in Equations 1 and 4 above. When used in Formula 1.6-1a of the AISC Specification, Cm was taken as .85 for the columns. However, when the actual behavior of the frames is considered, a more appropriate value of Cm should be used. For the case in which only gravity load is applied, the single story unbraced frames, whether utilizing rigid or semi-rigid connections, initially displaces in a manner identical to that of a braced frame due to the symmetry of the structure and of the loading. [4] Therefore, for this loading condition, Cm was taken to be $.6 - .4\ M_1/M_2$, in which the ratio M_1/M_2 becomes zero because the columns utilize non-rigid base plate connections.

Table 4.1 presents a list of the values of the various terms that are used in Equations (1) through (6). Note that the values for P_{crx}, P_{EX}, and the slenderness ratio differ for the column in the semi-rigid frame and the column in the rigid frame. This is due to the difference in the inelatic K factors, as discussed earlier.

The analyses at first distress and at the limit state were performed for both the rigid frame and the semi-rigid frame for a uniform gravity load. The column and beam moment diagrams and

00418

the appropriate response equations for these analyses are shown in Appendix D.

For the frame with semi-rigid connections the initial distress occurs as first yielding at the midspan of the beam at a load 1.56 times the service gravity load. Note that the summations of the terms in interaction formulas (1) and (2) on page 77 of Appendix D are considerably less than one at that load. This suggests that the columns can support greater loads before they experience first distress.

The rigid frame experiences first distress at a load of 1.64 times the service gravity load. However this distress occurs as first yielding at the top of the columns due to the presence of the fully rigid connections, which attract more moment to the ends of the beam (relative to that of the semi-rigid frame). It may be noted that the Equation (3) on page 78 of Appendix D has a value of 0.96, which indicates that yielding at the beam midspan is also imminent at the same 1.64 load factor.

The semi-rigid frame exhibits first plastic hinge formation at the beam midspan at a load of 1.73 times the gravity service load. The limit state interaction formulas, Equations (4) and (5), indicate that the columns have sufficient capacity to resist additional load at this time. However, it was assumed that the semi-rigid connections had essentially reached their full capacity at the 1.73 load factor, thereby creating a collapse "mechanism" for the beam, and negating the possibility of applying additional load to the frames.

00419

The justification for this assessment of the limit state is as follows. Fig. 4.3 shows the M-Ø curve for the connection used in the semi-rigid frame. Also shown in the figure is the point along the M-Ø curve that corresponds to the moment in the connection when plastic hinge formation occurs at the beam midspan. Note that this point is on the flattened portion of the M-Ø curve, suggesting that rotations are becoming large and that the connection has little additional reserve capacity. Therefore, the load corresponding to plastic hinge formation at the beam midspan was also considered to be the total collapse load for the semi-rigid frame.

For the rigid frame the first plastic hinge also forms at the midspan of the beam, but at a load of 3.6 k/ft, 1.92 times the service gravity load. Because this frame utilizes fully rigid connections, however, total collapse does not occur until additional plastic hinges form at the tops of the columns, creating a collapse mechanism. (The analysis is shown on page 81 of Appendix D). Collapse of the rigid frame occurs at a load of 3.7 k/ft, an overload factor of 1.97 times the service load.

Fig. 4.4 shows a comparison between the behavior of the rigid frame and that of the semi-rigid frame. The figure illustrates the relationship between the connection moment and the ratio of the applied gravity load to the service gravity load for both frames. Shown on the curves are the points which correspond to the moment in the connection at first distress, and at first plastic hinge formation. Also shown on the curve

08420

representing the rigid frame is the point which corresponds to the moment in the connection at total collapse of the frame. It should be recalled that, for the semi-rigid frame, the first plastic hinge formation was assumed to correspond also to collapse of that frame.

It is also of interest to compare the beam midspan deflections of the rigid and the semi-rigid frames, as shown in Fig. 4.5. As expected, the frame which utilizes semi-rigid connections has greater midspan beam deflections than does the rigid frame; however, the differences are relatively small, particularly under service load conditions.

4.2.3 Combined Gravity Plus Wind Loading

AISC specifies that, for frames subject to combined gravity plus wind loading, the allowable stresses may be increased by 1/3 (or the combined loading may be multiplied by a factor of 0.75). Therefore the design load for combined gravity plus wind was taken to be 0.75 times the service gravity load plus 0.75 times the wind load. This resulted in the frame being subjected to a uniform gravity load of 1.41 k/ft and a lateral wind load of 1.8 k applied at the top of the windward column. This load combination will be referred to as Load Case 2, while the previous load case involving the full gravity load alone will be referred to as Load Case 1.

The results of the analyses of Load Case 2 for both the rigid and semi-rigid frames, together with the AISC checks

80421

specified in Section 1.6, are presented in Appendix E. Both frames passed the AISC requirements for this Load Case 2 as they did for Load Case 1. The beam of the rigid frame again carries less moment in the span than the beam in the semi-rigid frame. Correspondingly, the columns of the semi-rigid frame carry less moment than the columns of the rigid frame, with the leeward connections experiencing larger moments than the windward connections. The axial effects in the leeward columns of both frames were small compared to the bending effects; thus, interaction formula 1.6-2 was checked instead of formulas 1.6-1a and 1.6-1b. For the leeward column of the rigid frame, the interaction formula summation was 0.958, compared to Load Case 1, for which the interaction summation was 0.926. This suggests that the gravity and wind load combination represents a more critical loading condition for this rigid frame. For the semi-rigid frame, the leeward column also was the more critical member under combined gravity plus wind loading. However, for the semi-rigid frame, if the values of the interaction formulas are considered, the beam of Load Case 1 had a higher formula 1.6-2 summation (0.945) than the leeward column of Load Case 2 (summation = 0.853). It is of interest to compare the values of the AISC interaction formulas of all members of both frames for Load Case 1 and Load Case 2. According to the formulas, the most critical member at service load is the leeward column of the rigid frame under Load Case 2; however, the beam of the semi-rigid frame under Load Case 1 follows very closely, with the

00422

values of their interaction formula summations being 0.958 and 0.945, respectively.

Both frames were then checked in accordance with the strength requirements in Part 2 of the AISC Specification for the combined effects of gravity plus wind load. Loads of 1.3 times the service gravity load plus 1.3 times the wind load were applied to the rigid and semi-rigid frames. The members of both frames were then checked according to the interaction formulas of Part 2 of the AISC Specification; all members passed the requirements. The results of these analyses and checks are shown in Appendix E. As indicated by interaction formulas 2.4-2 and 2.4-3, the leeward column of the rigid frame is more critical than any of the members of the semi-rigid frame. However, this should not be construed to indicate that the semi-rigid frame exhibits better performance under the gravity plus wind load than does the rigid frame. The maximum drift for each frame is a factor that must be taken into consideration. Fig. 4.6 shows a comparison between the maximum drift of the rigid frame and that of the semi-rigid frame. The abscissa is non-dimensionalized as the ratio of the applied gravity plus wind load to the combination of gravity and wind at service load. At factored load (L.F. = 1.3), the drift at the top of the columns for the rigid frame is 0.69 inches, while the drift for the semi-rigid frame is 1.31 inches. While the leeward column of the semi-rigid frame is far from reaching a limit state (interaction summations of 0.744 and 0.663 in formulas 2.4-2 and 2.4-3, respectively),

00423

the extent of sway is 90 percent greater than the drift of the frame which utilizes fully rigid connections. It may be noted also that the drift at service load was 0.40 inches for the rigid frame and 0.55 inches for the semi-rigid frame, an increase of only 37.5 percent for the structure utilizing the semi-rigid connections.

A behavioral analysis for first distress and for the limit state (collapse) was attempted for the combined loading of gravity plus wind. However, it was not possible to obtain this limit state analysis for the semi-rigid frame. This was due to the sensitivity of the computer program in its ability to achieve convergence in the calculation of connection moments in the region where the slope of the M-ϕ curve is very flat. This was indeed the case for the leeward column in the semi-rigid frame at loads well beyond service load conditions. Thus, in this presentation, the effects of combined gravity plus wind loading have been limited to Section 1.6 and Part 2 of the AISC Specification in the analyses of the two frames.

4.3 Use of the Revised Initial Slope

4.3.1 Monotonically Applied Loadings

In Section 3.1, a comparison was made between two analyses performed on a beam attached to fixed supports by semi-rigid connections. One analysis used the full M-ϕ curve of the connection while the other used the revised initial slope (RIS); the results were shown in Fig. 3.3. The RIS predicted a

00424

connection moment at working load which was 48 percent greater than the moment predicted by the full M-Ø curve.

Because the above beam example is analogous to a beam that is connected to infinitely stiff columns in a frame, this suggests an upper limit to which the RIS could be used in the analysis of frames at service load conditions. Note that the beam used in the example was a W14X38 section with a span of 24 feet, which is the same beam section and span that was used in the example frame which utilizes semi-rigid connections.

Comparisons were made of the analyses of the semi-rigid frame in which one analysis incorporated the full M-Ø curve of the connections while the other analysis used the RIS for the connections. The RIS for the connection used in the semi-rigid frame is 205,800 in-kips/rad,as shown in Table 2.1. The analyses were performed for gravity loading and for the combined gravity plus wind loading. Shown in Fig. 4.7 are two curves, one which predicts the connection moment on the basis of the RIS, and the other, which predicts the moment on the basis of the complete non-linear connection behavior. Both curves represent the moment at the connection that is produced upon the application of a specific proportion of the service or working gravity load. As shown in the figure, the RIS and non-linear M-Ø curve prediction are nearly identical up to and somewhat past the service load range. At working gravity load, the RIS predicts a connection moment of 402.2 in-kips, while use of the full M-Ø curve predicts a moment of 397.3 in-kips.

80425

A comparison of the frame connection moment predicted by the RIS with that predicted by the complete M-Ø curve is shown in Figures 4.8 and 4.9 for combined gravity and wind loading. (Figure 4.8 represents the moment at the windward column of the frame, while Figure 4.9 corresponds to the leeward column moment.) As with the case of gravity load alone, these predictions are very close for loads up to and including the service loads. Note that the abscissa in these figures represents a specific proportion of the combined service gravity plus service wind load. Therefore, a ratio of 0.4 represents the load state at which 40 percent of the service gravity load plus 40 percent of the wind load are applied to the frame, and a ratio of 1 represents the combined gravity plus wind load at the reduced load factor permitted by AISC (i.e., 0.75 times full gravity load plus 0.75 times full wind load). The moments predicted by the RIS for the windward and leeward connections at service load are 159.9 in-kips and 419.0 in-kips, respectively, while the connection moments predicted using the full M-Ø curve are 158.3 in-kips and 417.4 in-kips, respectively.

From the preceding analyses, it can be seen that, for the frame and semi-rigid connections examined, the RIS offers a reasonable and close approximation to the moments developed under both gravity loading alone, and under combined gravity and wind loading, at least up to service load conditions. Additional studies are required, however, to determine whether the same closeness of predicted behavior would hold for frames with more

but for ultimate load check in design process no good?

complex configurations and containing a variety of semi-rigid connections.

4.3.2 Loading and Unloading Effects

To further verify that the RIS closely predicts the behavior of the semi-rigid connection for the subject frame at working load, the frame was subjected to different combinations of loading and unloading of the gravity and wind forces. For this frame example, the dead load was taken as 40 percent, and the live load as 60 percent of the total service gravity load. (In the following discussions, the total gravity working load will be denoted G, while the dead load and the gravity live load will be referred to as D and L, respectively.)

The structure was next loaded in the following order. The total dead load (D=.4G) was applied; then only enough gravity live load was added so that the final gravity load, present on the frame was 0.75 times the total service gravity load (0.75G). Then, 75 percent of the wind load (W) was added to the gravity load so that the final load consisted of the combined gravity plus wind load specified by AISC. Hereafter, this final load case will be designated as 0.75 (G+W) for ease of reference.

The imposed loading sequence described above was analyzed by three different methods, each of which took into account a different representation of the connection's stiffness.

The first method (Method 1) used the complete M-Ø curve throughout the entire loading sequence, which resulted in

09427

windward and leeward moments of 158.3 in-kips and 417.4 in-kips, respectively, at the final loading of 0.75 (G+W). The moment vs. load relationships for the windward and leeward columns of the frame are shown in Figs. 4.10 and 4.11, respectively. The analysis used to generate these curves bears further explanation. For example, to obtain the point on the moment-load curve of the windward column corresponding to 0.75G + 0.4W, the computer program that was used, actually loaded the frame proportionally in increments until the final load combination was achieved. Thus, the windward connection was not actually loaded to the full gravity load moment and then unloaded (moment reversed) as the wind was applied. This procedure introduces some inaccuracies in the analysis as this connection would actually follow an unloading path corresponding to a stiffer M-Ø slope (resulting from reversal of moment) than that used to obtain the line from 0 to 0.75W in Fig. 4.10. As seen subsequently, however, this error was not appreciable and the entire loading history corresponded to moments in the nearly linear portion of the M-Ø curve for the connection.

In order to account for the moment reversal in the windward connection upon application of wind load, a second analytical procedure was used. This second method (Method 2) utilized the M-Ø curve for the application of the gravity load from zero to 0.75G; however, as the wind load was applied, different stiffnesses were used for the windward and leeward connections in the analysis procedure. This was done to account for the fact

that, as the wind load was applied following the application of the total gravity load, the leeward connection continues to follow the loading curve while the windward connection begins to unload (sense of the moment reverses). For the frame being considered, the moment in both connections was 297.7 in-kips before the wind load was applied. Fig. 4.12 shows the point on the M-Ø curve of the connection which corresponds to this moment. Because the structure is already loaded and each connection is experiencing a moment of 297.7 in-kips, they are no longer as stiff as what they were initially. Therefore, a more appropriate reduced stiffness of 87160 in-kips/rad (shown in Fig. 4.12) was used on the leeward connection since it continued to load upon the application of wind force. The reduced stiffness of the leeward connection was calculated by first estimating the value of the leeward connection moment at the final load of 0.75(G+W). The first estimate was taken to be 417 in-kips (the value obtained from the analytical procedure in Method 1). This point was then plotted on the full M-Ø curve along with the point which corresponds to the moment in the connection (297.7 in-kips) before the wind load was applied (0.75G). Referring to Fig. 4.12, a straight line was then drawn between these two points, the slope of which was taken to be the reduced stiffness in the leeward connection. This reduced stiffness for the leeward connection was used in the analysis for the application of the wind load. The final moment in the connection at the total load of 0.75(G+W) did not agree with the estimated moment (417.0

00429

in-kips); therefore, a new estimated moment was used and the above procedure was repeated until convergence was achieved. This corresponded to a final moment of 415.9 in-kips, which resulted in a reduced stiffness in the leeward connection of 87,160 in-kips load as shown in Fig. 4.12.

While the leeward connection continues to load upon applications of wind load the windward connection follows an unloading path. The RIS (205,800 in-kips/rad) was used for the adjusted stiffness of the windward connection; it was shown in the NSF study [2] that the initial stiffness closely predicts the unloading behavior of these semi-rigid connections. Using these newly defined stiffnesses for the windward and leeward connections, the frame was then subjected to a wind force of 0.75W and the analysis performed. The moments at the final load of 0.75(G+W) were 156.8 in-kips for the windward connection and 415.9 in-kips for the leeward connection. It should be noted that the values predicted by Method 2 are nearly identical to those predicted by Method 1 (158.3 in-kips and 417.4 in-kips, respectively), which incorporated the full M-Ø curve throughout the entire loading sequence.

A third procedure (Method 3) was used to analyze the frame for the same loading sequence used in Method 1 and Method 2. Method 3 utilized only the RIS for each load increment, which resulted in windward and leeward connection moments of 160.0 in-kips and 419.1 in-kips, respectively. Again, note the closeness of these values to those obtained by Method 1 and

00439

Method 2.

The loading sequence for each of the three methods detailed above is shown in Figures 4.10-4.16. To summarize, Method 1 utilized the full M-Ø curve for each load increment; Method 2 utilized the M-Ø curve for gravity load increments but incorporated adjusted stiffnesses upon the addition of wind loading; and Method 3 employed the RIS for each load increment. For the three methods, the moments at the windward connection for the final loading of 0.75(G+W) were 158.3 in-kips, 156.8 in-kips, and 160.0 in-kips, and for the leeward connection, the moments were 417.4 in-kips, 415.9 in-kips, and 419.1 in-kips.

The next consideration was to compare the residual moments in the connections after unloading of the wind load and the gravity live load. The frame was loaded according to the sequence described above, in which the connection behavior was predicted by each of the three methods just discussed. For each method, the unloading path was predicted by the RIS. The unloading sequence was accomplished in the following manner. First the wind load, then the gravity live load was removed, leaving only the dead load on the frame. When the connection behavior for the loading sequence was described by Method 1, the residual moment in both connections after unloading was 152.9 in-kips; when described by Method 2, the residual moment after unloading was 151.5 in-kips; and when described by Method 3, the residual moment was 154.5 in-kips. A second unloading sequence was then considered in which the gravity live load and the wind

00431

load were reduced proportionately. Using this sequence, each of the three methods yielded the same value as it did with the first unloading sequence. Figures 4.10, 4.11, 4.13-4.16 illustrate the response of the connections for each of the loading and unloading sequences just described. Separate curves are presented for the windward and leeward connection for each of the three loading methods. The solid line represents the connection moment upon loading while the dashed line describes the unloading path (first sequence) of the connection. Note that the loading and unloading sequence in which the connection behavior is described entirely by the RIS (shown in Figures 4.15, 4.16) closely approximates the behavior of the connections predicted by the more rigorous analytical approaches (Methods 1, 2).

The same closeness of response predicted by each of the three methods was also evident when the frame was subjected to a sequence of full gravity load application, followed by removal of the gravity live load only. Fig. 4.17 represents the connection moment vs. load response when it is described by the full M-Ø curve in the loading process, and Fig. 4.18 corresponds to the connection moment-load behavior when the RIS is used to define the connection stiffness in the loading process. (Both analyses employed the RIS for the unloading path). The residual moment in the connection was found to be 156.0 in-kips when the M-Ø curve was used, and 160.9 in-kips when the RIS was used. This again illustrates that, for this frame example and the loadings considered, the RIS gives a very good approximation to the

00432

behavior of the connections predicted using the analysis based on the non-linear moment-rotation curves, at least at service load conditions. This suggests that the RIS may be used in place of the full M-Ø curve to describe connection behavior at service loads, thus permitting the use of simpler analytical procedures in the design of frames which utilize semi-rigid connections. Further work is needed, however, to determine if similar correlations can be found for structures with more complex geometries and loading histories.

00433

SUMMARY AND CONCLUSIONS

Semi-empirical moment-rotation relationships developed from an experimental investigation [2] were used to formulate preliminary design aids which may be applicable to the direct utilization of semi-rigid connections in building systems. Several series of moment-rotation (M-Ø) curves were generated for connections of varying stiffness, within reasonable limits of extrapolation beyond the connections tested in that investigation.

The initial slopes to the empirically determined moment-rotation curves were found to provide unconservative predictions of the connection moment transfer capability and corresponding beam rotations. However, a revised initial slope (RIS) was considered and found to closely predict the initial stiffness of the M-Ø curves obtained from the actual test data. The values of the RIS were tabulated for all of the connections for which moment-rotation curves were generated.

A procedure was demonstrated for the design of a beam which utilizes semi-rigid connections attached to non-rotating supports. The procedure involved superimposing the beam line at working load over a series of M-Ø curves to select the appropriate semi-rigid connection. This beam and semi-rigid connection assembly was then compared to the behavior of a beam which utilized fully rigid connections at its ends. As expected, the rigid beam experienced a greater overload capacity than did the beam which utilized semi-rigid connections. The overload

00434

capacity of the beam with semi-rigid connections was assumed to occur at the point of first plastic hinge formation at the beam midspan. It was reasoned that, beyond this point, the connection had little reserve capacity; i.e., the beam line at that load intersected the M-Ø curve of the connection in a region of very low stiffness.

A procedure was also developed for a preliminary selection of member and connection sizes for a simple framed structure utilizing semi-rigid connections. A single story, single bay frame with a uniform gravity load was considered. A comparison was then made of the behavior of this semi-rigid frame with a similar frame utilizing fully rigid connections; both frames consisted of the same members and had the same loadings imposed. The frames were unbraced in the plane of bending, but considered to be fully supported laterally. At service load, the semi-rigid frame developed smaller moments at the connection in comparison to the rigid frame, while the mid-span beam moment of the semi-rigid frame was correspondingly greater than that of the rigid frame. The columns and beams of each frame were then checked by the provisions of Section 1.6 of the AISC Specification. All members of both frames satisfied the specification requirements for gravity loading (Load Case 1) and for combined gravity plus wind loading (Load Case 2). There were some interesting results obtained in comparing the values of the interaction formula summations for the members of both frames for Load Case 1 and Load Case 2. According to the formulas, the most

00435

critical member at service load was the leeward column of the rigid frame of Load Case 2, while the beam of the semi-rigid frame of Load Case 1 followed closely; the values of their interaction formula summations were 0.958 and 0.945, respectively. Both frames were also checked according to the strength and stability requirements specified in Part 2 of the AISC Specification for gravity loading and for gravity plus wind loading. Again, similar results were found in the summations of the interaction formulas - the leeward column of the rigid frame under combined gravity plus wind loading was found to be the more critical member. However, it was noted that, under the combined gravity plus wind loading, the story drift in the frame with semi-rigid connections was 90 percent greater than the drift in the frame which utilized rigid connections.

A limit-state analysis was performed for the rigid and the semi-rigid frames to obtain a measure of the overload capacity associated with the frames under gravity load. For the semi-rigid frame the first plastic hinge formation, at the beam midspan, was considered to correspond to the total collapse of the frame (for the same reasons as discussed above with the beam example). A collapse mechanism which involved three plastic hinges defined the collapse load for the rigid frame. These analyses resulted in overload factors of 1.73 and 1.97 times the service loads for the semi-rigid and the rigid frames, respectively.

The use of the Revised Initial Slope (RIS) in the analyses

00436

of the beam and frame which utilized semi-rigid connections was studied. A beam attached to fixed supports by semi-rigid connections was analyzed first by using the full M-Ø curve of the connection, and then, by using the RIS of the connection. The RIS predicted a connection moment at service load which was 48 percent greater than that which was predicted by the M-Ø curve. Since this beam is analogous to a beam which is connected to infinitely stiff columns in a frame, it represented an upper limit for which the RIS can be used to predict the behavior of an actual frame at service load conditions.

Two analytical comparisons were then made of the behavior of the semi-rigid frame; one incorporated the full M-Ø curve of the connections and the other utilized the RIS. The semi-rigid frame was subjected to different combinations of the loading and unloading of gravity load and wind load. It was shown that, for this frame example and the loadings considered, the RIS gives a very good approximation to the behavior of the connections predicted using the analyses based on the non-linear moment-rotation curves, at least at service load conditions. This suggests that the RIS may be used in place of the full M-Ø curve to describe connection behavior at service loads, thus permitting the use of simpler analytical procedures in the design of frames which utilize semi-rigid connections. However, further work is needed, to determine if similar correlations can be found for structures with more complex geometries and loading histories.

00437

Further work needs to be completed in the area of computer analysis of structures utilizing semi-rigid connections. More sophisticated computer programs which incorporate the non-linear M-Ø relationship of the semi-rigid connections need to be developed. ALREADY AVAILABLE

Lastly, additional studies should be performed to compare the behavior of the simple, single-story frame used in this study to the behavior of frames with more complex configurations and containing a variety of semi-rigid connections. However, the results of this investigation have served to illustrate preliminary procedures that could be used to incorporate semi-rigid connections directly in future designs.

00438

REFERENCES

1. Manual of Steel Construction, Eighth Edition, American Institute of Steel Construction, Inc., Chicago, Illinois, 1980.

2. Altman, W.G., Azizinamini, A., Bradburn, J.H., and Radziminski, J.B., "Moment-Rotation Characteristics of Semi-Rigid Steel Beam-Column Connections," Department of Civil Engineering, University of South Carolina, Columbia, South Carolina, June 1982.

3. Azizinamini, A., Monotonic Response of Semi-Rigid Steel Beam to Column Connections, Master's Thesis, Department of Civil Engineering, University of South Carolina, Columbia, South Carolina, August 1982.

4. Gaylord, E.H. and Gaylord, C.N., Design of Steel Structures, McGraw-Hill Book Company, New York, 1972.

5. Defalco, F., and Marino, F., "Column Stability and Type 2 Connections," Engineering Journal, AISC, Vol. 3, No. 2, April 1966.

80439

Appendix A

Moment-Rotation Curves

99449

Nomenclature for M-Ø Curves

Symbol

d = depth of beam

g = gage in flange angle; from heel of angle to center of bolt hole in leg adjacent to column face

L = overall length of flange angle

t = thickness of flange angle

t_c = thickness of web angle

00441

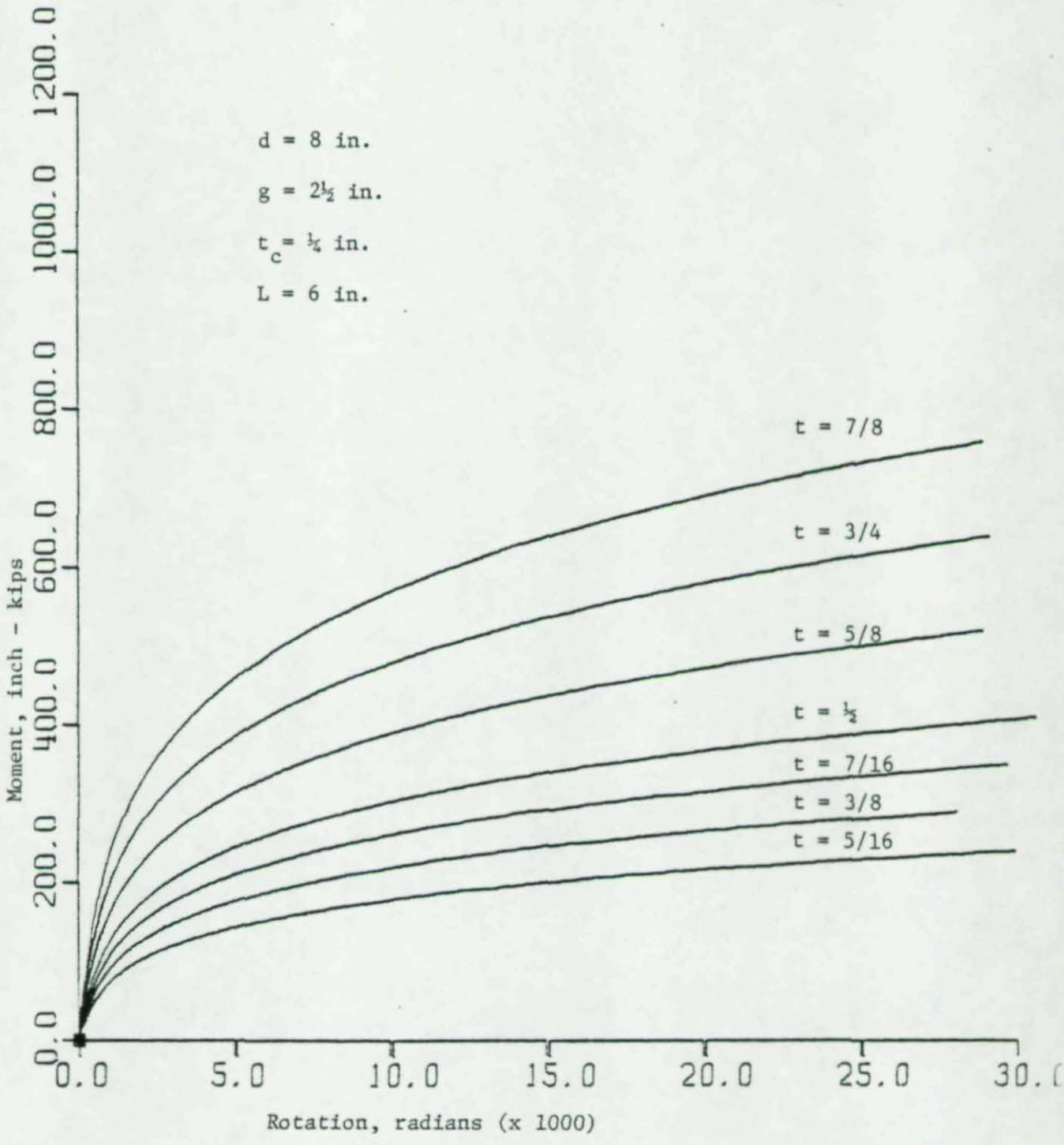

Fig. A1 M-Ø Curves for Connections Used to Frame Beam Depth of 8 in. with a 2½ in. Gage in the Flange Angles

00442

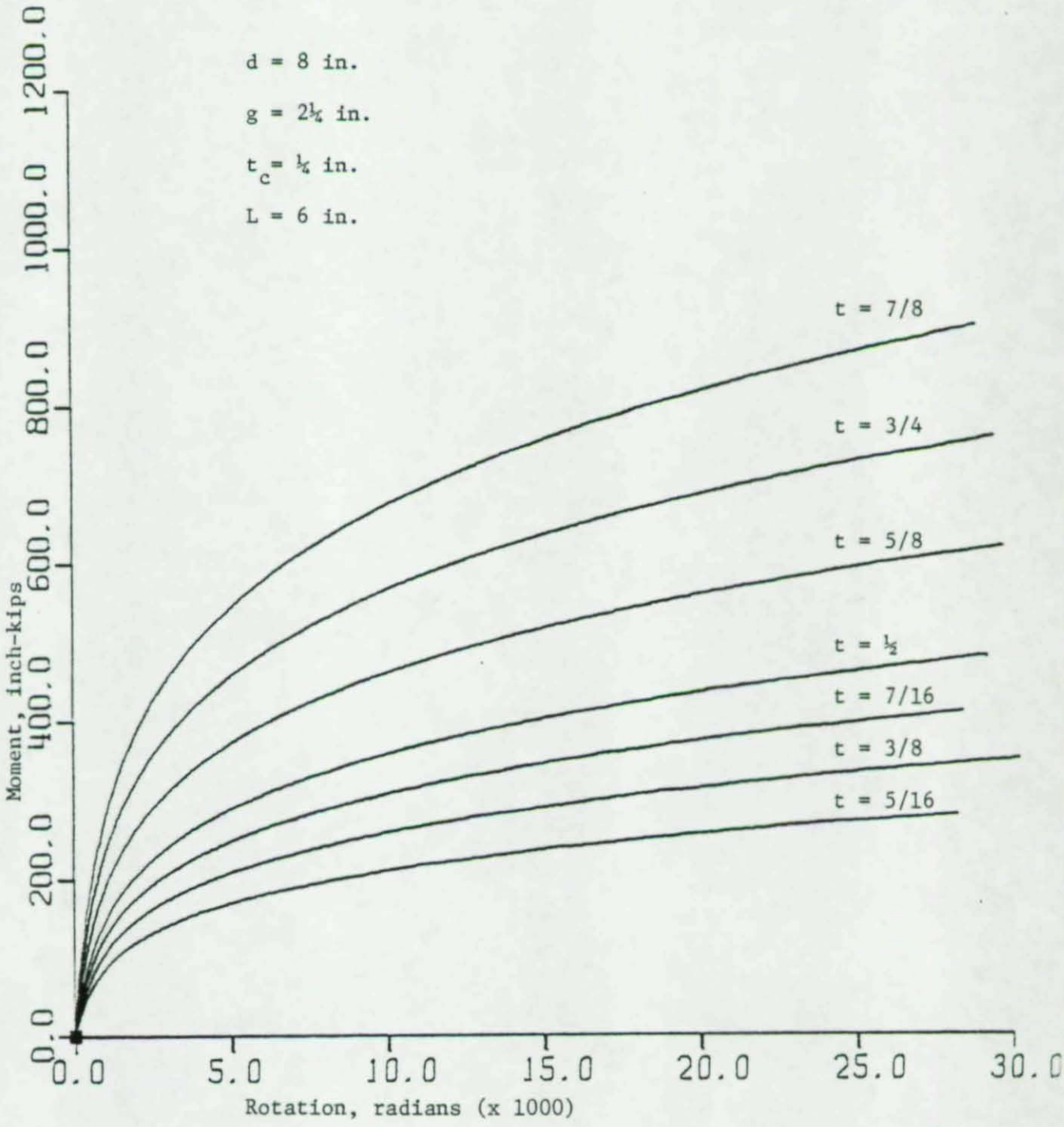

Fig. A2 M-Ø Curves for Connections Used to Frame Beam Depths of 8 in. with a 2½ in. Gage in the Flange Angles

00443

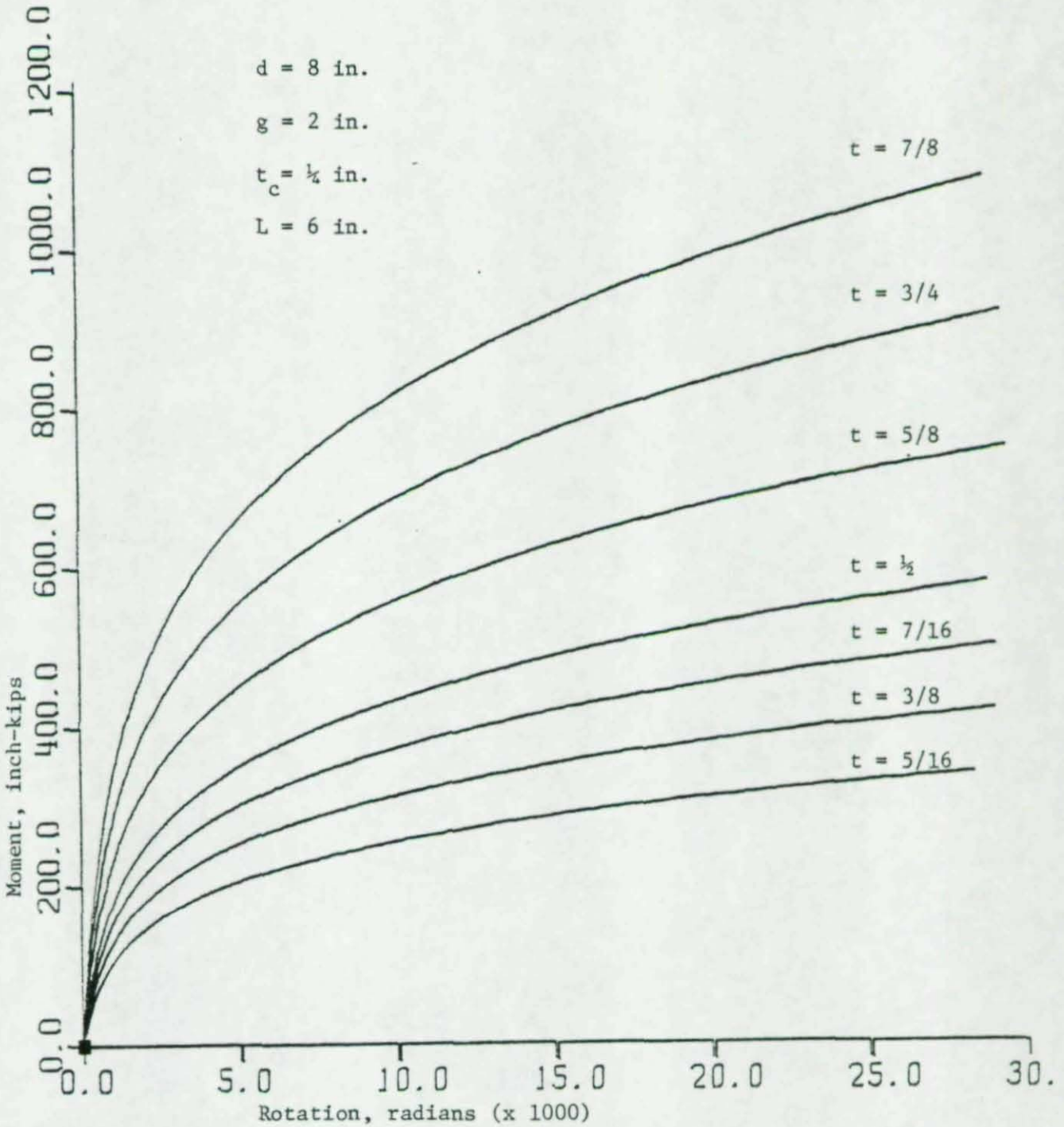

Fig. A3 M-Ø Curves for Connections Used to Frame Beam Depths of 8 in. with a 2 in. Gage in the Flange Angles

00444

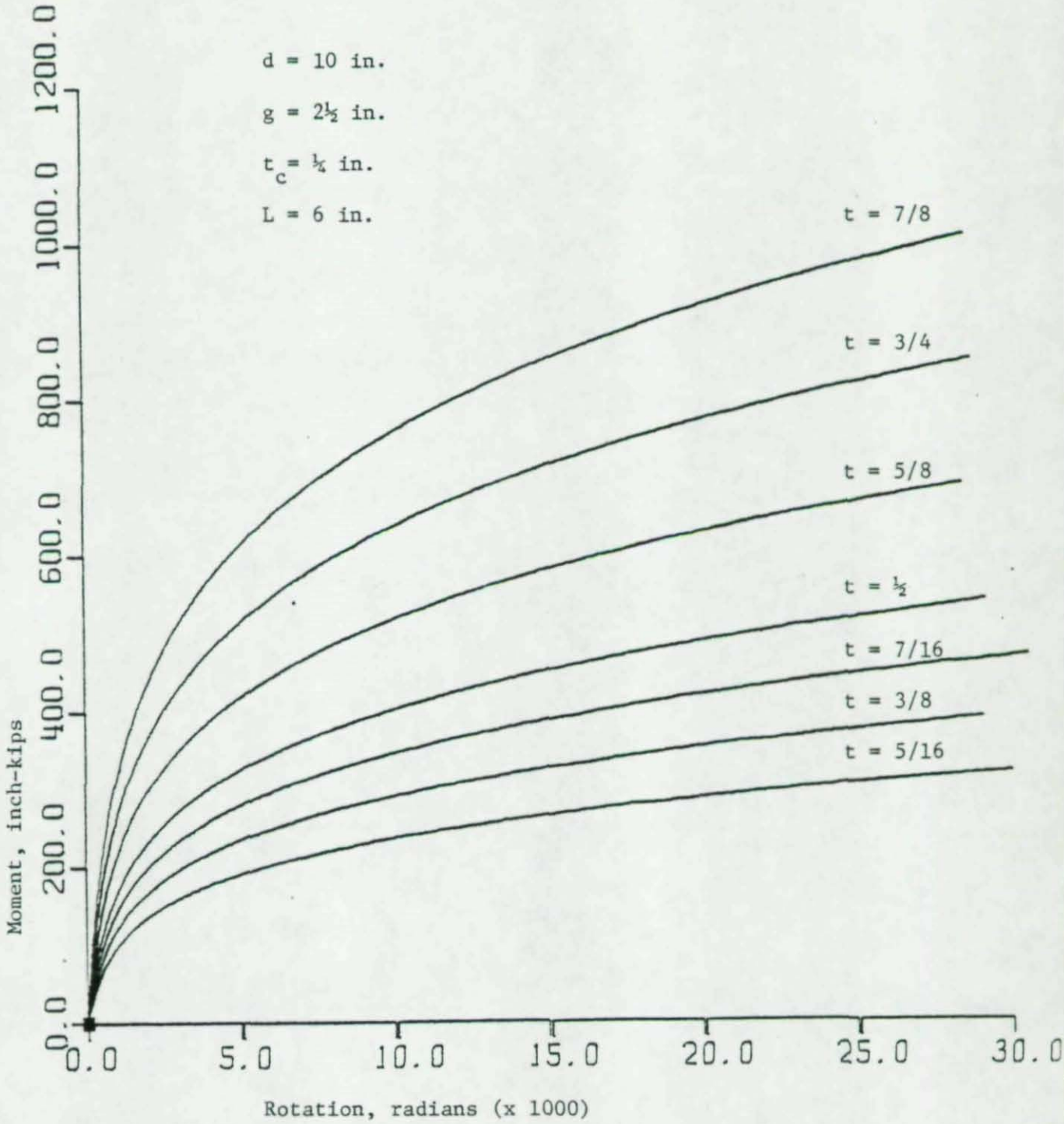

Fig A4 M-Ø Curves for Connections Used to Frame Beam Depths of 10 in. with a 2½ in. Gage in the Flange Angles

00445

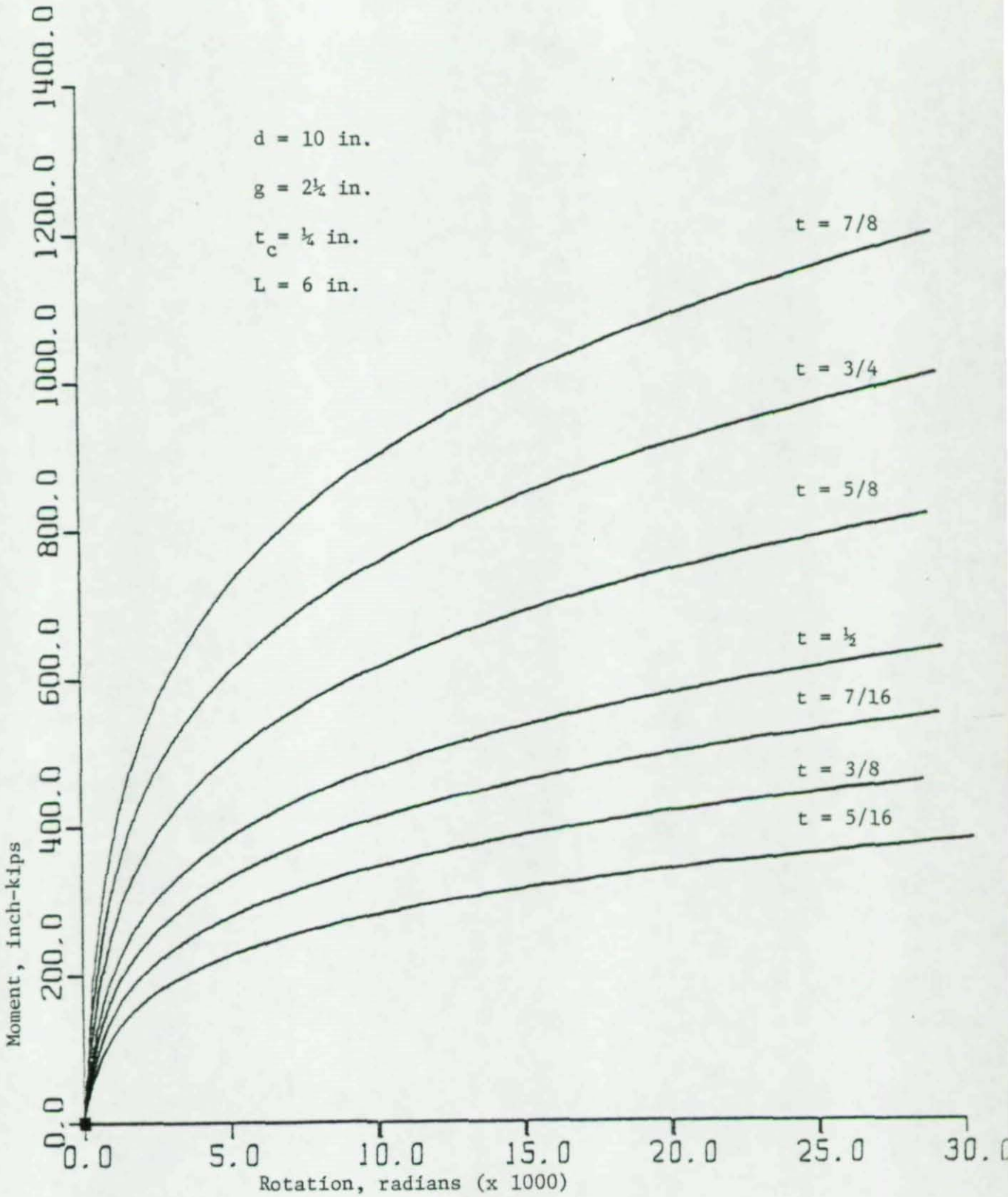

Fig. A5 M-Ø Curves for Connections Used to Frame Beam Depths of 10 in. with a 2½ in. Gage in the Flange Angles

00446

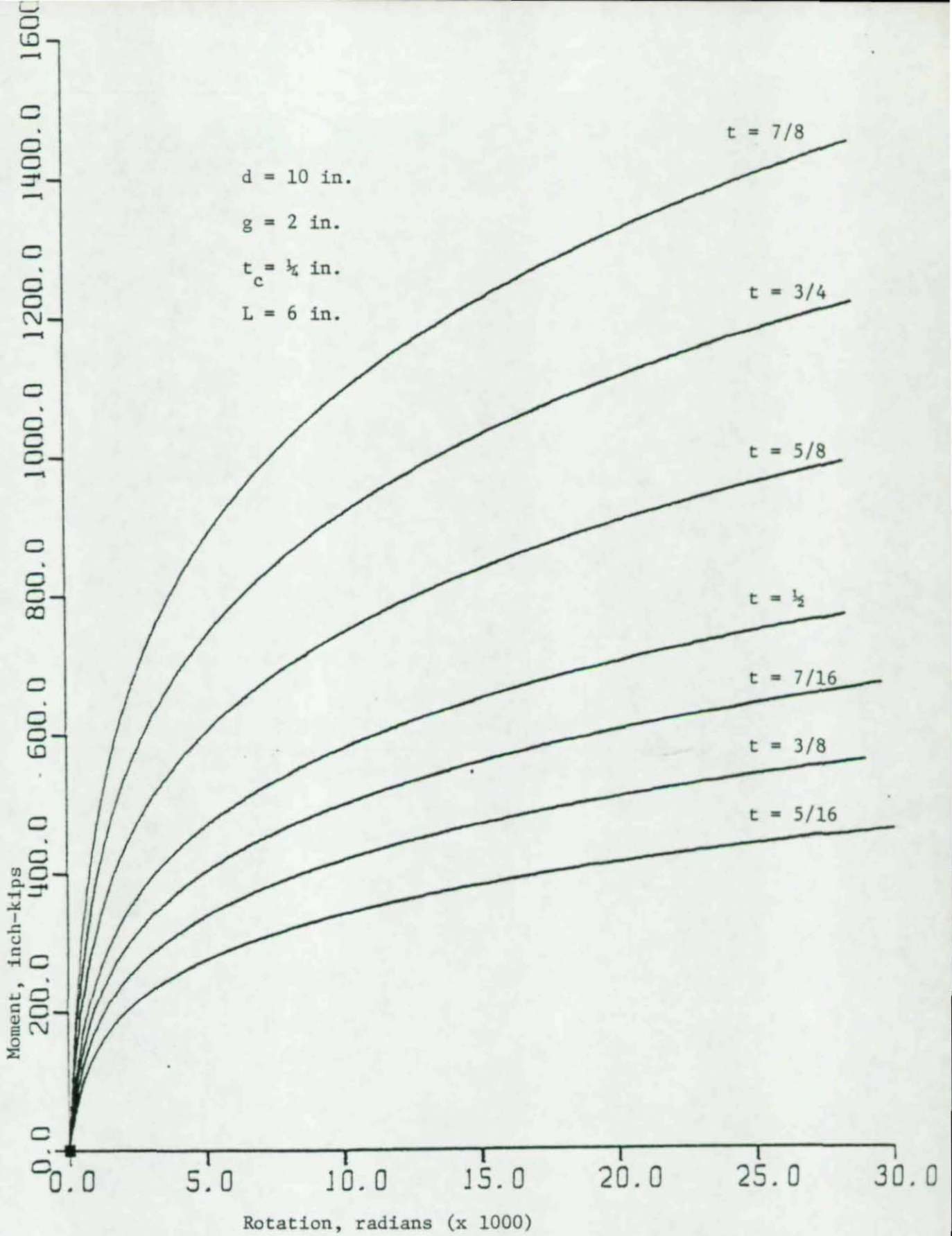

Fig. A6 M-Ø Curves for Connections Used to Frame a Beam Depth of 10 in. with a 2 in. Gage in the Flange Angles

00447

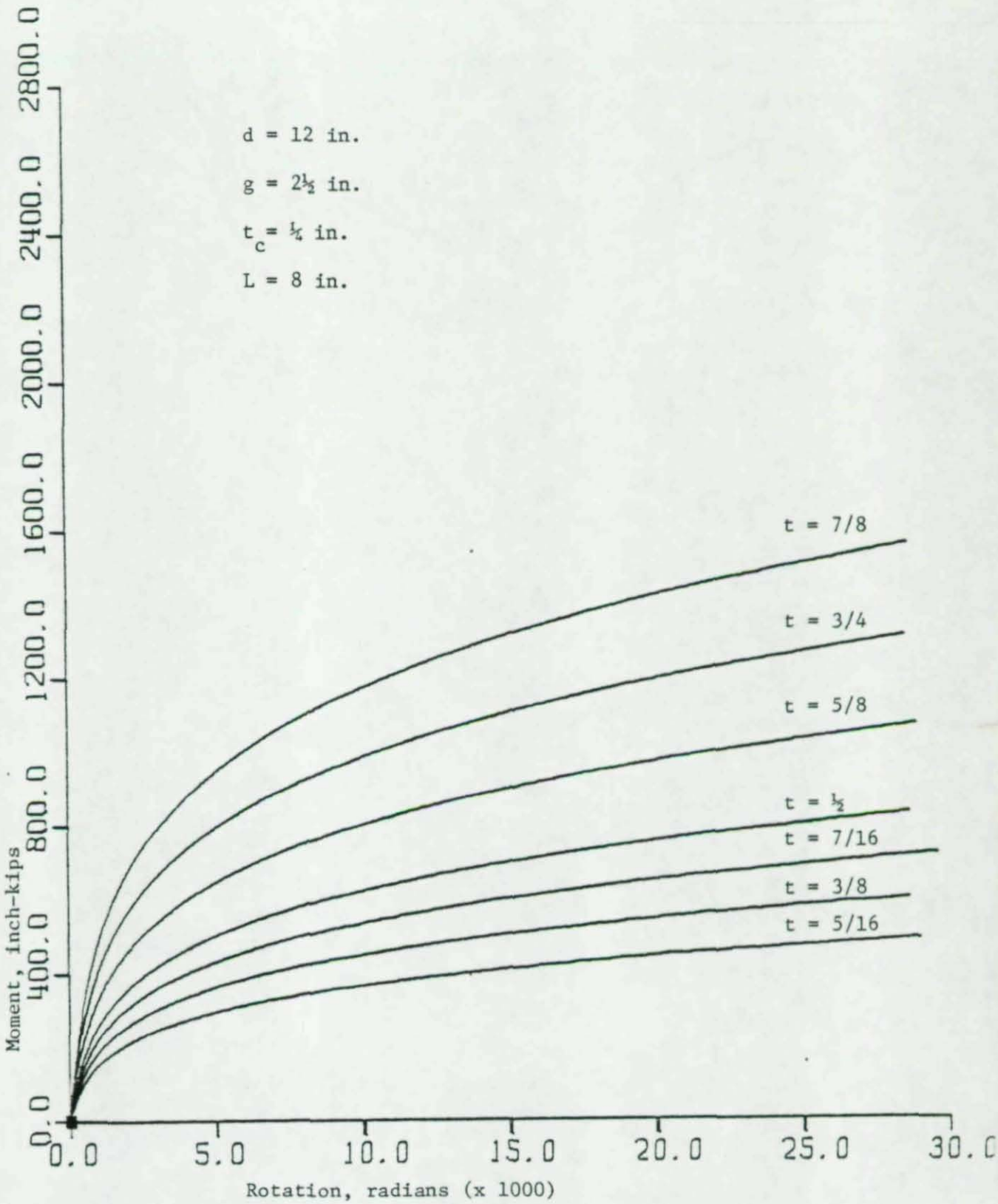

Fig. A7 M-Ø Curves for Connections Used to Frame a Beam Depth of 12 in. with a 2½ in. Gage in Flange Angles

00448

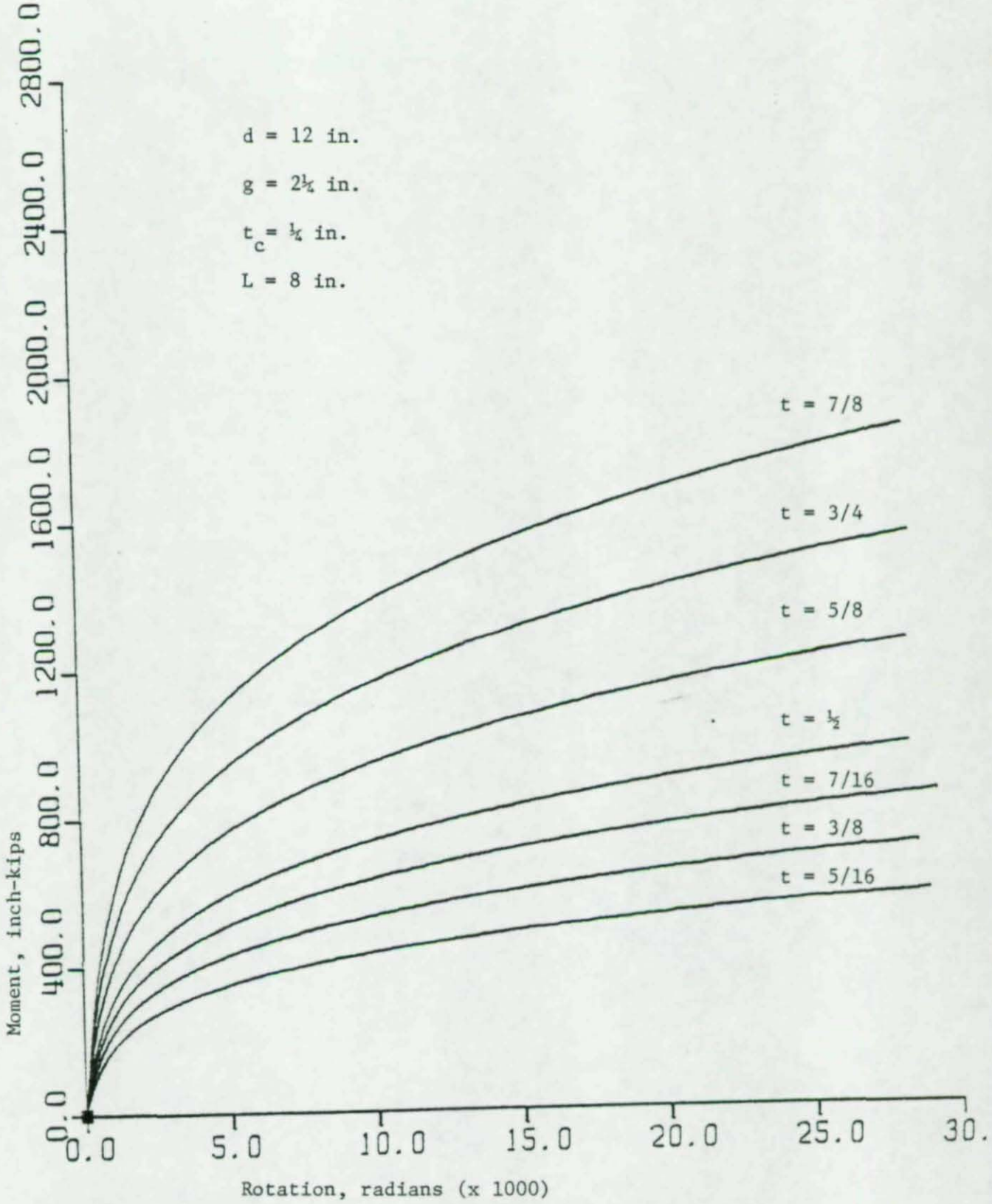

Fig. A8 M-Ø Curves for Connections Used to Frame Beam Depths of 12 in. with a 2½ in. Gage in the Flange Angles

00449

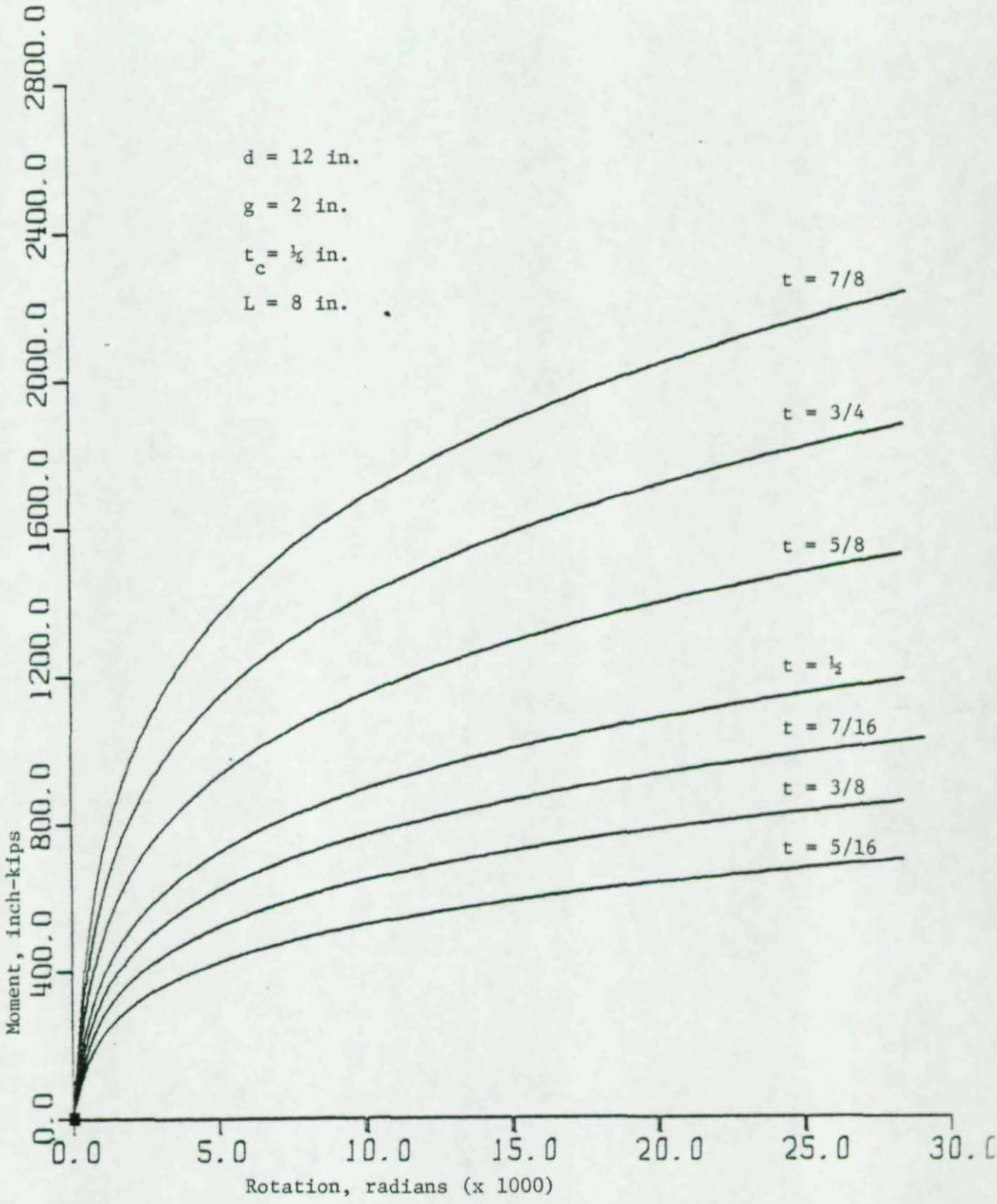

Fig. A9 M-Ø Curves for Connections Used to Frame Beam Depths of 12 in. with a 2 in. Gage in the Flange Angles

00450

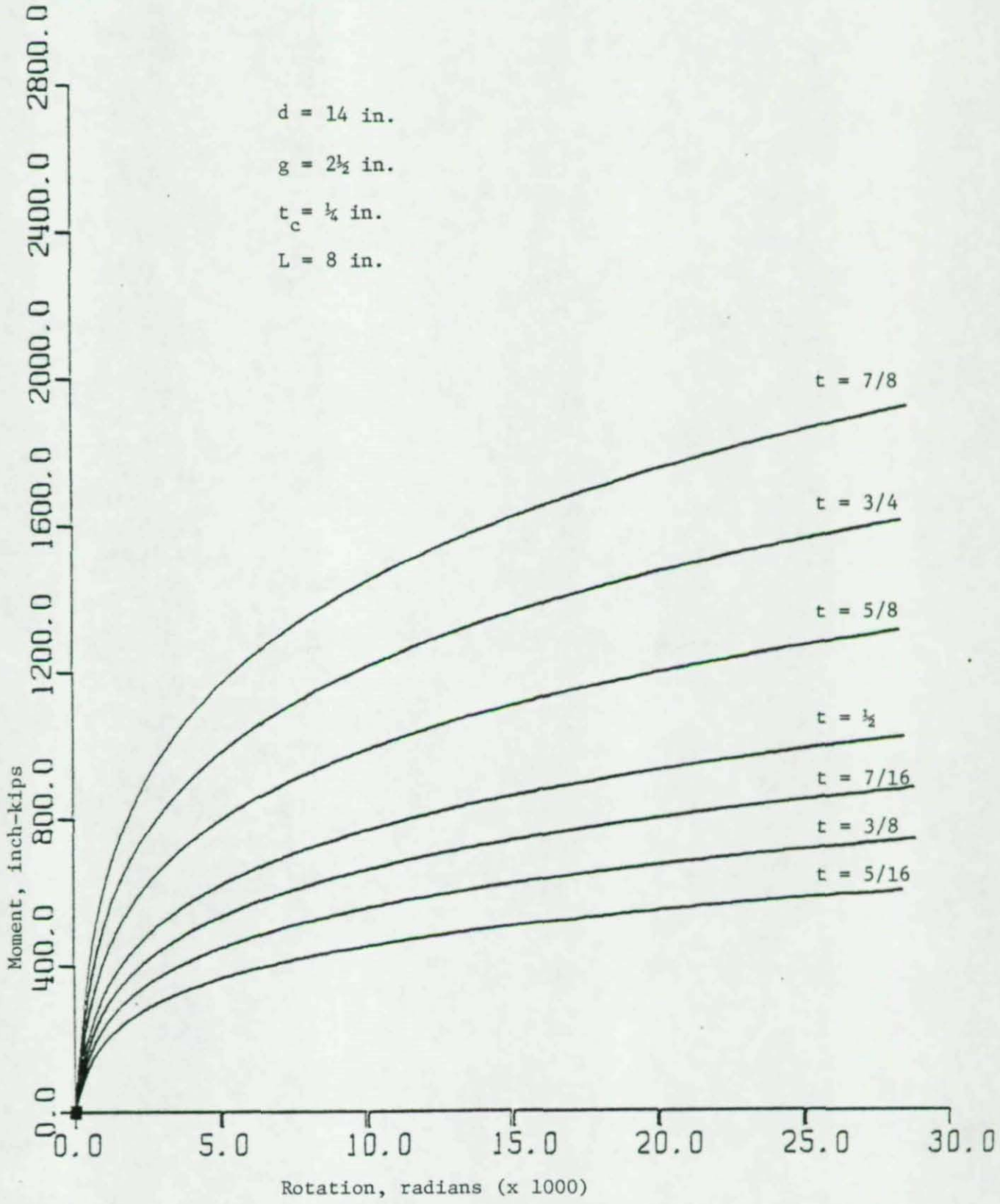

Fig. A10 M-Ø Curves for Connections Used to Frame Beam Depths of 14 in. with a 2½ in. Gage in the Flange Angles

00451

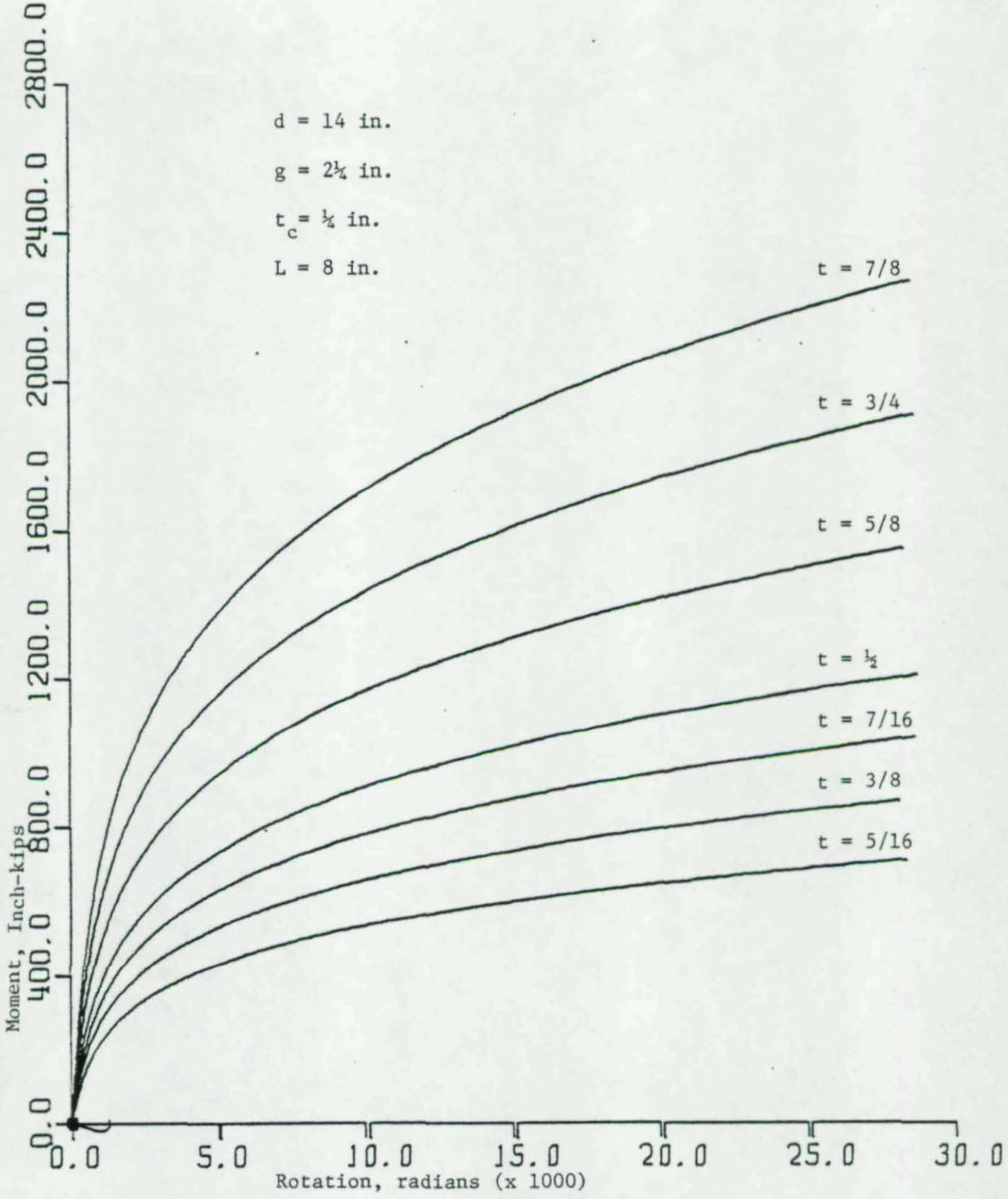

Fig. A11 M-Ø Curves for Connections Used to Frame Beam Depths of 14 in. with a 2¼ in. Gage in the Flange Angles

00452

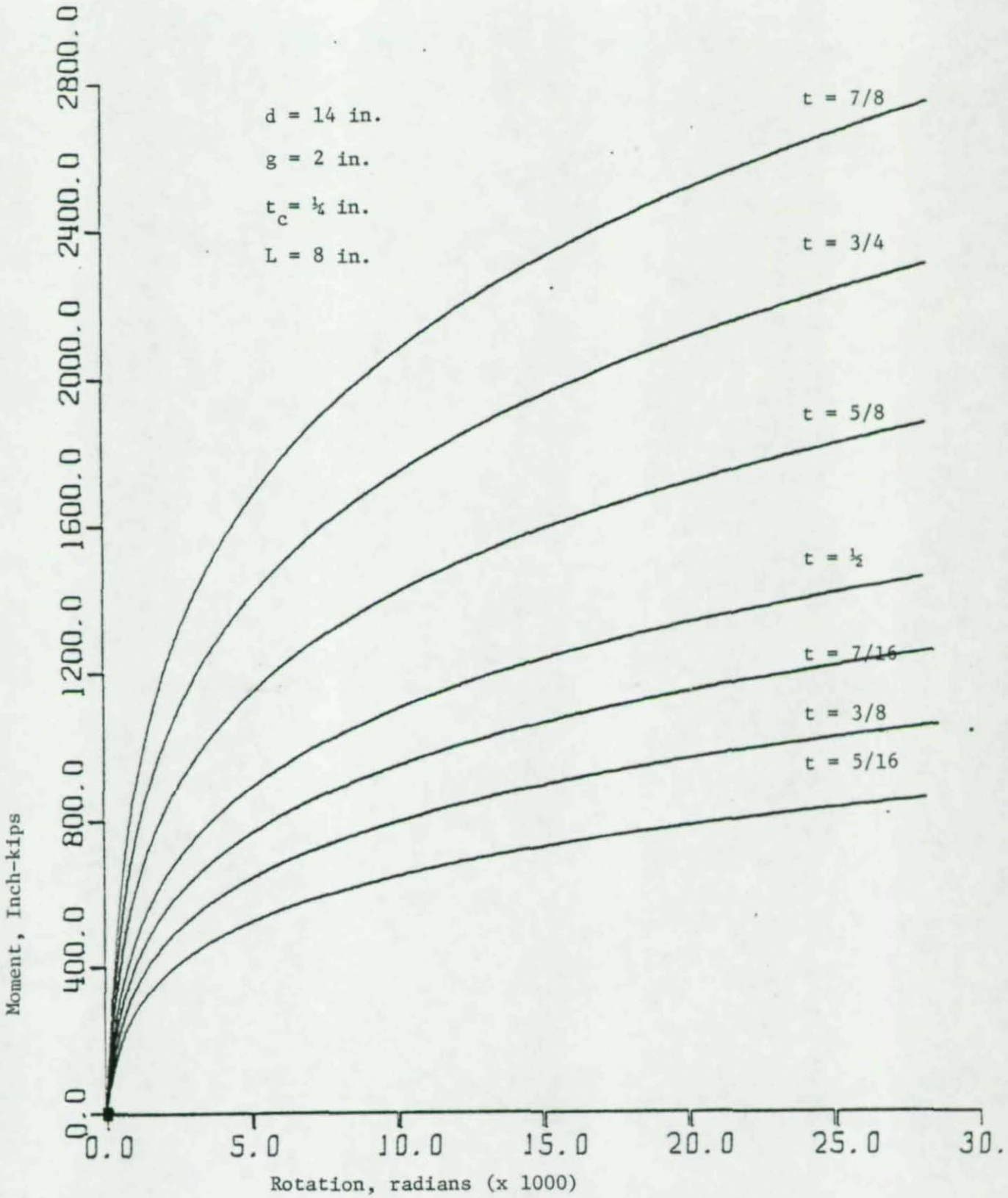

Fig. A12 M-Ø Curves for Connections Used to Frame Beam Depths of 14 in. with a 2 in. Gage in the Flange Angles

00453

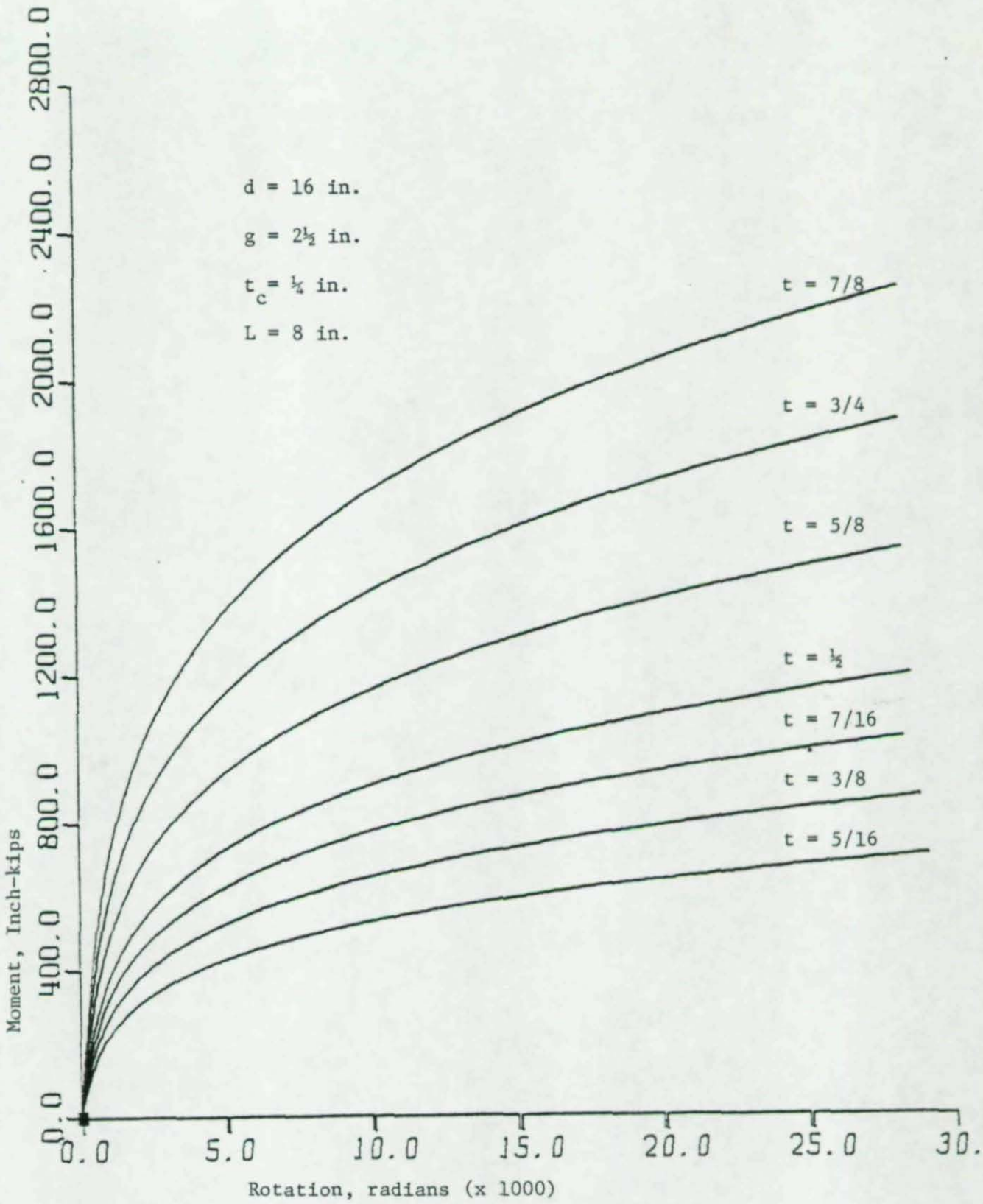

Fig. A13 M-Ø Curves for Connections Used to Frame Beam Depths of 16 in. with a 2½ in. Gage in the Flange Angles

80454

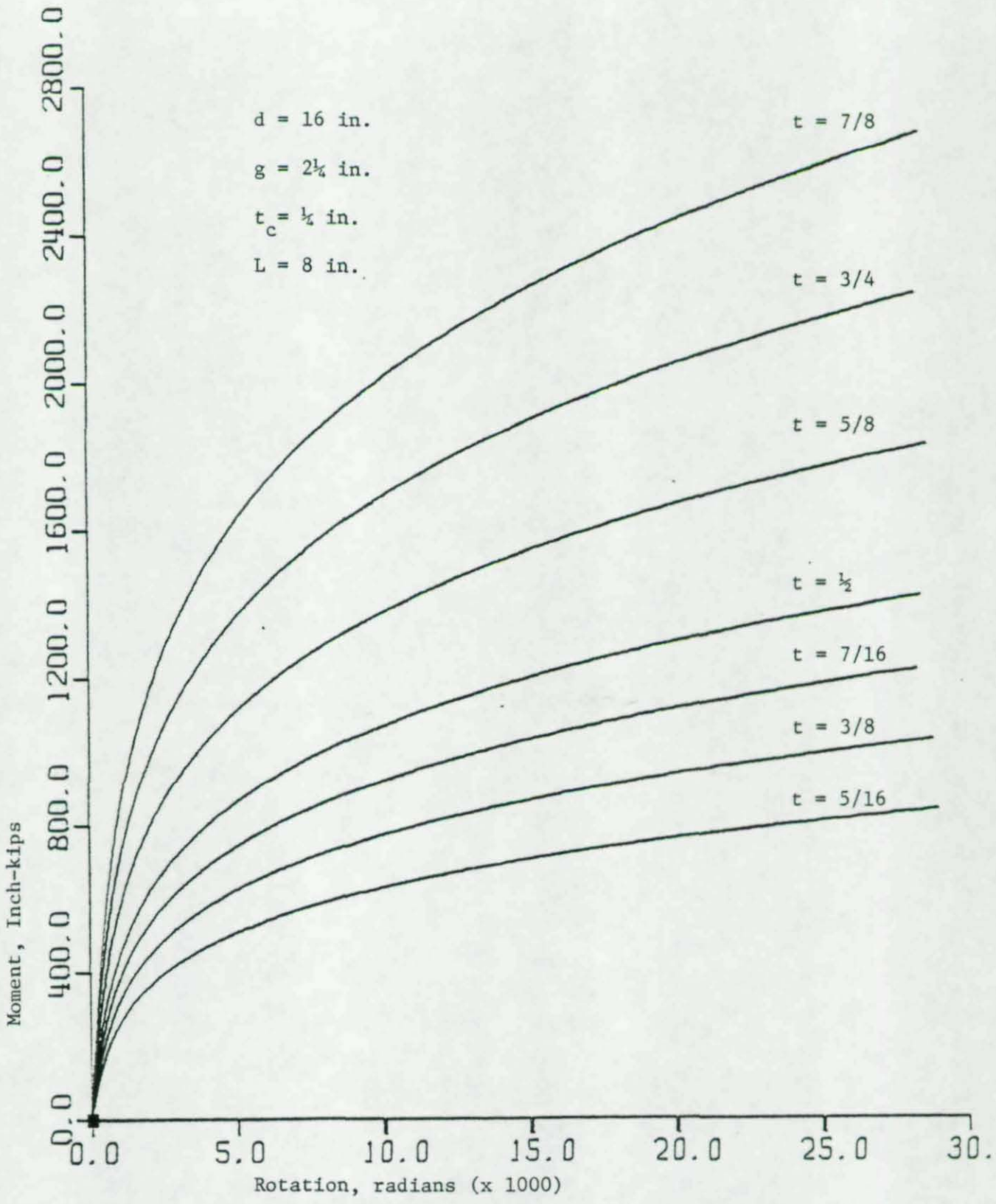

Fig. A14 M-Ø Curves for Connections Used to Frame Beam Depths of 16 in. with a 2¼ in. Gage in the Flange Angles

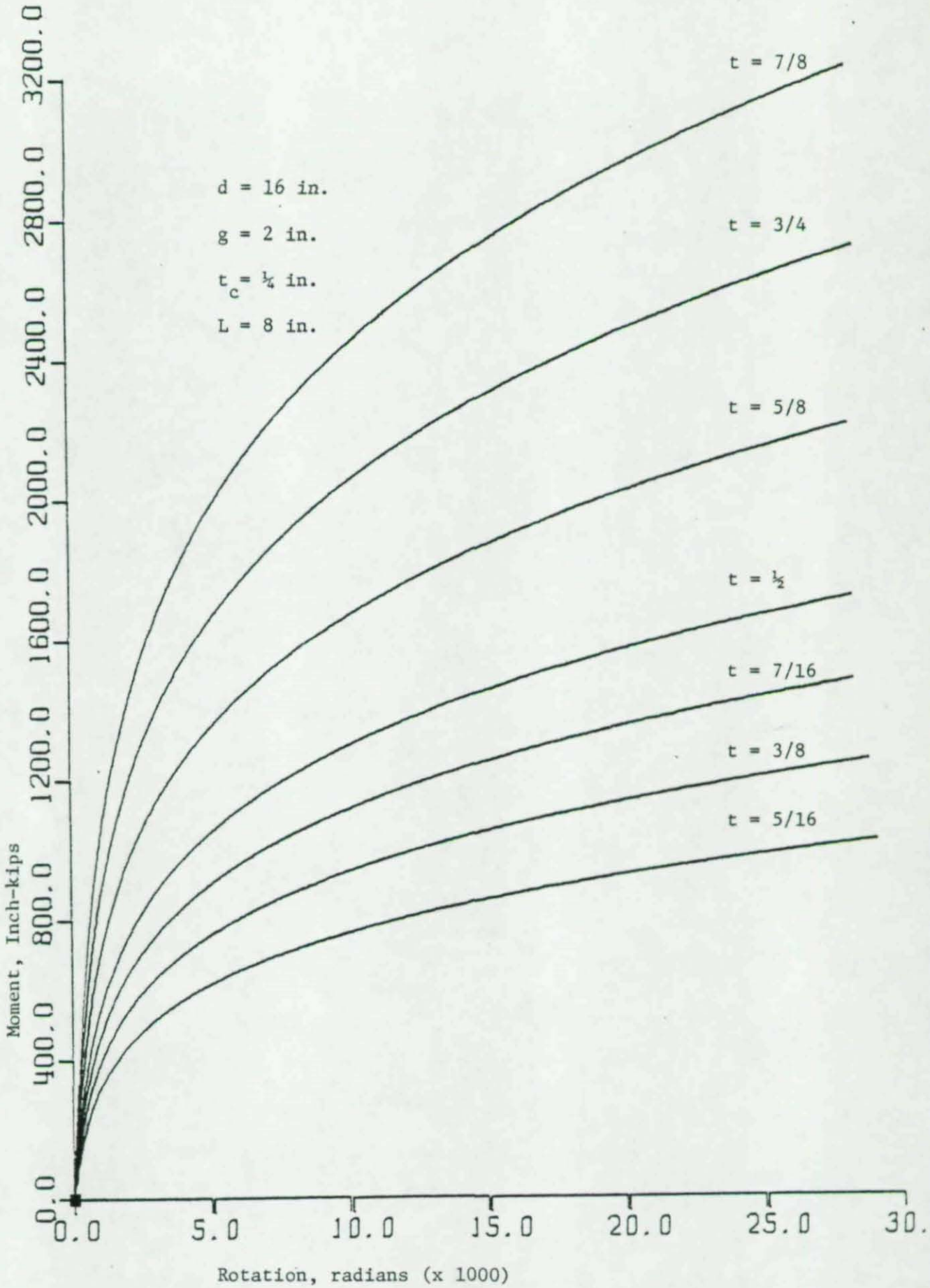

Fig. A15 M-Ø Curves for Connections Used to Frame Beam Depths of 16 in. with a 2 in. Gage in the Flange Angles

00456

Appendix B

Computer Program for RIS

00457

Nomenclature for Variables, Used in RIS Program

BP = overall length of leg of flange angle adjacent to the column face

BPC = overall leg length of web angle adjacent to the column face

D = depth of beam

DB = diameter of bolt

DW = diameter of washer

G = gage in flange angle (from heel of angle to center of bolt hole in the leg adjacent to column face)

GC = gage in web angle (from heel of angle to center of bolt hole in leg adjacent to column face)

L = overall length of flange angle

LC = overall length of web angles

PC = pitch (spacing of bolts in each leg of web angle)

S = number of interior flexible sections in the web angle
(s = 2 when 3 bolts are used)
(s = 1 when 2 bolts are used)

T = thickness of flange angle

TC = thickness of web angle

00458

COMPUTER PROGRAM TO CALCULATE RIS

```
      DIMENSION T(7)
      REAL L,LC,LF
      READ(41,*)BP,BPC,D,DB,DW,G,GC,L,LC,PC,S,TC
      DO 2 I=1,7
      READ(43,*)T(I)
      E=29000.0
      GE=0.5
      B=G-DB/2.0-T(I)/2.0
      BB=BP-T(I)/2.0
      BBC=BPC-TC/2.0
      BC=GC-DB/2.0-TC/2.0
      DB=D+T(I)/2.0
      LF=L-2.0*DW
      IF(S.EQ.1.0)GO TO 10
      IF(S.EQ.2.0)GO TO 20
   10 DF1=D/2.0
      DF2=0.0
      DE1=DF1+LC/2.0-GE/2.0
      DE2=DF1-LC/2.0+GE/2.0
      DR1=DF1+LC/2.0-GE-DW/2.0
      DR2=DF1-LC/2.0+GE+DW/2.0
      DR3=0.0
      GO TO 30
   20 DR2=D/2.0
      DE1=DR2+LC/2.0-GE/2.0
      DE2=DR2-LC/2.0+GE/2.0
      DR1=DR2+LC/2.0-GE-DW/2.0
      DR3=DR2-LC/2.0+GE+DW/2.0
      DF1=DR2+PC/2.0
      DF2=DR2-PC/2.0
   30 Z=2.0/3.0
      ASR=Z*2.0*DW*T(I)
      ASF=Z*LF*T(I)
      ASCF=Z*(PC-DW)*TC
      ASCR=Z*DW*TC
      X=1.0/12.0
      BIR=X*2.0*DW*(T(I)**3.0)
      BIF=X*LF*(T(I)**3.0)
      BICE=X*GE*(TC**3.0)
      BICF=X*(PC-DW)*(TC**3.0)
      BICR=X*DW*(TC**3.0)
      W=(12.0*E)/11000.0
      PR=(W*BIR)/(ASR*BB**2.0)
      PF=(W*BIF)/(ASF*BB**2.0)
      PCF=(W*BICF)/(ASCF*BBC**2.0)
      PCR=(W*BICR)/(ASCR*BBC**2.0)
      TRM1=((6.0*E*BIR*DD)/(B*BB*(1.0+PR)))*(2*DD/B+1.0)
      TRM2=(4.0*E*BIF*DD/(BB**3.0*(1.0+PF)))*(1.0-((2.0-PF)/(4+PF)))*(DD
     C+BB)
      TRM3=(12.0*E/(BBC**3.0*(1.0+PCF)))*(1.0-((2.0-PCF)/(4+PCF)))
      TRM4=(DE1*DE1+DE2*DE2)*BICE+(DF1*DF1+DF2*DF2)*BICF
      TRM5=(24.0*E*BICR/(BC**3.0*(1.0+PCR)))*(DR1*DR1+DR2*DR2+DR3*DR3)
      SLP=TRM1+TRM2+TRM3*TRM4+TRM5
      WRITE(42,35)BP,BPC,D,DB,DW,G,GC,L,LC,PC,S,TC,T(I)
   35 FORMAT(///8F10.5,/,5F10.5)
      WRITE(42,40)SLP
   40 FORMAT(/F12.2)
    2 CONTINUE
      STOP
      END
```

00459

SAMPLE INPUT

```
1.0  4.00  12.00  0.750  1.50  2.50  2.59375  8.0  8.5  3.0  2.0  .25


.3125
.375
.4375
.50
.625
.75
.875
```

SAMPLE OUTPUT

```
1.00000   4.00000  12.00000   0.75000   1.50000   2.50000   2.59375   8.00000
8.50000   3.00000   2.00000   0.25000   0.31250

 72619.38


1.00000   4.00000  12.00000   0.75000   1.50000   2.50000   2.59375   8.00000
8.50000   3.00000   2.00000   0.25000   0.37500

113067.34


4.00000   4.00000  12.00000   0.75000   1.50000   2.50000   2.59375   8.00000
8.50000   3.00000   2.00000   0.25000   0.43750

169237.11


4.00000   4.00000  12.00000   0.75000   1.50000   2.50000   2.59375   8.00000
8.50000   3.00000   2.00000   0.25000   0.50000

242881.27


4.00000   4.00000  12.00000   0.75000   1.50000   2.50000   2.59375   8.00000
8.50000   3.00000   2.00000   0.25000   0.62500

447015.75


4.00000   4.00000  12.00000   0.75000   1.50000   2.50000   2.59375   8.00000
8.50000   3.00000   2.00000   0.25000   0.75000

729760.50


4.00000   4.00000  12.00000   0.75000   1.50000   2.50000   2.59375   8.00000
8.50000   3.00000   2.00000   0.25000   0.87500

1090222.63
```

09469

Appendix C

Frame Design

Gravity Loading - AISC Checks

00461

SEMI-RIGID FRAME - SERVICE GRAVITY LOAD

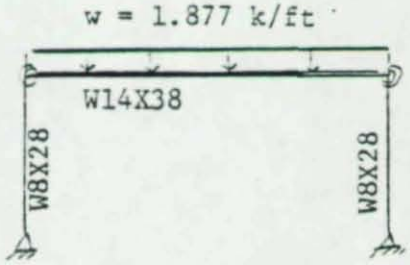

Beam Moment Diagram

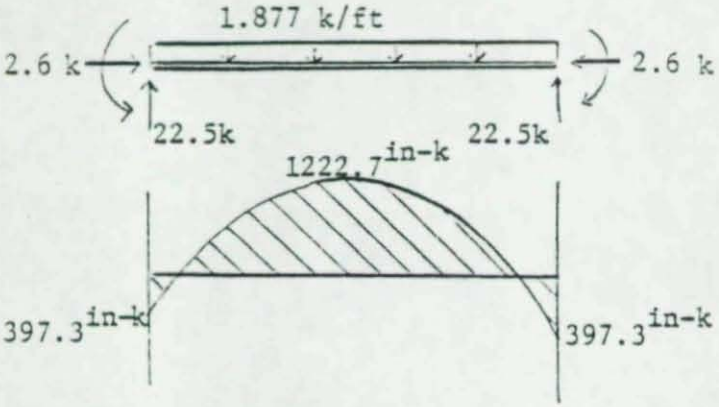

W14X38 Properties

$A = 11.2\ in^2$

$Ix = 385\ in^4$

$Sx = 54.6\ in^3$

$rx = 5.87\ in$

$zx = 61.5\ in^3$

AISC Check - Section 1.6

$$fa = \frac{P}{A} = \frac{2.6^{k}}{11.2 in^2} = .232\ ksi \qquad \frac{Kx\ell}{rx} = \frac{1.0(24X12)}{5.87} = 49.06$$

$Fa = 18.43\ ksi$ $\qquad \frac{fa}{Fa} = \frac{.232}{18.43} = .0126 < .15$

$Fbx = 24\ ksi$ $\qquad fbx = \frac{M}{S} = \frac{1222.7^{in-k}}{54.6^{in^3}} = 22.39\ ksi$

eqn. [1.6-2] $\frac{.232}{18.43} + \frac{22.39}{24.0} = .0126 + .933 \approx .945$

Deflection at midspan = .885 inches

SEMI-RIGID FRAME - SERVICE GRAVITY LOAD

Column Moment Diagram

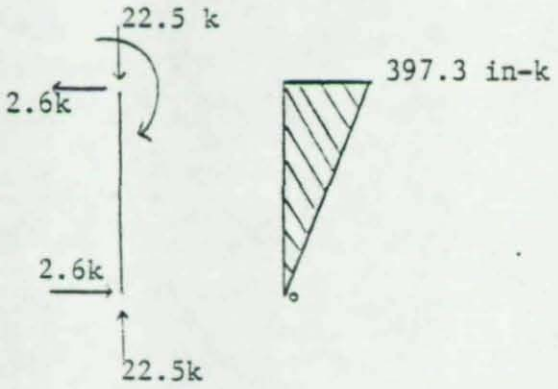

W8X28 Properties

$A = 8.25\ in^2$

$Ix = 98.0\ in^4$

$Sx = 24.3\ in^3$

$rx = 3.45\ in$

$Zx = 6.63\ in^3$

AISC Check

$$fa = \frac{P}{A} = \frac{22.50^{k}}{8.25in^2} = 2.73\ ksi$$

$$G_{Bot} = 10 \qquad G_{Top} = \frac{\Sigma(I/L)C}{Ce\ \Sigma(I/L)g} = \frac{98/12}{.532(385/24)} = .96$$

Ce is a modification factor which takes into account the stiffness of the semi-rigid connections.

Kx = 1.88 (from alignment chart - sway permitted) Fa = 15.53 ksi
F'ex = 24.25 ksi

$$\text{Since } \frac{Kx\ell}{rx} = \frac{1.88(144)}{3.45} = 78.47 \leq C_c\ Kx \text{ inelastic will be used}$$

$$G_{T_{inelastic}} = \left(\frac{Fa}{F'ex}\right)G_T = \frac{15.53}{24.25}(.96) = .615 \qquad Kx_{inel} = 1.82$$

$$\frac{Kx_{inel}\ell}{rx} = \frac{1.82(144)}{3.45} = 75.97 \qquad Fa = 15.79\ ksi \quad F'ex = 25.87\ ksi$$

Cm = .85 (as specified by AISC)

$$fbx = \frac{M}{Sx} = \frac{397.3^{in-k}}{24.3in^3} = 16.35\ ksi$$

$$\text{eqn [1.6-1a]}\ \frac{2.73}{15.74} + \frac{.85(16.35)}{\left(1 - \frac{2.73}{25.87}\right)24} = .173 + .648 = \underline{.821}$$

$$\text{eqn [1.6-1b]}\ \frac{2.73}{22} + \frac{16.35}{24.0} = .124 + .681 = \underline{.805}$$

RIGID FRAME - SERVICE GRAVITY LOAD

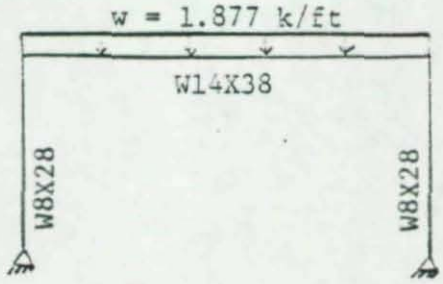

Beam Moment Diagram

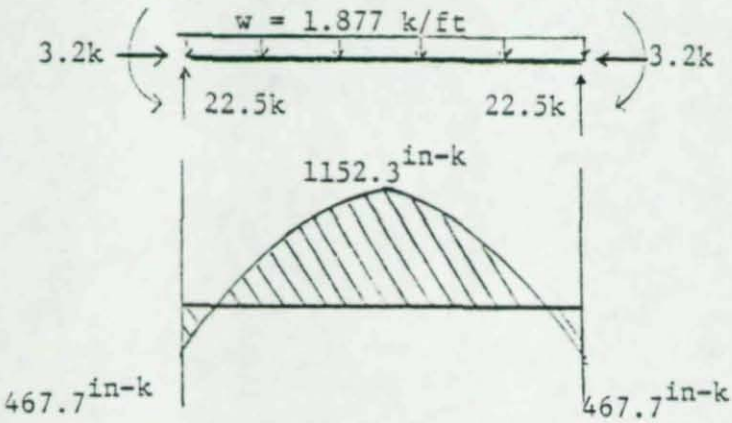

W14X38 Properties

$A = 11.2\ in^2$

$Ix = 385\ in^4$

$Sx = 54.6\ in^3$

$rx = 5.87\ in$

$Zx = 61.5\ in^3$

AISC Check - Section 1.6

$$fa = \frac{P}{A} = \frac{3.2^{k}}{11.2 in^2} = .286\ ksi \qquad \frac{Kx\ell}{rx} = \frac{1.0(24x12)}{5.87} = 49.06$$

$$Fa = 18.43\ ksi$$

$\frac{fa}{Fa} = .0155 < .15$ use eqn 1.6-2

$$fbx = \frac{M_{max}}{Sx} = \frac{1152.3^{in-k}}{54.6 in^3} = 21.1\ ksi$$

$Fbs = 24\ ksi$

eqn [1.6-2] $\frac{.286}{18.43} + \frac{21.1}{24} = .0155 + .879 = \underline{.895} < 1.0$

Deflection at beam midspan = .834 inches

RIGID FRAME - SERVICE GRAVITY LOAD

Column Moment Diagram

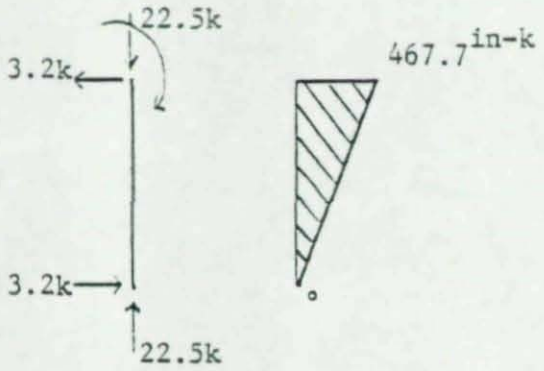

W8X28 Properties

$A = 8.25\ in^2$

$Ix = 98.0\ in^4$

$Sx = 24.3\ in^3$

$rx = 3.45\ in$

$Zx = 6.63\ in^3$

AISC Check - Section 1.6

$$fa = \frac{P}{A} = \frac{22.5^{k}}{8.25 in^2} = 2.73\ ksi$$

$$G_{Bot} = 10 \quad G_{Top} = \frac{\Sigma(I/L)c}{\Sigma(I/L)g} = \frac{98/12}{385/24} = .51$$

Kx = 1.80 (from AISC alignment chart - sway permitted)

$$\frac{Kx\ell}{rx} = \frac{1.80(144)}{3.45} = 75.13 < C_c = 126.1$$ use inelastic Kx

(Fa = 15.89 ksi F'ex = 26.46 ksi)

$$G_{Top(inelastic)} = \frac{Fa}{Flex} \cdot G_{Top} = \frac{15.89}{26.46}(.51) = .306$$

$$Kx_{inelastic} = 1.75$$

$$\frac{Kx_{inel}\ell}{rx} = \frac{1.75\ (144)}{3.45} = 73.04$$

Fa = 16.12 ksi
F'ex = 27.49 ksi

Cm = .85 (as specified by AISC)

$$fbx = \frac{M}{Sx} = \frac{467.7^{in-k}}{24.3 in^3} = 19.25\ ksi$$ Fbx = 24 ksi

eqn [1.6-1a] $\frac{2.73}{16.12} + \frac{.85(19.25)}{(1-2.73/27.44)24} = .169 + .755 = \underline{.924}$

eqn [1.6-1b] $\frac{2.73}{22} + \frac{19.25}{24} = .124 + .802 = \underline{.926}$

00465

SEMI-RIGID FRAME - 1.7 SERVICE GRAVITY LOAD

Column Moment Diagram

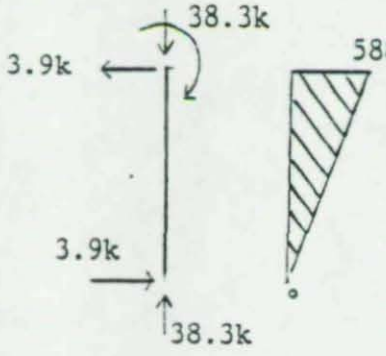

Beam Moment Diagram

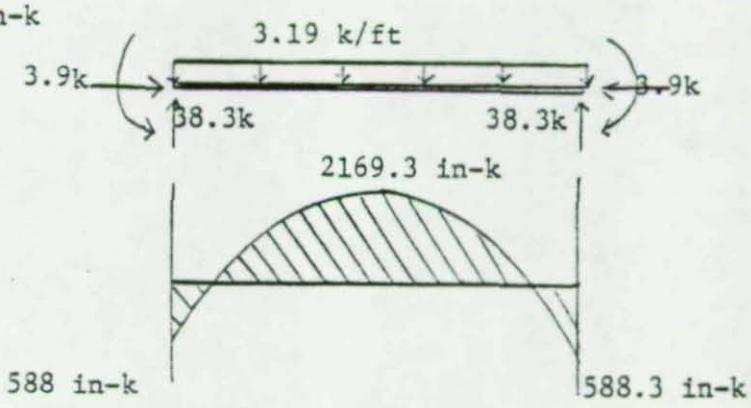

AISC - Check Part 2

Column: $Py = A \cdot F_y = 297^k$

$P_{CR} = 1.7\ AFa = 1.7(8.25\ in^2)(15.79\ ksi) = 221.45^k$

$P_{EX} = 23/12\ A \cdot F'e = 409.14^k$

$M_P{}^c = 979.2\ ^{in\text{-}k}$

Eqn [2.4-2] $\frac{38.3}{221.45} + \frac{.85(588.3)}{(1-38.3/409.16)979.2} = .173 + .563 = \underline{.736}$

Eqn [2.4-3] $\frac{38.3}{297} + \frac{588.3}{1.18(979.2)} = .129 + .509 = \underline{.638}$

Beam: $Py = A \cdot F_y = 403.2^k$

$P_{CR} = 1.7AFa = 1.7(8.25in^2)(18.43ksi) = 350.9^k$

$P_{EX} = 28/12\ F'e = 1331.9^k$

$M_P{}^b = 2214\ ^{in\text{-}k}$

Eqn [2.4-2] $\frac{3.9}{350.9} + \frac{1.0(2169.3)}{(1-3.9/1331.9)2214} = .011 + .983 = .994$

Eqn [2.4-3] $\frac{3.9}{403.2} + \frac{2169.3}{1.18(2214)} = .01 + .830 = .840$

Delection at Beam Midspan = 1.59 in

Rigid Frame - 1.7 X Design Gravity Load

Column Moment Diagram

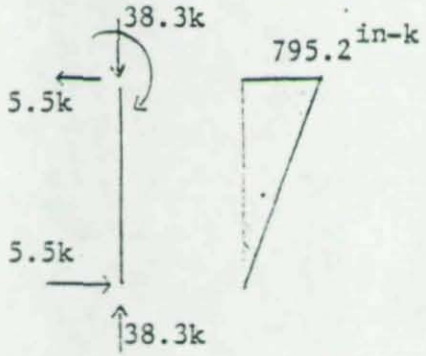

Beam Moment Diagram

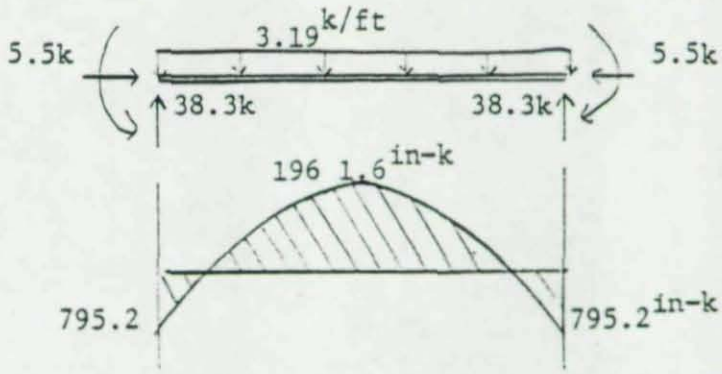

AISC Check Part Two

Column: $P_y = A \cdot Fy = 297k$

$P_{CR} = 1.7\ A \cdot Fa = 1.7(8.25)(16.12) = 226k$

$P_{EX} = 23/12\ A \cdot Fe' = 442.62k$

$M_p^c = 979.2^{in\text{-}k}$

eqn[2.4-2] $\frac{38.29}{226} + \frac{.85\ (795.2)}{(1-383/442.6)\ 979.2} = .169 + .756 = \underline{.925}$

eqn[2.4-3] $\frac{38.3}{297} + \frac{795.2}{1.18(979.2)} = .129 + .688 = \underline{.817}$

Beam: $P_y = A.Fy = 403.2k$

$P_{CR} = 1.7\ A \cdot Fa = 1.7(11.2)(18.43) = 350.9k$

$M_p = 2214^{in\text{-}k}$

eqn[2.4-2] $\frac{5.5}{350.9} + \frac{1.0(1961.6)}{(1-5.5/1331.9)\,2214} = .016 + .890 = \underline{.906}$

eqn[2.4-3] $\frac{5.5}{403.2} + \frac{1961.6}{1.18(2214)} = .014 + .751 = \underline{.765}$

Deflection at Beam Midspan = 1.418 in.

004467

Appendix D

Frame Design

Gravity Loading - Behavioral Checks

00468

SEMI-RIGID FRAME - GRAVITY LOAD - FIRST DISTRESS

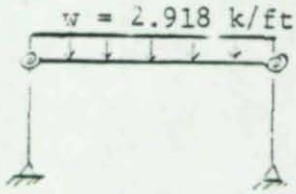

Column Moment Diagram

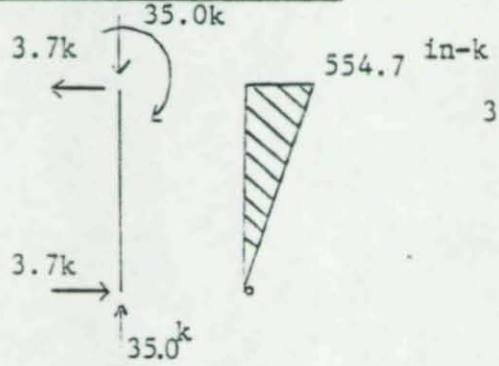

Beam Moment Diagram

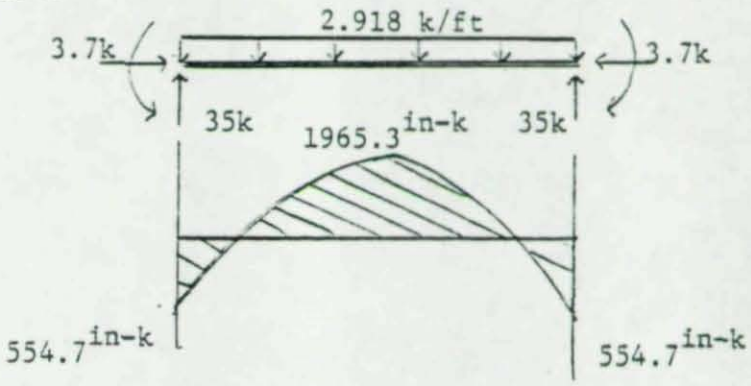

First Distress Response

Column: (1) $\frac{P}{P_{cr_x}} + \left(\frac{Cm}{1-P/P_{EX}}\right) \cdot \frac{M}{M_y} \leq 1.0$

$$\frac{35.0}{243.10} + \left(\frac{.6}{1-35/409.14}\right) \frac{554.7}{874.8} = .144 + .416 = \underline{.560}$$

(2) $\frac{P}{Py} + \frac{M}{M_y} \leq 1.0$

$$\frac{35}{297} + \frac{554.7}{874.8} = .118 + .634 = \underline{.752}$$

Beam: (3) $\frac{M}{M_y} \leq 1.0$

$$\frac{1965}{1965} = 1.0$$

(First Distress Occurs at Beam Midspan)

Deflection at Beam Midspan = 1.43 inches

00469

RIGID FRAME - GRAVITY LOAD - FIRST DISTRESS

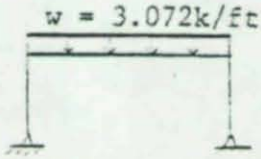

Column Moment Diagram

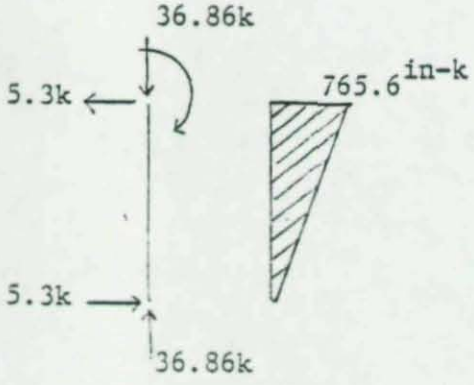

Beam Moment Diagram

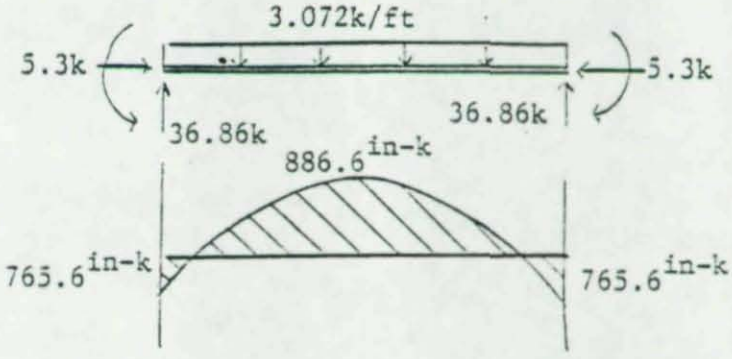

First Distress Response

Column: (1) $\frac{P}{P_{crx}} + \left(\frac{Cm}{1-P/P_{EX}}\right) \cdot \frac{M}{My} \leq 1.0$

$$\frac{36.86}{247.18} + \left(\frac{.6}{1-36.86/442.62}\right) \cdot \frac{765.61}{874.61} =$$

$$.149 + .573 = \underline{.722}$$

(2) $\frac{P}{Py} + \frac{M}{My} \leq 1.0$

$$\frac{36.86}{297} + \frac{765.61}{874.8} = .124 + .874 = \underline{1.0}$$

(first distress occurs at top of column)

Beam: (3) $\frac{M}{My} \leq 1.0$

$$\frac{886.6}{1965} = .96 \leq 1.0$$

Deflection at midspan of beam = 1.365 in.

SEMI-RIGID FRAME - GRAVITY LOAD - LIMIT STATE

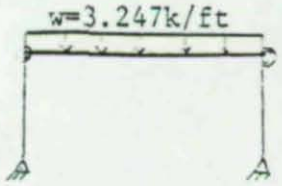

Column Moment Diagram

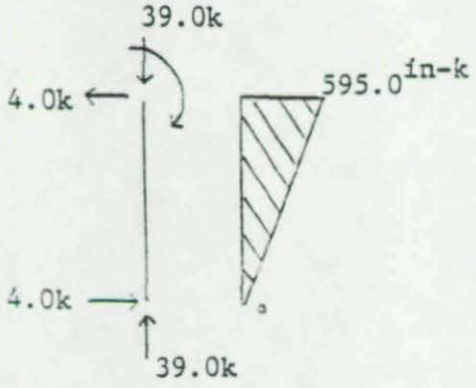

Beam Moment Diagram

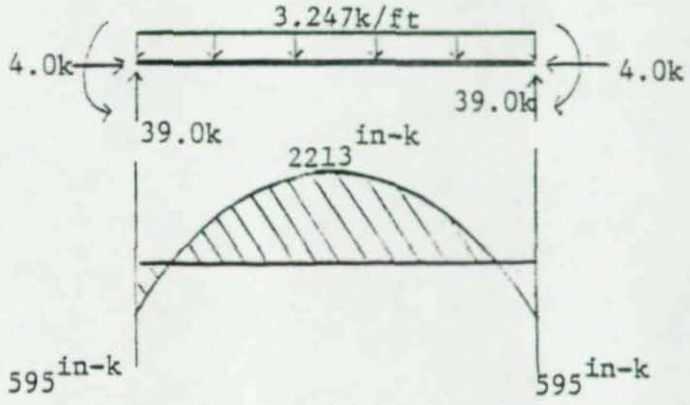

Limit State Response

Column: (4) $\frac{P}{P_{crx}} + (\frac{Cm}{1-P/P_{EX}})\frac{M}{Mp} \leq 1.0$

$$\frac{39.0}{243.10} + (\frac{.6}{1-39.0/409.14})\frac{595.0}{479.2} = .160 + .402 = \underline{.562}$$

(5) $\frac{P}{Py} + \frac{M}{1.18Mp} \leq 1.0;\ M \leq Mp$

$$\frac{39.0}{297} + \frac{595}{1.18(979.2)} = .131 + .515 + \underline{.642}$$

Beam: (6) $\frac{M}{Mp} \leq 1.0$

$$\frac{2213}{2214} = .9995 \sim 1.0$$

(Plastic hinge formation at beam midspan).

Midspan Beam Deflection = 1.62 inches

09471

RIGID FRAME - GRAVITY LOAD - FIRST PLASTIC HINGE

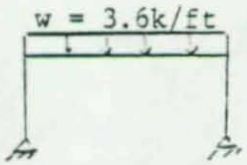

Column Moment Diagram

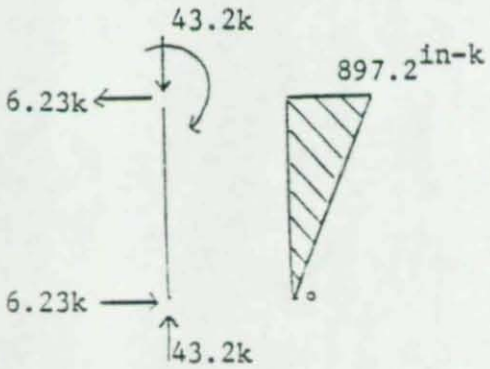

Beam Moment Diagram

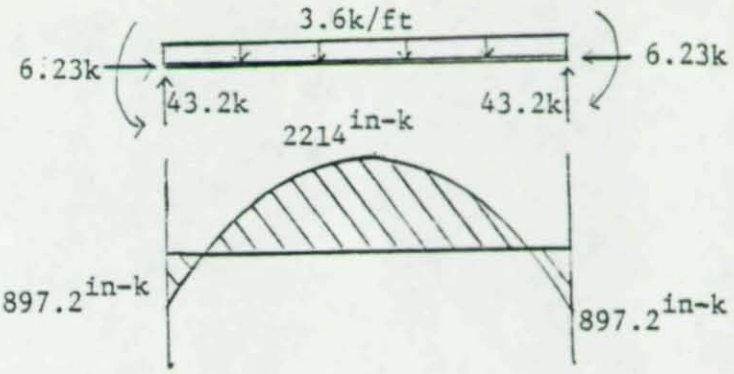

Limit State Response

Column: (4) $\frac{P}{P_{crx}} + \left(\frac{Cm}{1-P/P_{EX}}\right)\frac{M}{Mp} \leq 1.0$

$$\frac{43.2}{247.18} + \left(\frac{.6}{1-43.2/442.6}\right)\frac{897.2}{979.2} = .175 + .609 = \underline{.784}$$

(5) $\frac{P}{Py} + \frac{M}{1.18M_p} \leq 1.0; \quad M \leq Mp$

$$\frac{43.2}{297} + \frac{897.2}{1.18(979.2)} = .146 + .777 = \underline{.923}$$

Beam: (6) $\frac{M}{Mp} \leq 1.0$

$$\frac{2214}{2214} = 1.0 \text{ (Plastic hinge formation at beam midspan)}$$

Deflection at beam midspan = 1.60 inches

00472

RIGID FRAME - GRAVITY LOAD - COLLAPSE OF FRAME

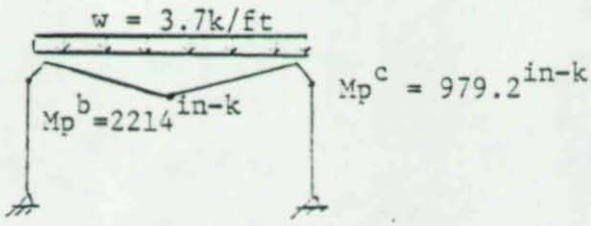

Column Moment Diagram

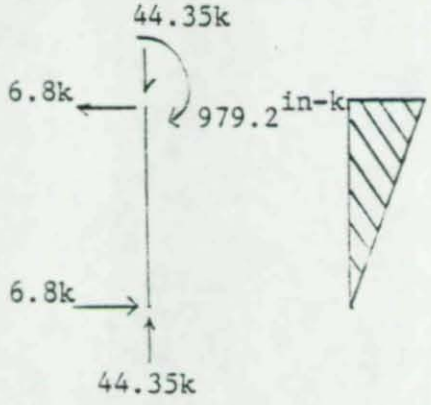

Beam Moment Diagram

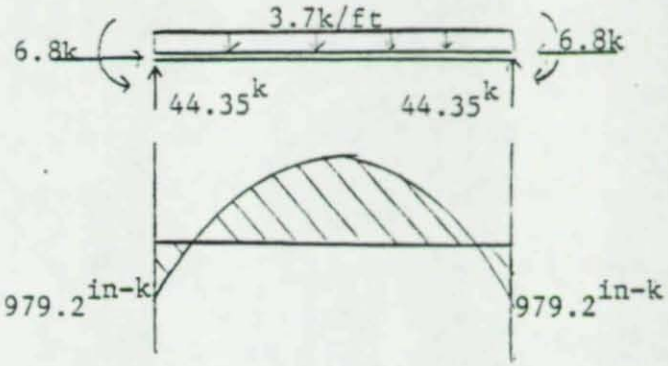

Limit State Response of Column at Collapse

$$(4)\quad \frac{P}{P_{crx}} + \left(\frac{Cm}{1-P/P_{EX}}\right)\cdot\frac{M}{Mp} \leq 1.0$$

$$\frac{44.35}{247.18} + \left(\frac{.6}{1-44.35/442.62}\right)\frac{979.2}{979.2} = .179 + .667 = \underline{.845}$$

$$(5)\quad \frac{P}{Py} + \frac{M}{1.18Mp} \leq 1.0; \qquad M \leq Mp$$

$$\frac{44.35}{297} + \frac{979.9}{1.18(979.9)} = .149 + .847 = \underline{.996}$$

(Additional plastic hinges have formed at the tops of columns - the frame collapses)

and $M = 979.2^{\text{in-k}} = Mp$

00473

Appendix E

Gravity Plus Wind Loading - AISC Checks

SEMI-RIGID FRAME - .75 (Gravity Plus Wind Loads)

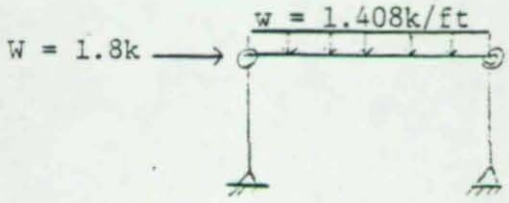

Column Moment Diagram

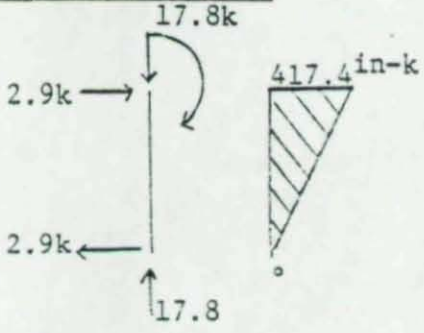

Beam Moment Diagram

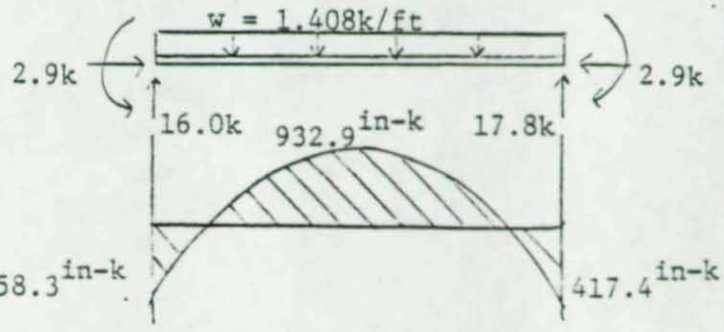

AISC Check - Section 1.6

Column: (leeward) $f_a = \frac{P}{A} = \frac{17.8k}{8.25in^2} = 2.158ksi$ $K_x = 1.82$ $\frac{K_x \ell}{r_x} = 75.97$

$F_a = 15.79$ ksi $F'_{ex} = 25.87$ ksi

$\frac{f_a}{F_a} = \frac{2.158}{15.79} = .137 < .15$ Use Eqn. [1.6-2]

$f_{bx} = \frac{M}{S_x} = \frac{417.4^{in-k}}{24.3in^3} = 17.18$ ksi $F_{bx} = 24.0$ ksi

Eqn. [1.6-2] $\frac{2.158}{15.79} + \frac{17.18}{24.0} = .137 + .716 = \underline{.853}$

Beam: $f_a = \frac{2.9k}{11.2in^2} = .259$ ksi $K_x = 1.0$(beams) $\frac{K_x \ell}{r_x} = 49.06$ $F_a = 18.43$ksi

$\frac{f_a}{F_a} = \frac{.259}{18.43} = .014 < .15$ Use Eqn. [1.6-2]

$f_{bx} = \frac{932.9}{54.6} = 17.09$ ksi $F_{bx} = 24.0$ ksi

Eqn. [1.6-2] $\frac{.259}{18.43} + \frac{17.09}{24.0} = .014 + .712 = \underline{.726}$

Deflection at Beam Midspan = 0.677 inches.

Maximum Drift = .548 inches.

80475

RIGID FRAME - .75 (Gravity plus Wind Load)

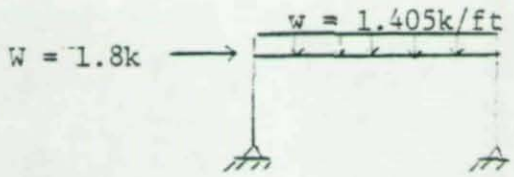

Column Moment Diagram

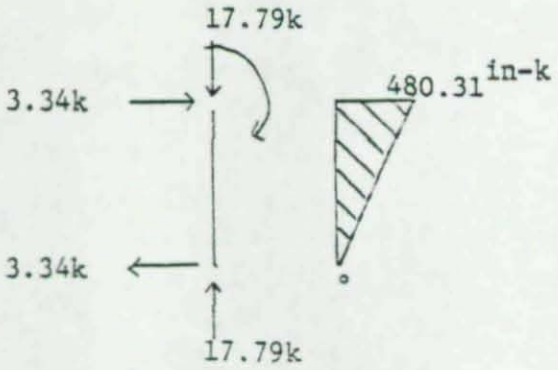

Beam Moment Diagram

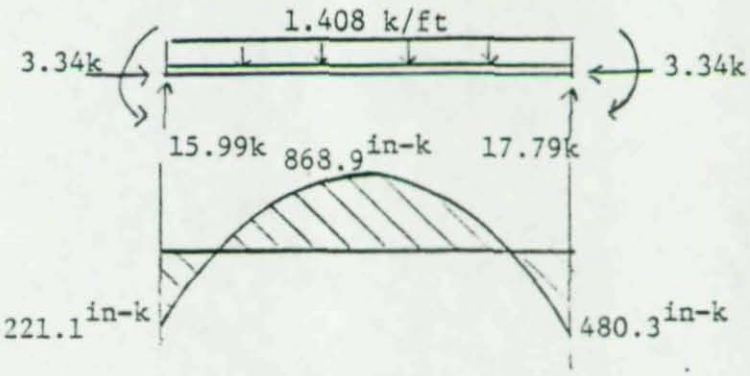

AISC Check - Section 1.6

Column: (leeward) $f_a = \frac{17.79}{8.25} = 2.156$ ksi $K_x = 1.75$ $\frac{K_x \ell}{r_x} = 73.04$ $F_a = 16.12$ ksi $F'_e = 27.99$ ksi

$\frac{f_a}{F_a} = \frac{2.156}{16.12} = .134 < .15$ Use Eqn. [1.6-2]

$f_{bx} = \frac{M}{S} = \frac{480.3}{24.3} = 19.77$ ksi $F_{bx} = 24.0$ ksi

Eqn. [1.6-2] $\frac{2.156}{16.12} + \frac{19.77}{24.0} = .134 + .824 = .958$

Beam: $f_a = \frac{3.34k}{11.2} = .298$ ksi $K_x = 1.0$ $\frac{K_x \ell}{r_x} = 49.06$ $F_a = 18.43$ ksi

$\frac{f_a}{F_a} = \frac{.298}{18.43} = .016 \leq .15$ Use Eqn. [1.6-2]

$f_{bx} = \frac{M}{S} = \frac{868.9}{54.6} = 15.91$ ksi $F_{bx} = 24.0$ ksi

Eqn. [1.6-2] $\frac{.298}{18.43} + \frac{15.91}{24.0} = .016 + .663 = .679$

Deflection at Beam Midspan = 0.616 inches.

Maximum Drift = .397 inches.

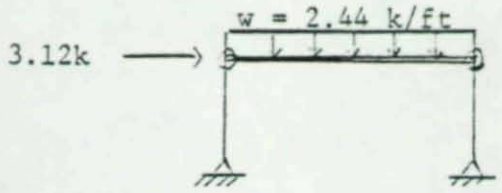

Column Moment Diagram

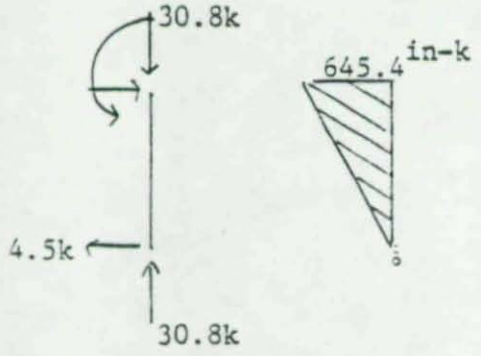

Beam Moment Diagram

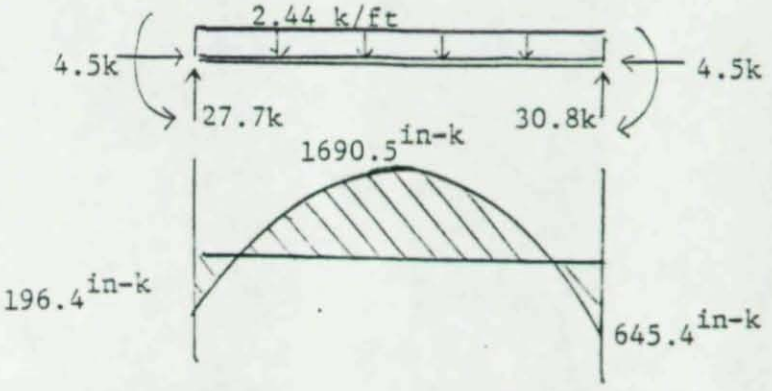

AISC Check - Part 2

Column: (leeward)

Eqn. [2.4-2] $\frac{30.8k}{221.45k} + \frac{.85(645.4^{in-k})}{(1-30.8k/409.14k)979.2^{in-k}} = .139 + .606 = \underline{.744}$

Eqn. [2.4-3] $\frac{30.8k}{297k} + \frac{645.4^{in-k}}{1.18(979.2^{in-k})} = .104 + .559 = \underline{.663}$

Beam:

Eqn. [2.4-2] $\frac{4.5k}{350.9k} + \frac{.85(1690.5^{in-k})}{(1-4.5k/1332k)2214^{in-k}} = .013 + .649 = \underline{.662}$

Eqn. [2.4-3] $\frac{4.5k}{403.2k} + \frac{1690.5^{in-k}}{1.18(2214^{in-k})} = .011 + .647 = .658$

Deflection at Beam Midspan = 1.243 inches.

Maximum Drift = 1.305 inches.

RIGID FRAME = 1.3 (Gravity Plus Wind Loads) - AISC Part 2

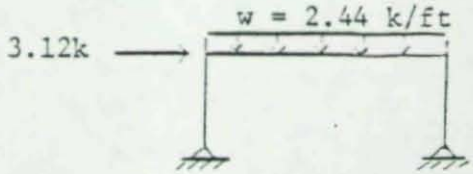

Column Moment Diagram

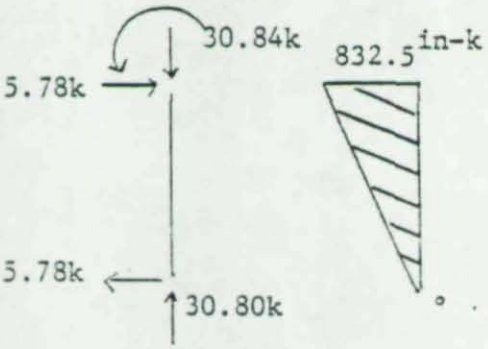

Beam Moment Diagram

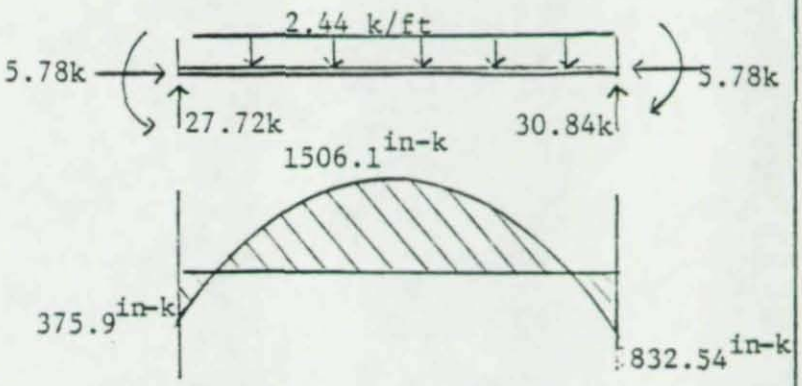

AISC Check-Part 2

Column (leeward) Eqn. [2.4-2] $\frac{30.84k}{226k} + \frac{.85(832.5^{in-k})}{(1-30.84k/442.6k)979.2^{in-k}} = .137 + .777 = \underline{.913}$

Eqn. [2.4-3] $\frac{30.84k}{297k} + \frac{832.54}{1.18(979.2)} = .104 + .721 = \underline{.825}$

Beam: Eqn. [2.4-2] $\frac{.578k}{350.9k} + \frac{.85(1506.09)}{(1-5.78/1332)2214^{in-k}} = .0165 + .581 = \underline{.597}$

Eqn. [2.4-3] $\frac{5.78k}{403.2} + \frac{1506.1^{in-k}}{1.18(2214)^{in-k}} = .014 + .576 = \underline{.590}$

Deflection at Beam Midspan = 1.073 inches.

Maximum Drift = .689 inches.

00478

Table 2.1

Connection Properties			Revised Initial Slope (RIS) (in.-k/rad)
	Flange Angle Gage (in.)	Flange Angle Thickness (in.)	
Beam Depth = 8 in. Web Angle Thickness = ¼ in. Length of Flange Angle = 6 in.	2½	5/16	29800
		3/8	48300
		7/16	74000
		1/2	107700
		5/8	201300
		3/4	331000
		7/8	496200
	2¼	5/16	40200
		3/8	66200
		7/16	101800
		1/2	148000
		5/8	273100
		3/4	441600
		7/8	650800
	2	5/16	57800
		3/8	95800
		7/16	147300
		1/2	212600
		5/8	384600
		3/4	608100
		7/8	878600
Beam Depth = 10 in. Web Angle Thickness = ¼ in. Length of Flange Angle = 6 in.	2½	5/16	45000
		3/8	73000
		7/16	111700
		1/2	162500
		5/8	303200
		3/4	497500
		7/8	744200
	2¼	5/16	61000
		3/8	100300
		7/16	154200
		1/2	224000
		5/8	412600
		3/4	665600
		7/8	978800
	2	5/16	87900
		3/8	145700
		7/16	223800
		1/2	322800
		5/8	582700
		3/4	919300
		7/8	1325400
Beam Depth = 12 in. Web Angle Thickness = ¼ in. Length of Flange Angle = 8 in.	2½	5/16	72600
		3/8	113100
		7/16	169200
		1/2	242900
		5/8	447000
		3/4	729800
		7/8	1090200
	2¼	5/16	95200
		3/8	151800
		7/16	229500
		1/2	329900
		5/8	601900
		3/4	967500
		7/8	1421500
	2	5/16	133400
		3/8	216400
		7/16	328300
		1/2	470200
		5/8	843000
		3/4	1326700
		7/8	1911700

69479

Table 2.1 (Cont.)

Connection Properties			Revised Initial Slope (RIS) (in.-k/rad)
	Flange Angle Gage (in.)	Flange Angle Thickness (in.)	
Beam Depth = 14 in. Web Angle Thickness = ¼ in. Length of Flange Angle = 8 in.	2½	5/16	98000
		3/8	152900
		7/16	229000
		1/2	328700
		5/8	604700
		3/4	986400
		7/8	1472100
	2¼	5/16	128900
		3/8	205800
		7/16	311200
		1/2	447400
		5/8	815800
		3/4	1310200
		7/8	1922900
	2	5/16	181200
		3/8	294000
		7/16	446200
		1/2	639000
		5/8	1144700
		3/4	1799700
		7/8	2590400
Beam Depth = 16 in. Web Angle Thickness = ¼ in. Length of Flange Angle = 8 in.	2½	5/16	124400
		3/8	194200
		7/16	290900
		1/2	417600
		5/8	768000
		3/4	1251900
		7/8	1867000
	2¼	5/16	163900
		3/8	261800
		7/16	396000
		1/2	569200
		5/8	1037400
		3/4	1664900
		7/8	2441700
	2	5/16	230700
		3/8	374600
		7/16	568500
		1/2	814000
		5/8	1457500
		3/4	2289800
		7/8	3293300

00480

Table 4.1

Values of Terms Used in Equations 1-6

Column (W8X28)	Rigid Frame	Semi-Rigid Frame
Area, A	8.25 in^2	8.25 in^2
Kx (inelastic)	73.04	75.97
$P_{crx} = Fy[1-\frac{1}{2}(K_x\ell/C_c)^2]A$	247.18 kips	243.10 kips
$P_{EX} = [\pi^2E/(K_x\ell/r_x)^2]A$	442.62 kips	409.14 kips
$P_y = F_y \cdot A$	297.0 kips	297.0 kips
$M_y{}^c = F_y \cdot S$	874.0 in-kips	874.0 in-kips
$M_p{}^c = F_y \cdot Z$	979.2 in-kips	979.2 in-kips
Beam (W14X38)		
Area	11.2 in^2	11.2 in^2
$M_y{}^b$	1965.6 in-kips	1965.6 in-kips
$M_p{}^b$	2214.0 in-kips	2214.0 in-kips

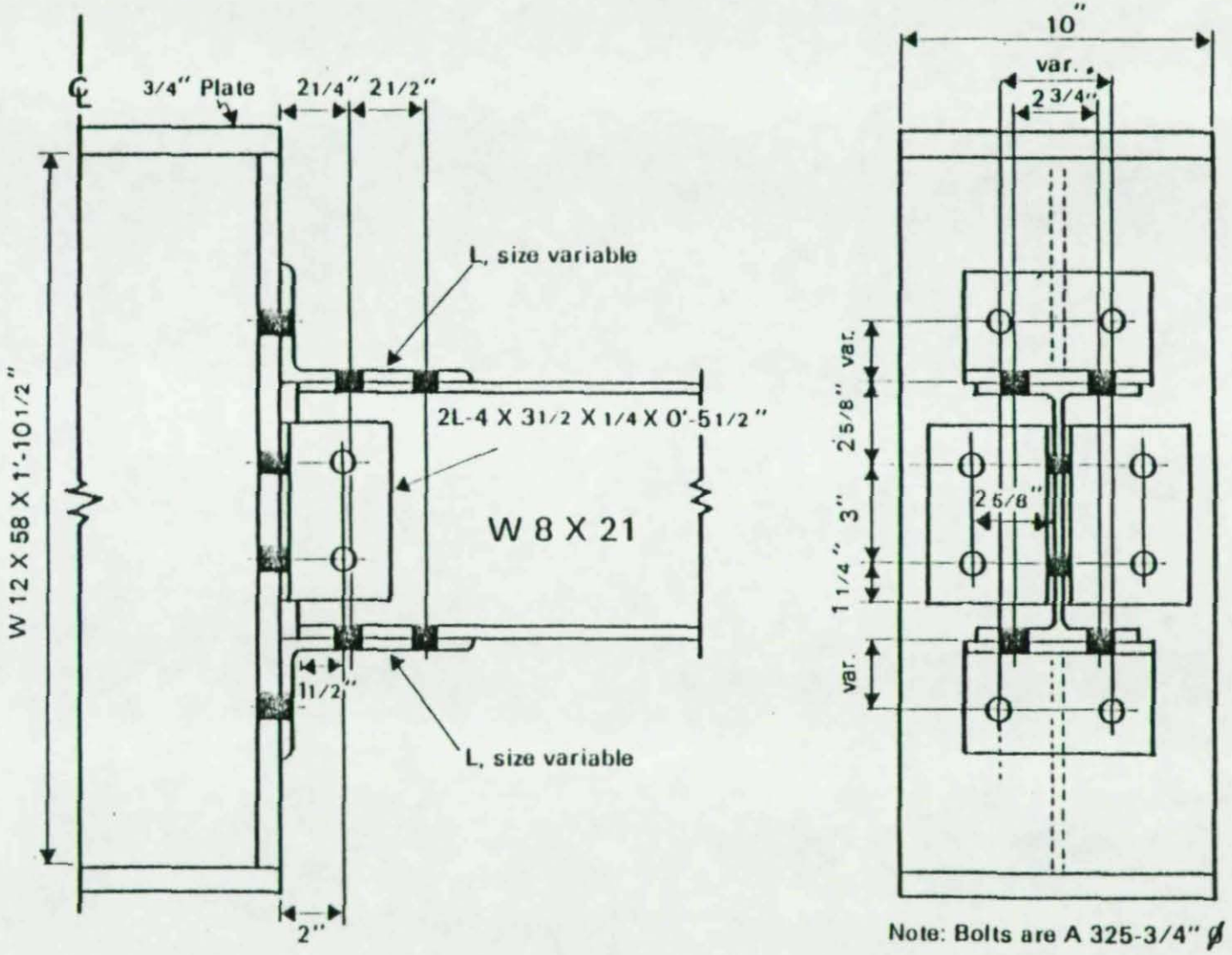

Fig. 1.1 DETAILS OF CONNECTION FOR W 8 X 21 BEAM

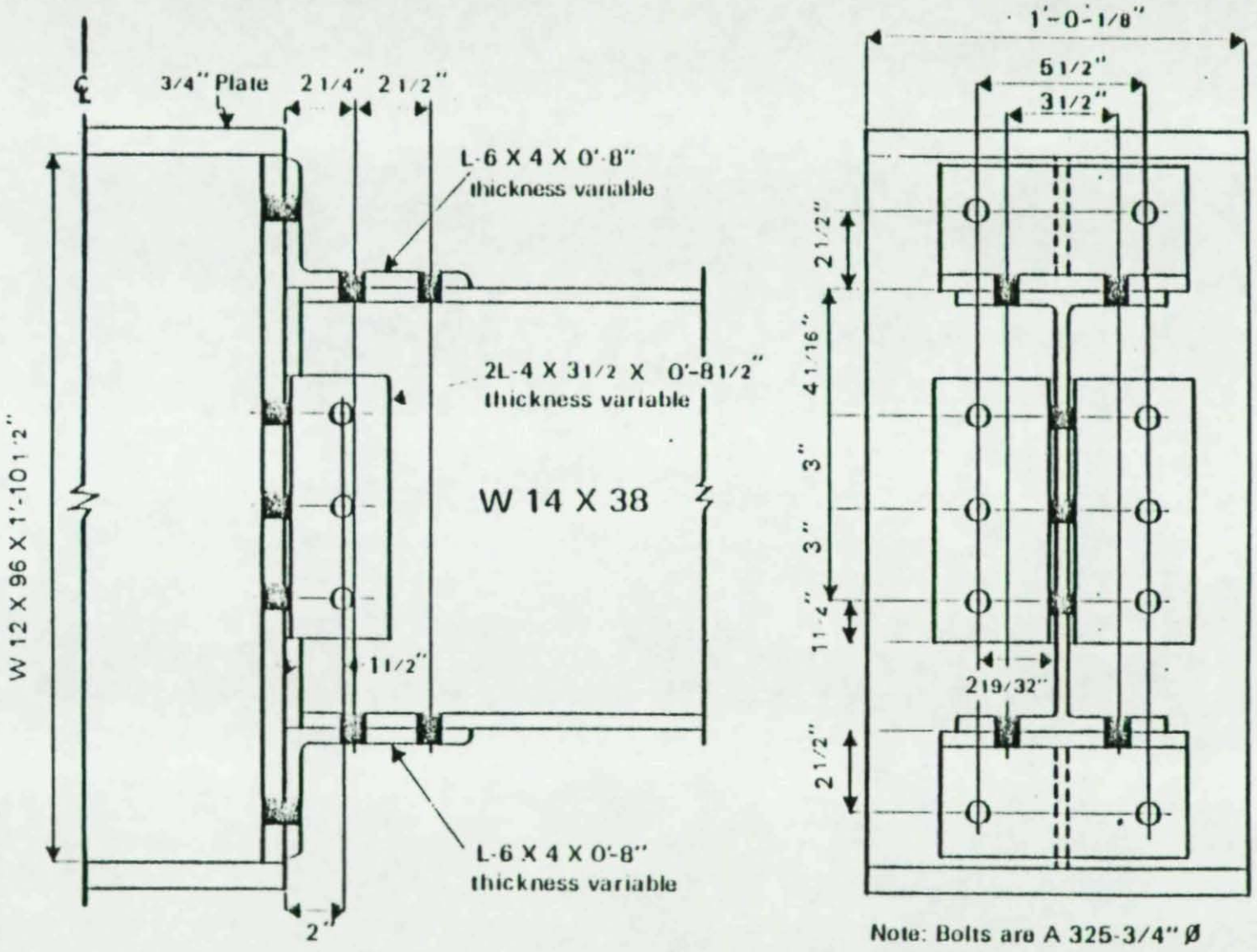

Note: Bolts are A 325-3/4" Ø

Fig. 1.2 DETAILS OF CONNECTION FOR W 14 X 38 BEAM

00483

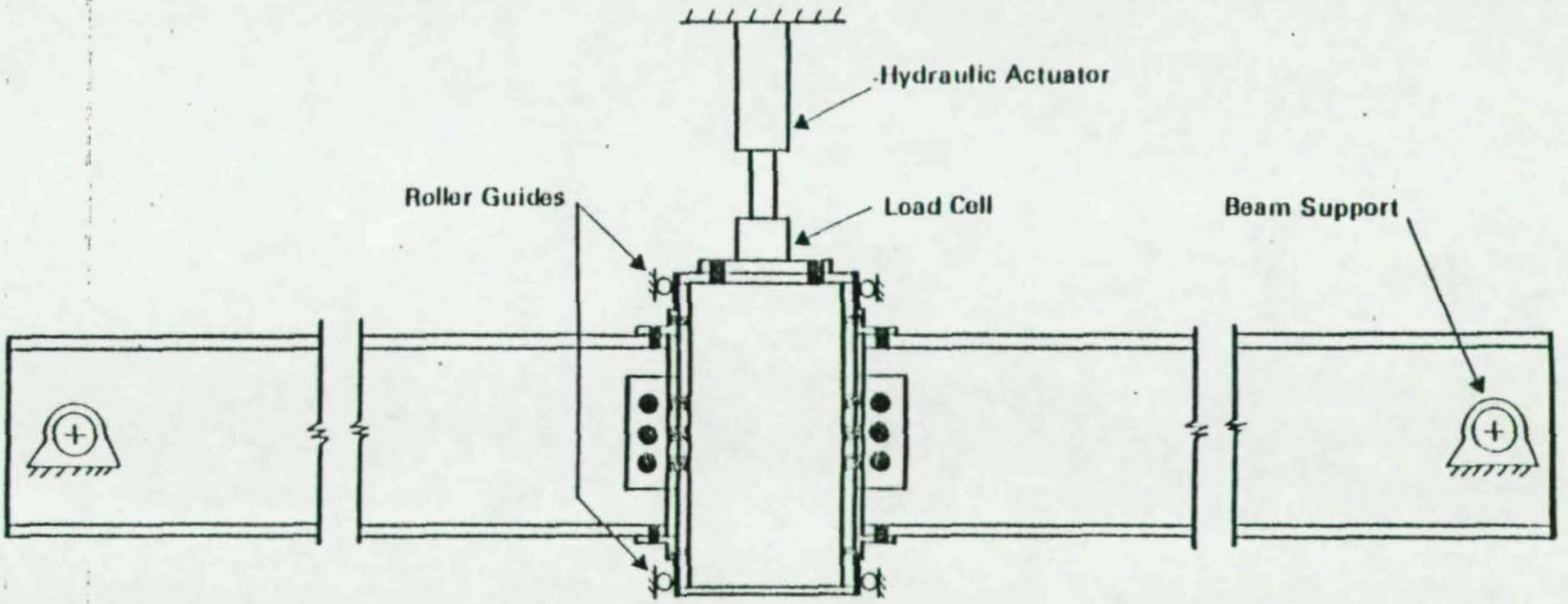

Fig. 1.3 SCHEMATIC OF LOADING SYSTEM FOR TEST BEAMS

00484

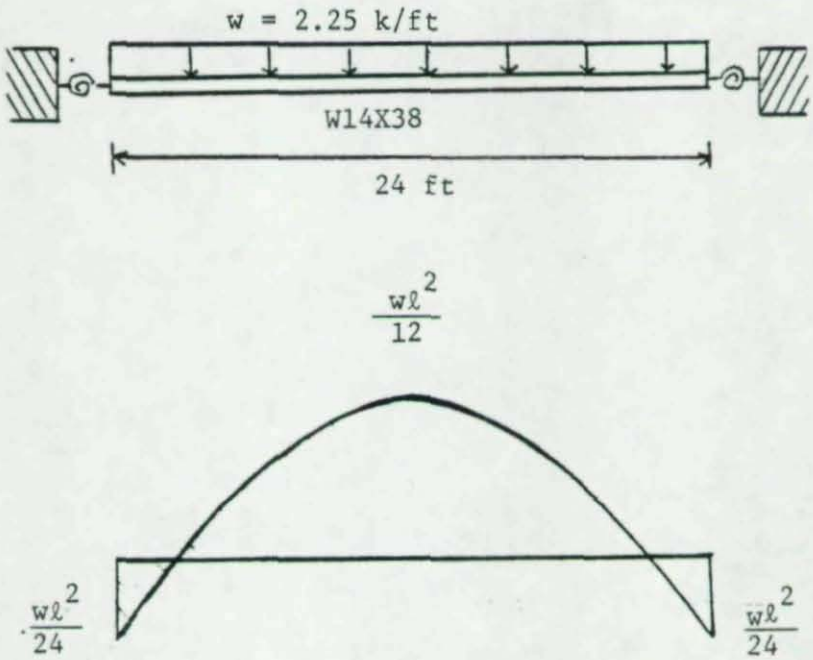

Connection Properties
- Flange Angle Gage = 2½ in.
- Flange Angle Length = 8 in.
- Flange Angle Thickness = ½ in.
- Web Angle Thickness = ½ in.
- Beam Depth = 14.1 in.

Fig. 3.1a BEAM WITH SEMI-RIGID CONNECTIONS

00485

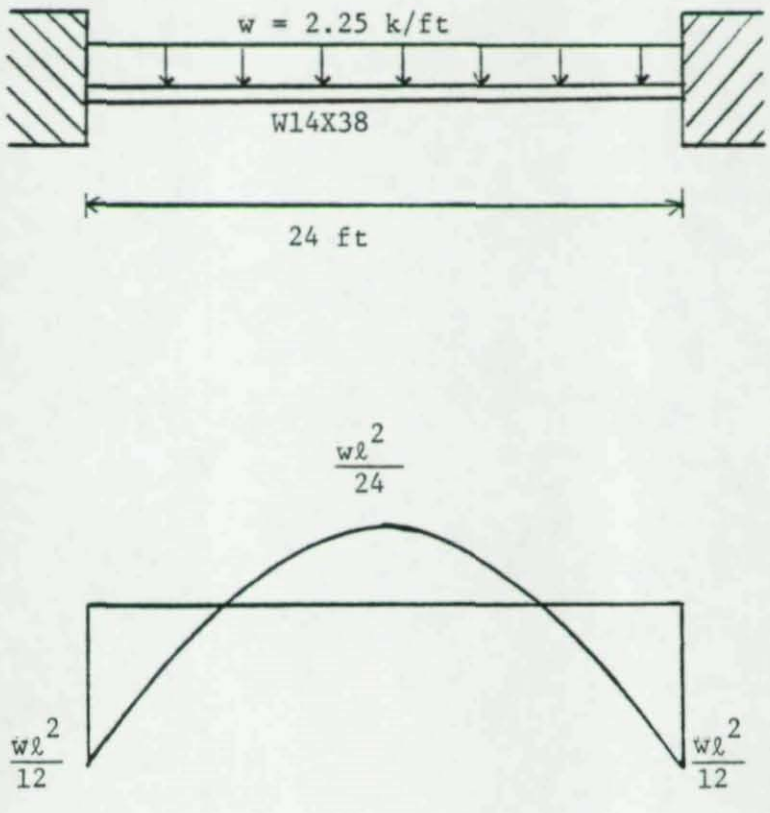

Fig. 3.1b BEAM WITH FULLY RIGID CONNECTIONS

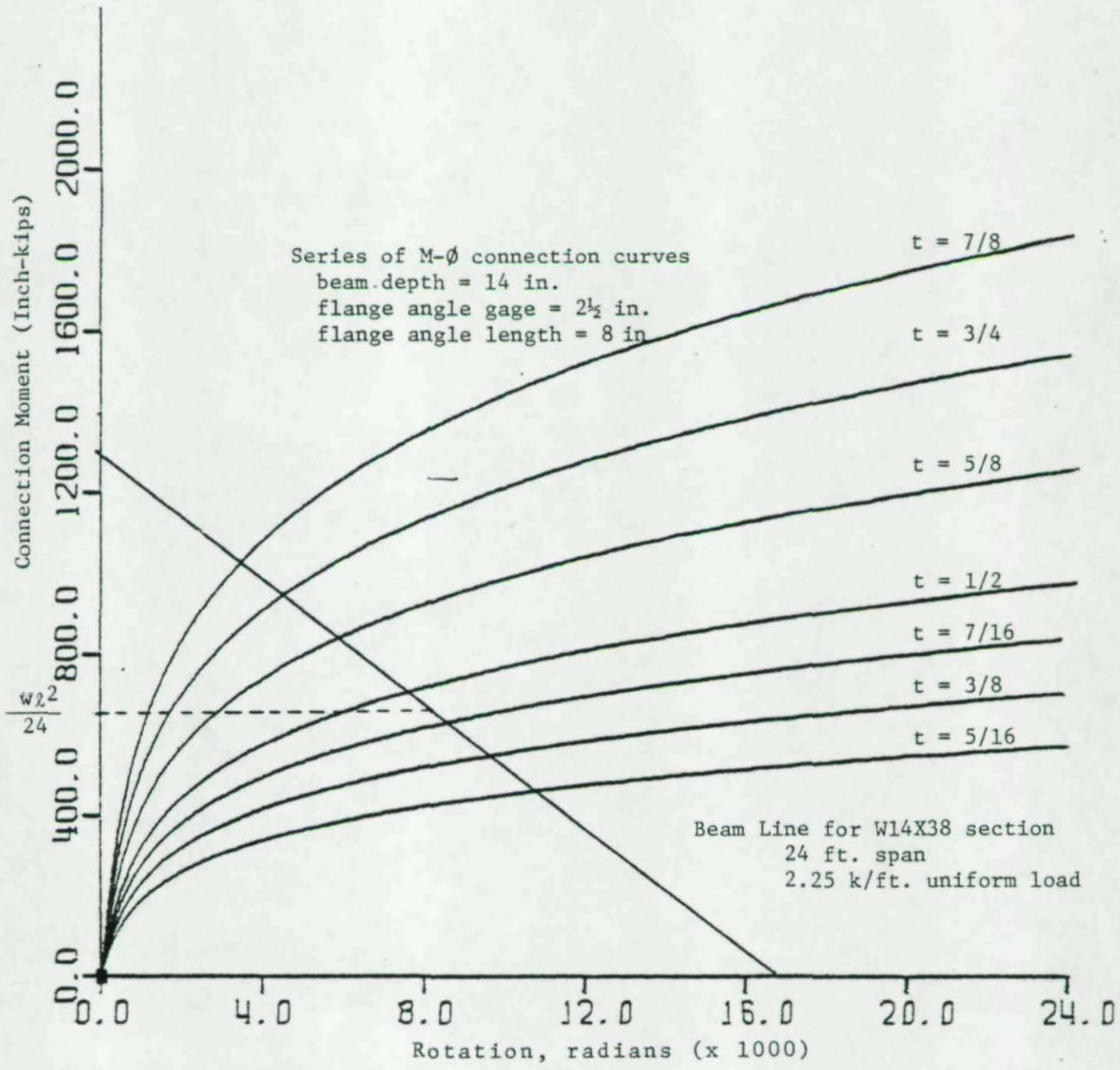

Fig. 3.2 SELECTION OF BEAM CONNECTION

00487

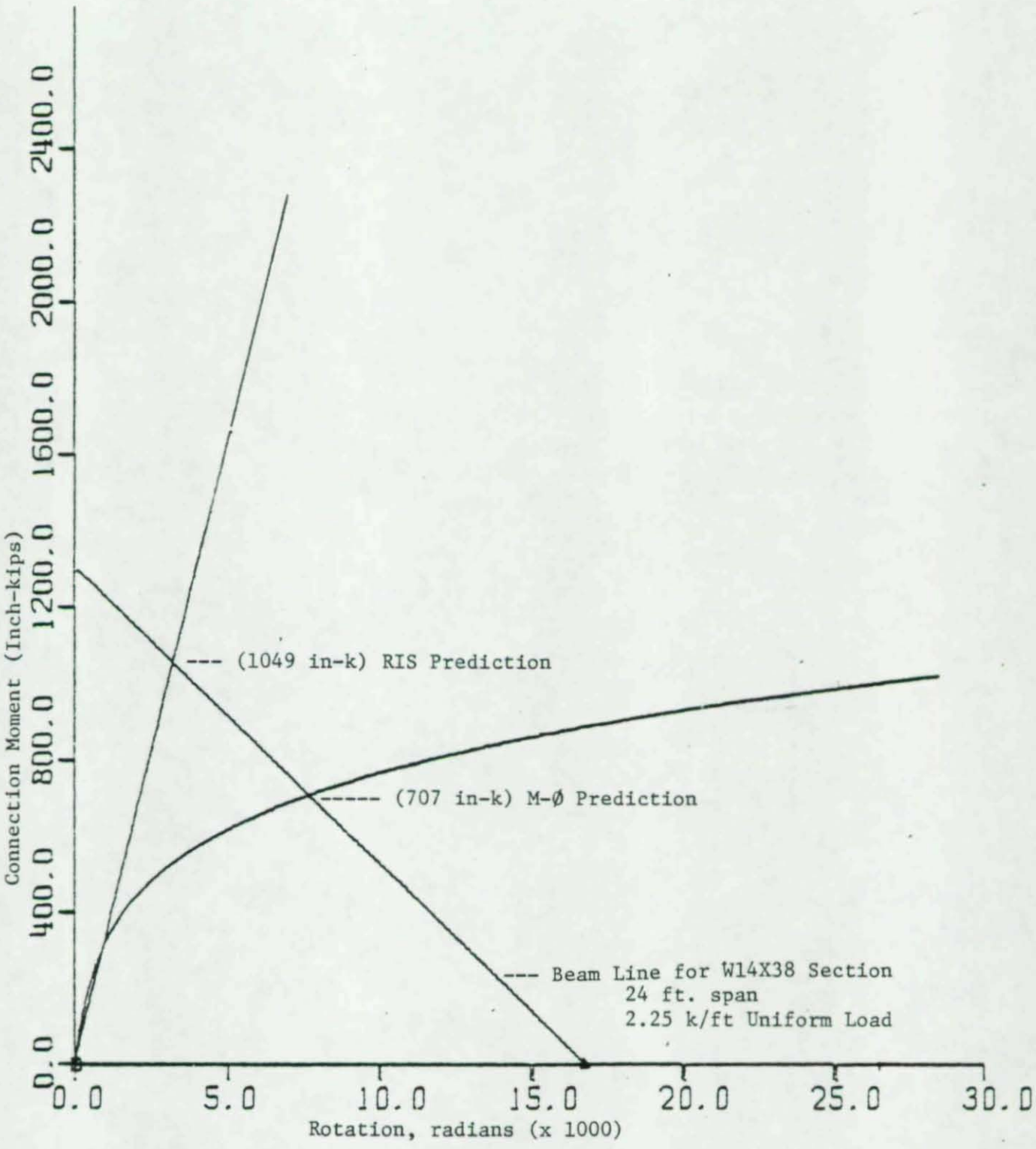

Fig. 3.3 COMPARISON OF CONNECTION MOMENT IN EXAMPLE BEAM USING M-Ø CURVE AND RIS LINE

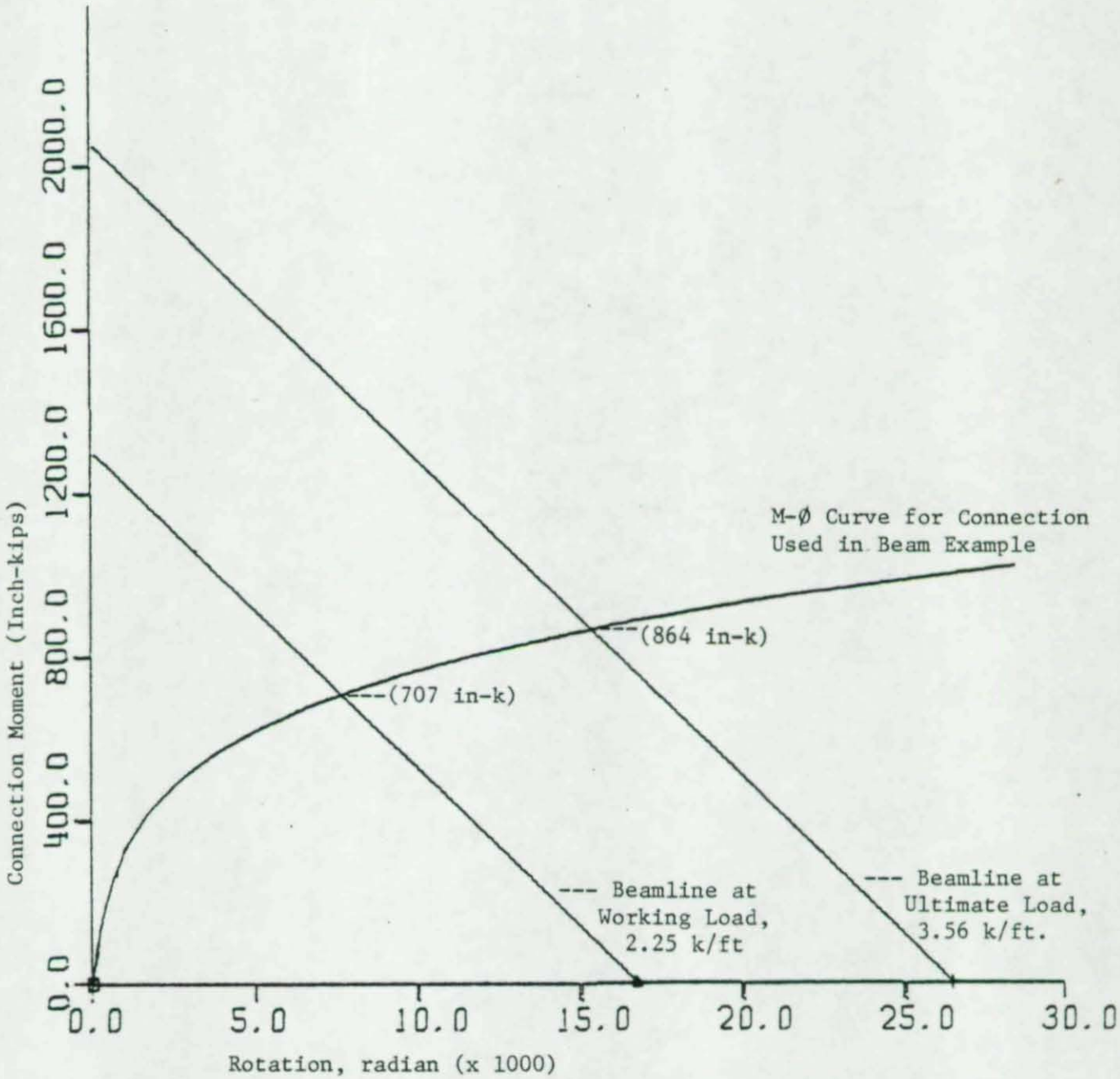

Fig. 3.4 CAPACITY OF CONNECTION AT COLLAPSE LOAD (BEAM EXAMPLE)

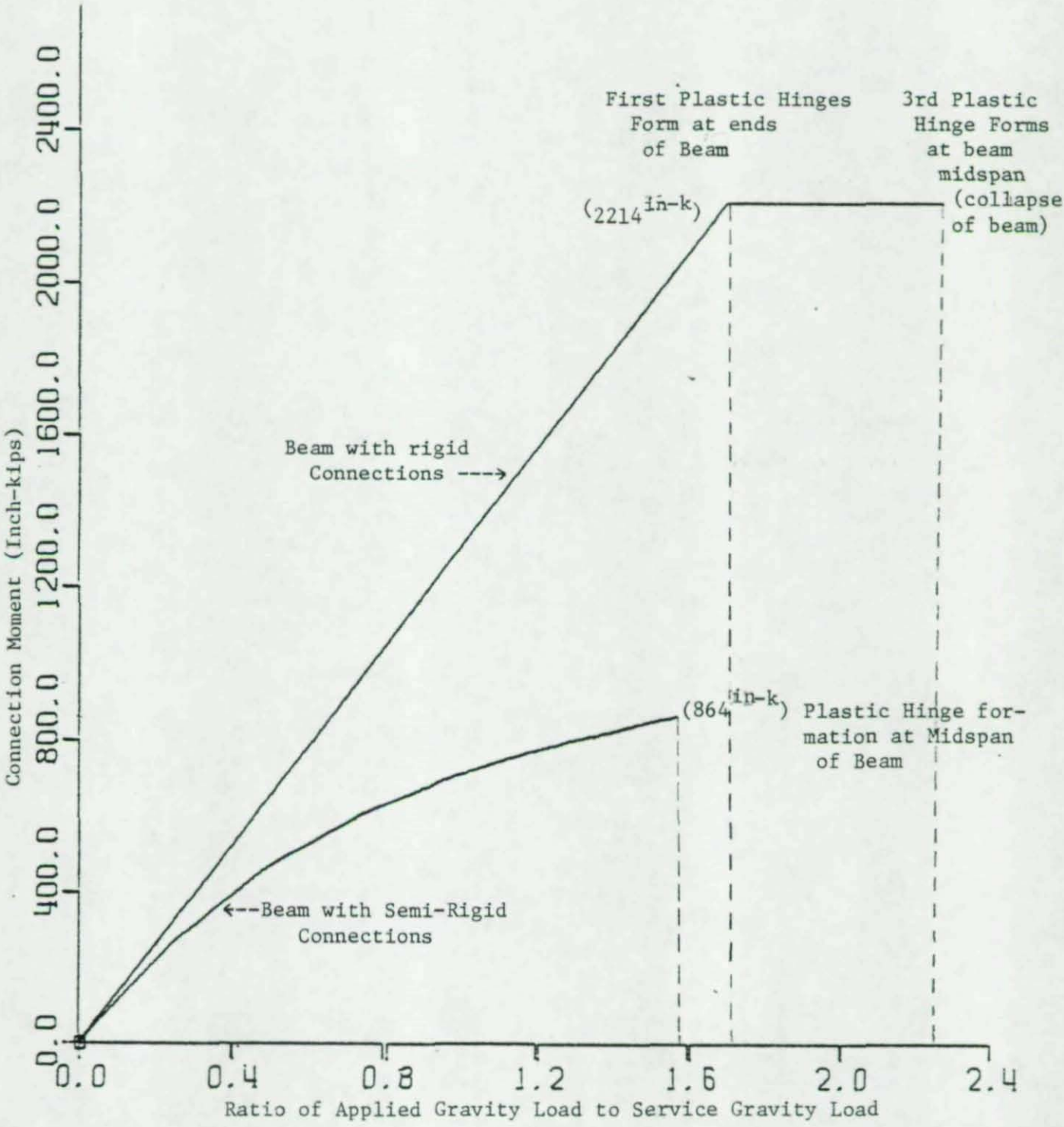

Fig. 3.5 Comparison of Rigid and Semi-Rigid Beam Behavior

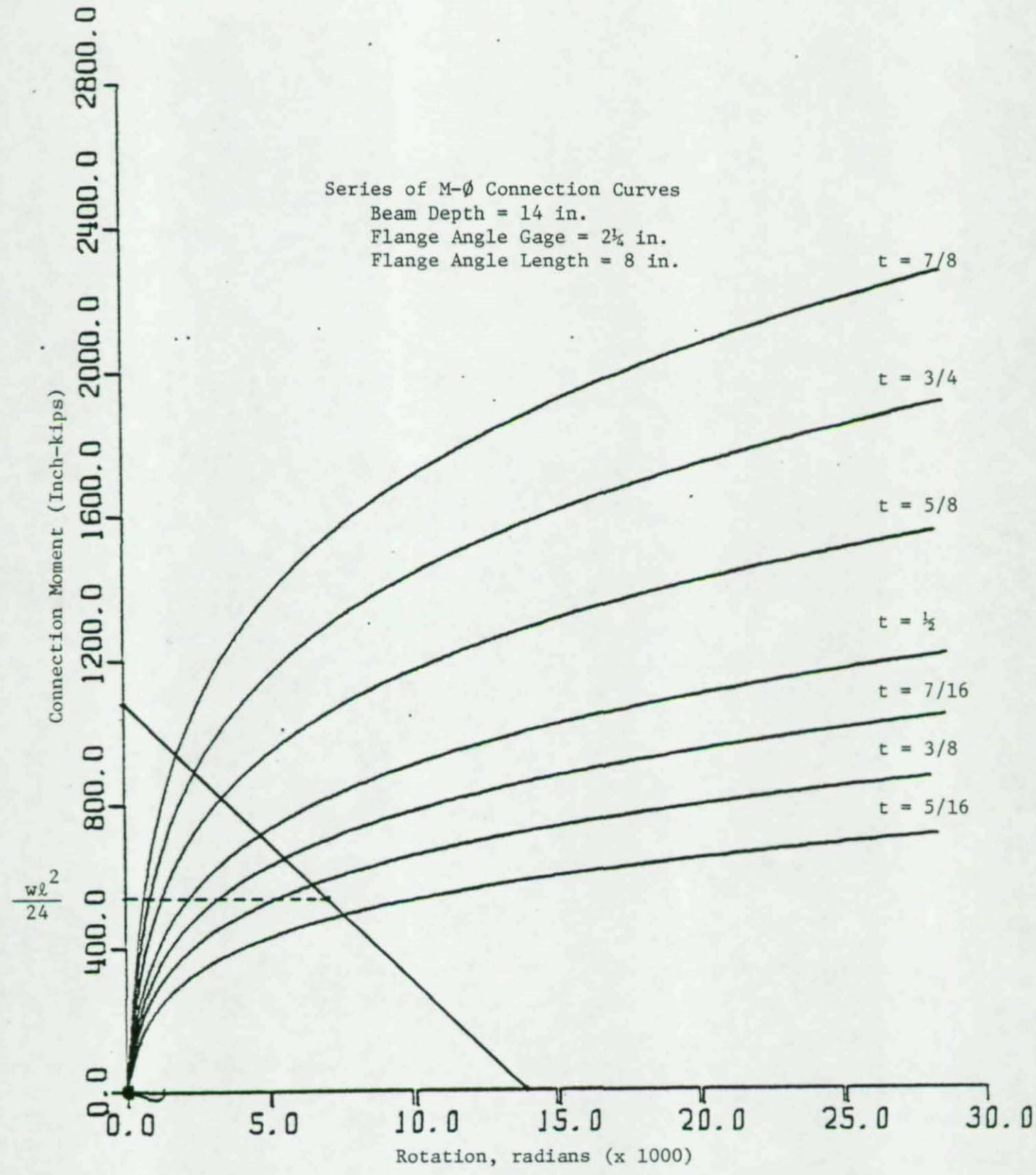

Fig. 4.1 Selection of Connection Used in Frame Example

00491

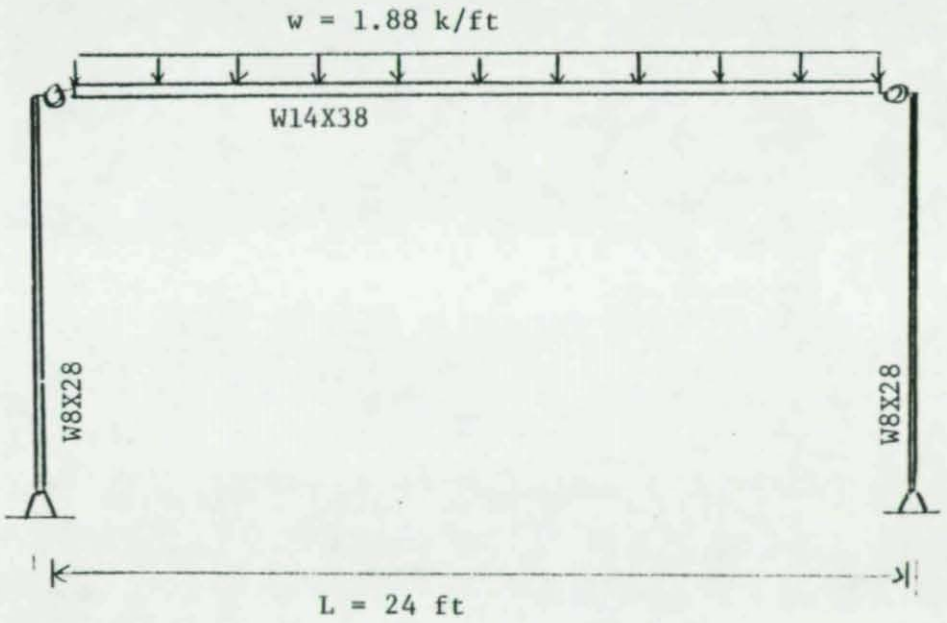

Semi-Rigid Connections:

top and seat angles - L 6 X 4 X 3/8 X 0'-8"

web angles - 2 L 4 X 3½ X ¼ X 0'-8½"

Fig. 4.2 Single Story, Single Bay Frame Utilizing Semi-Rigid Connections

00492

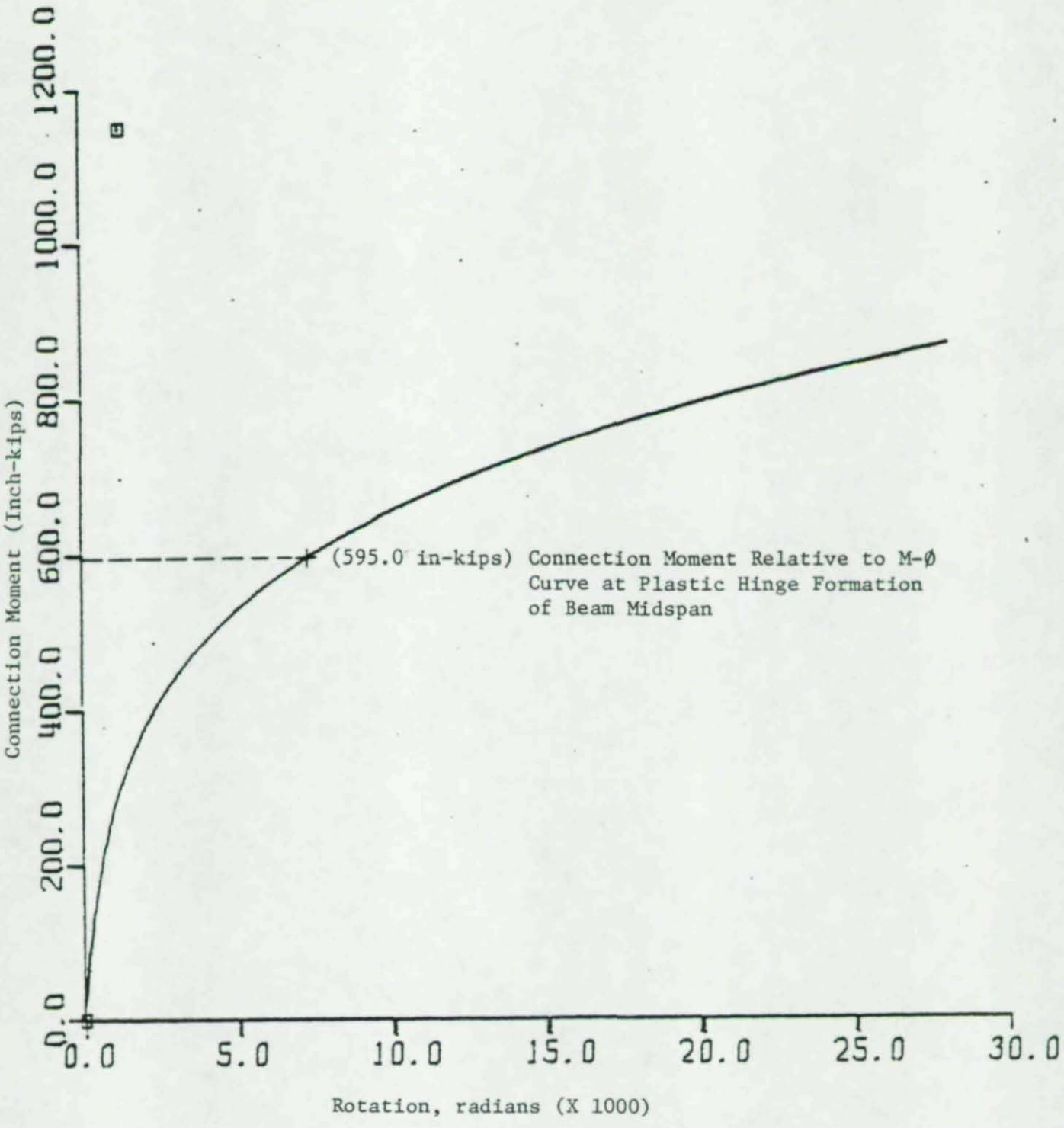

Fig. 4.3 M-Ø Curve for Connection Used In Semi-Rigid Frame

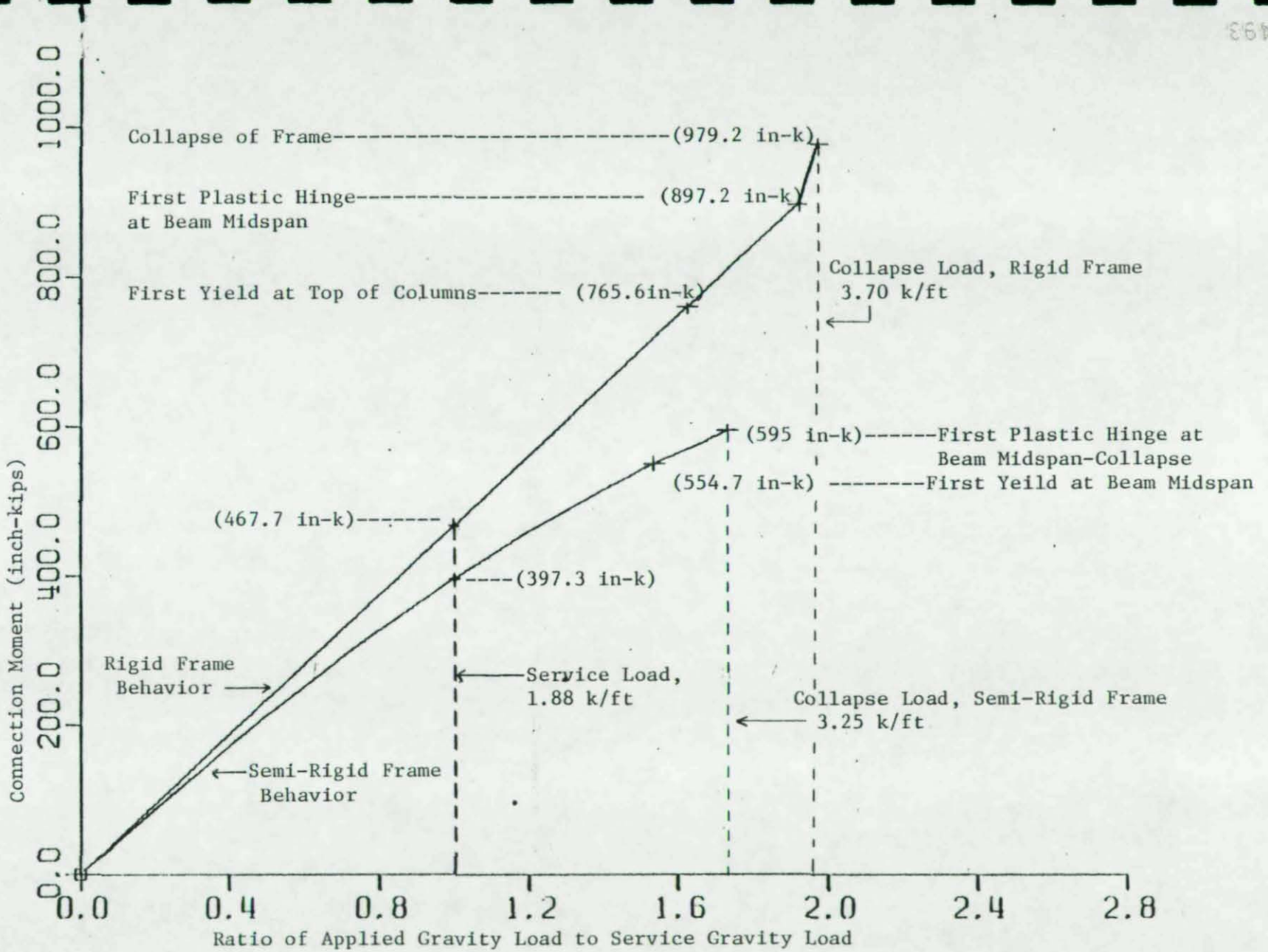

Fig. 4.4 Behavioral Comparison Between Rigid Frame And Semi-Rigid Frame Under Gravity Load

00494

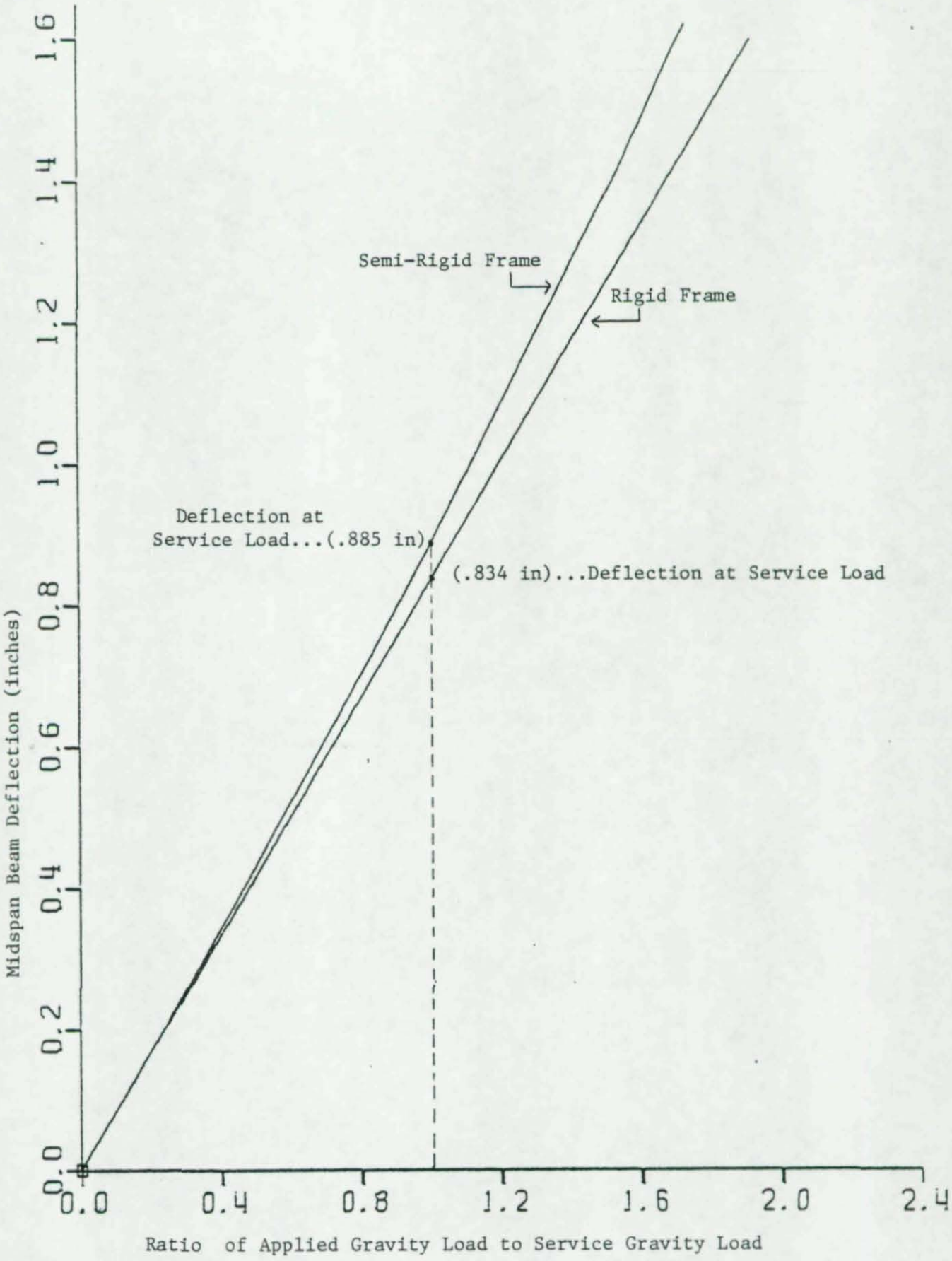

Fig. 4.5 Comparison of Midspan Beam Deflection Between Rigid and Semi-Rigid Frames - Gravity Load

004095

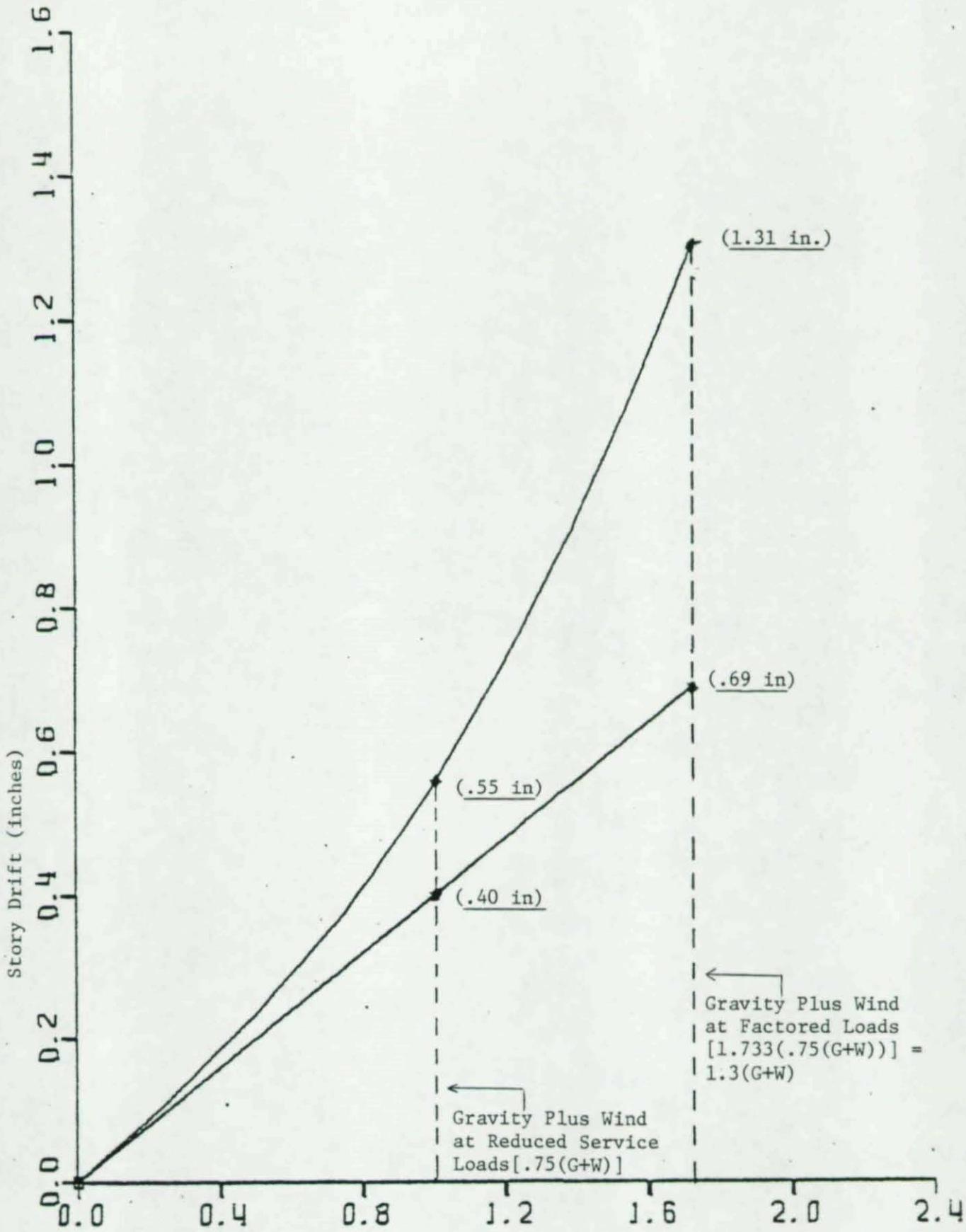

Fig. 4.6 Comparison of Story Drift Between Rigid Frame and Semi-Rigid Frame

00496

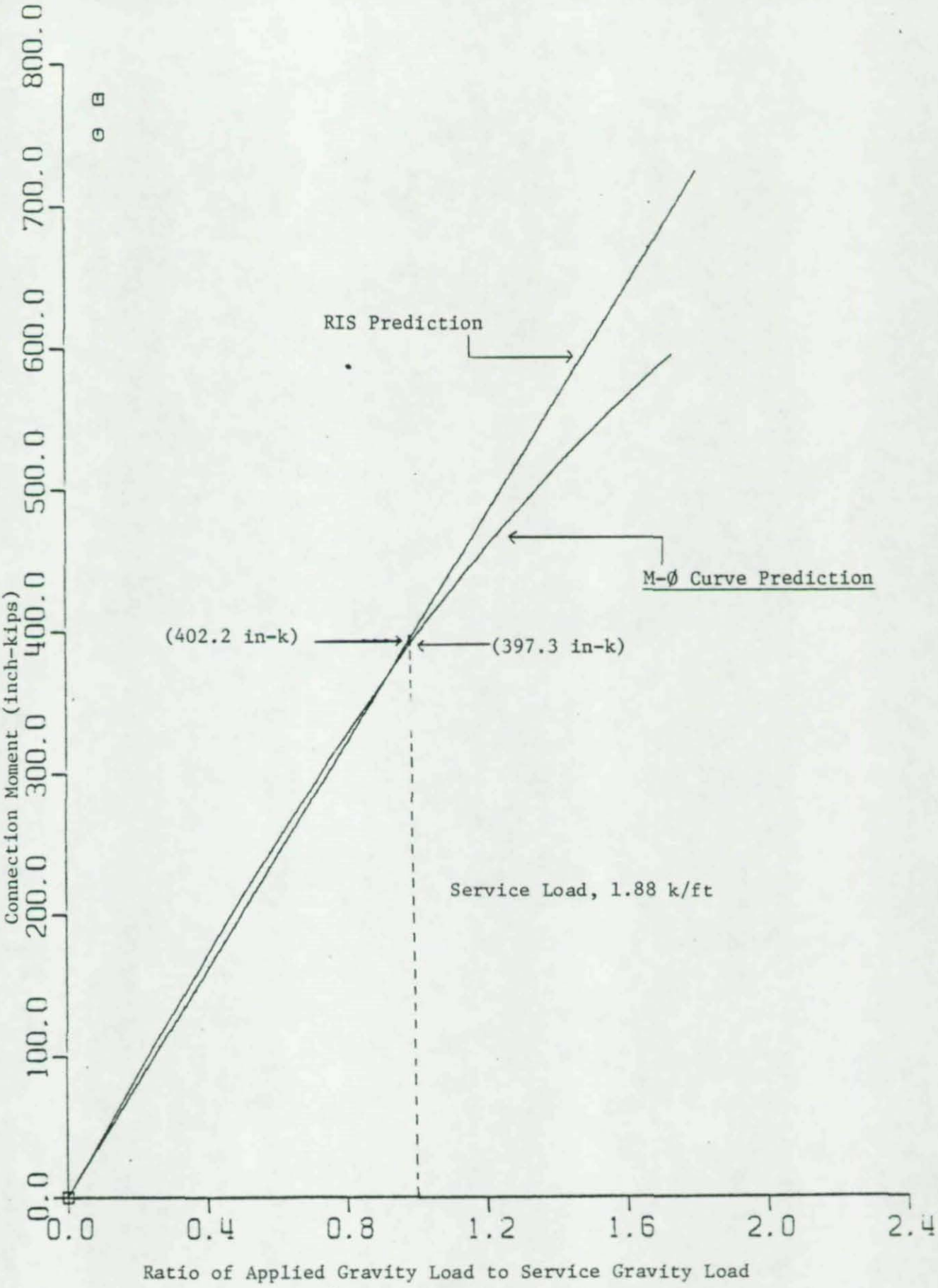

Fig. 4.7 Connection Moment Comparison Using RIS and M-Ø Curve - Gravity Loading

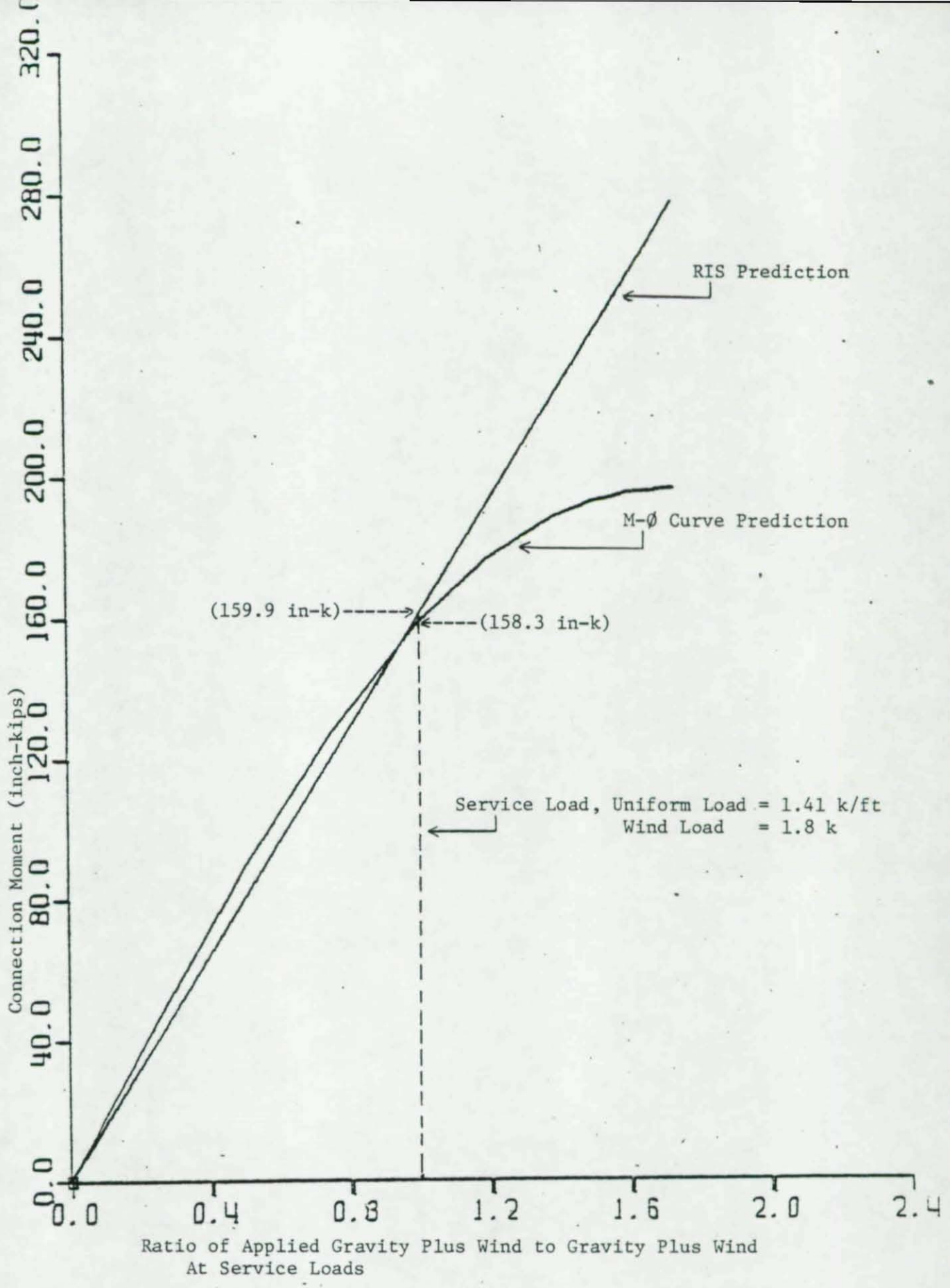

Fig. 4.8 Comparison of Windward Moment Using RIS and M-Ø Curve for Gravity Plus Wind Loading

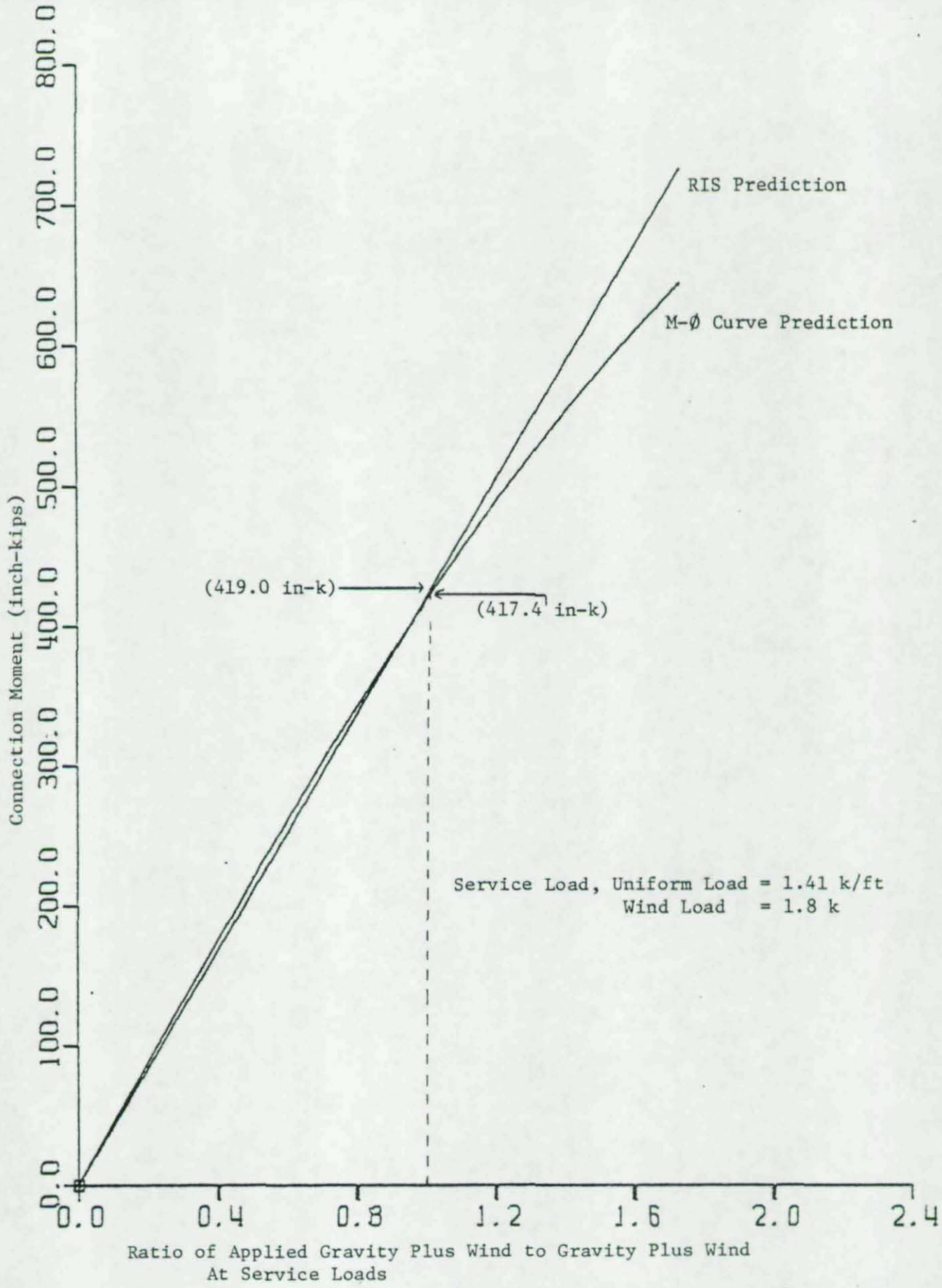

Fig. 4.9 Comparison of Leeward Moment Using RIS and M-Ø Curve for Gravity Plus Wind Loading

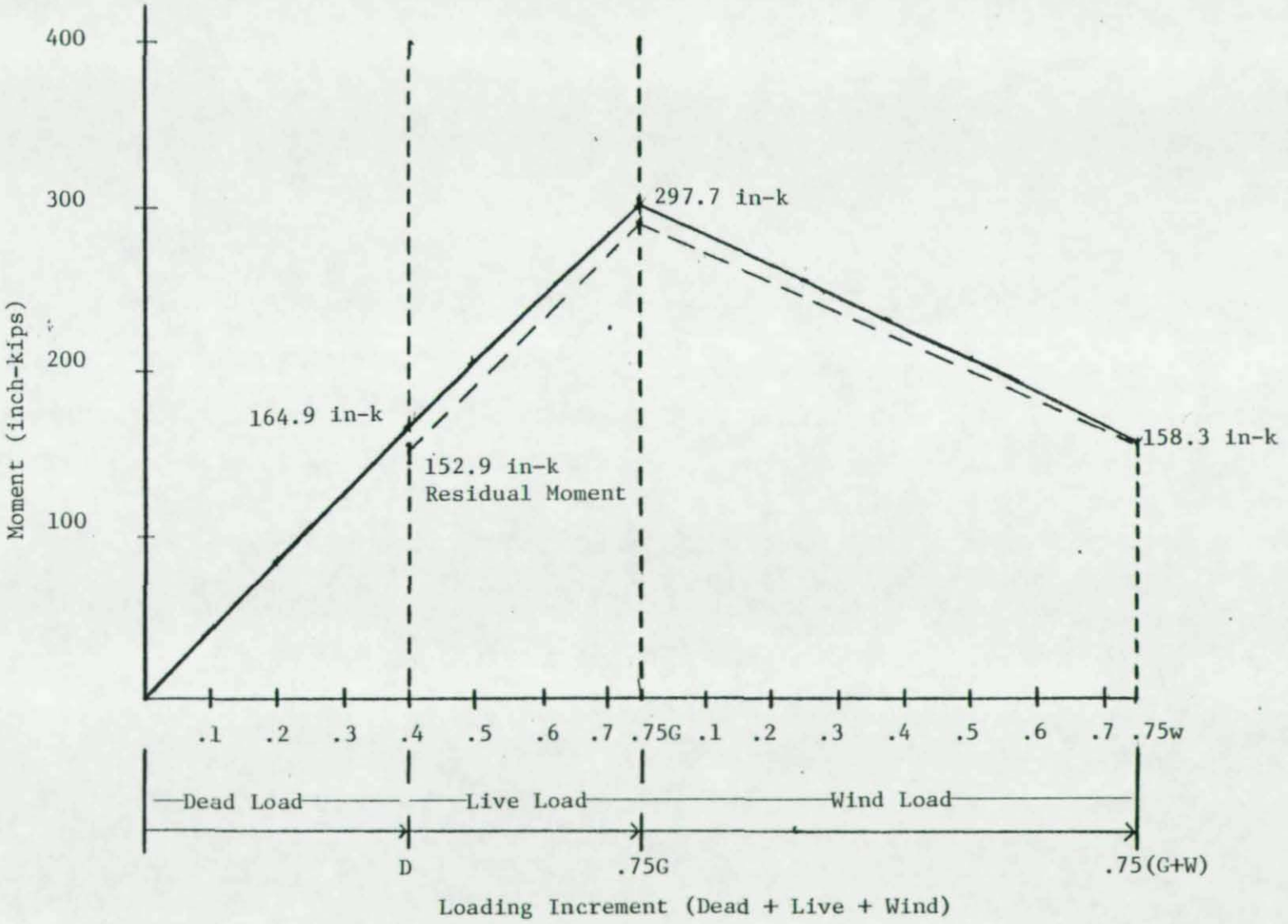

Fig. 4.10 Behavior of Windward Connection Upon Loading and Unloading - Method 1

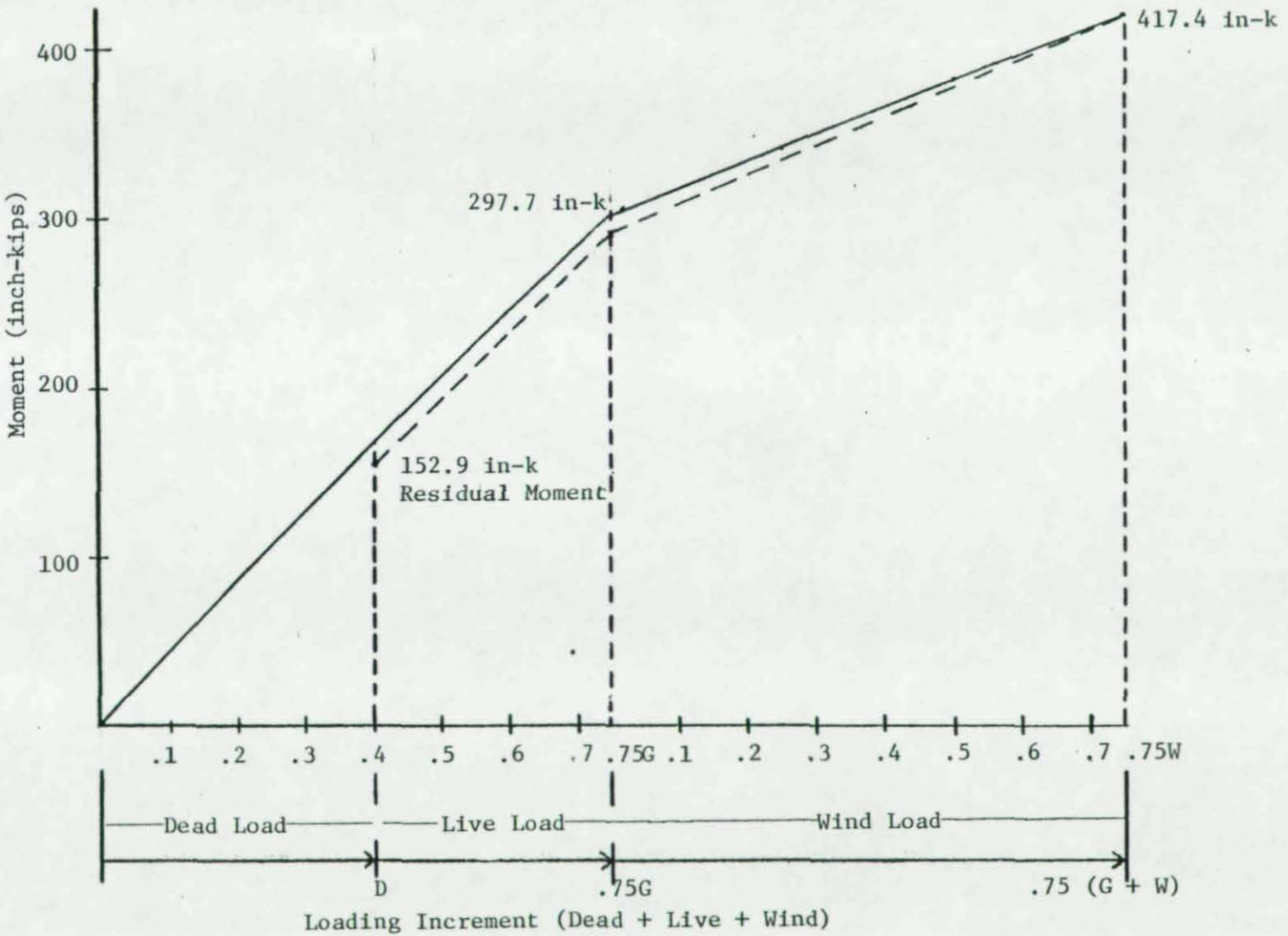

Fig. 4.11 Behavior of Leeward Connection Upon Loading and Unloading - Method 1

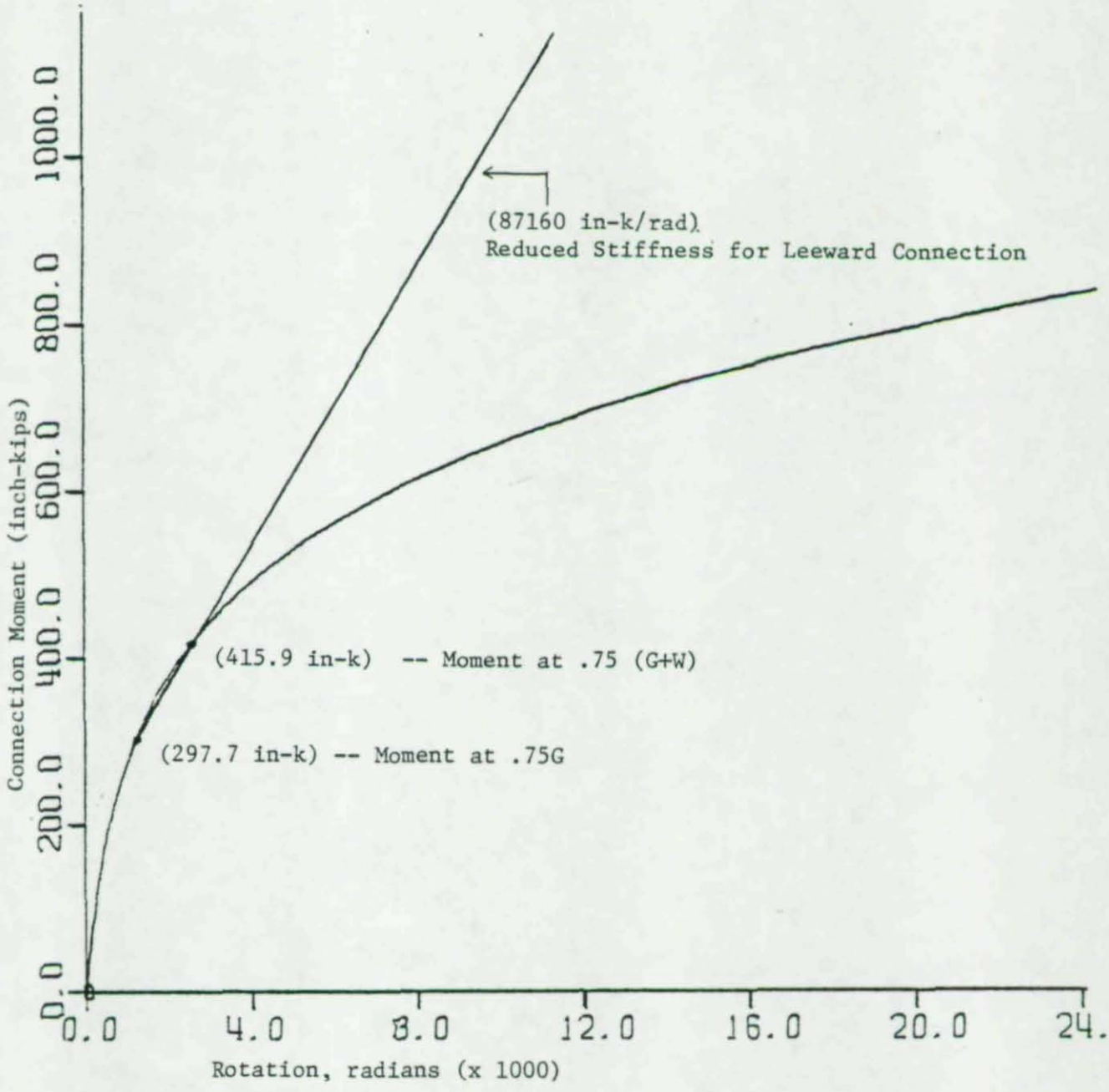

Fig. 4.12 Reduced Stiffness for Leeward Connection for Application of Wind Load

00502

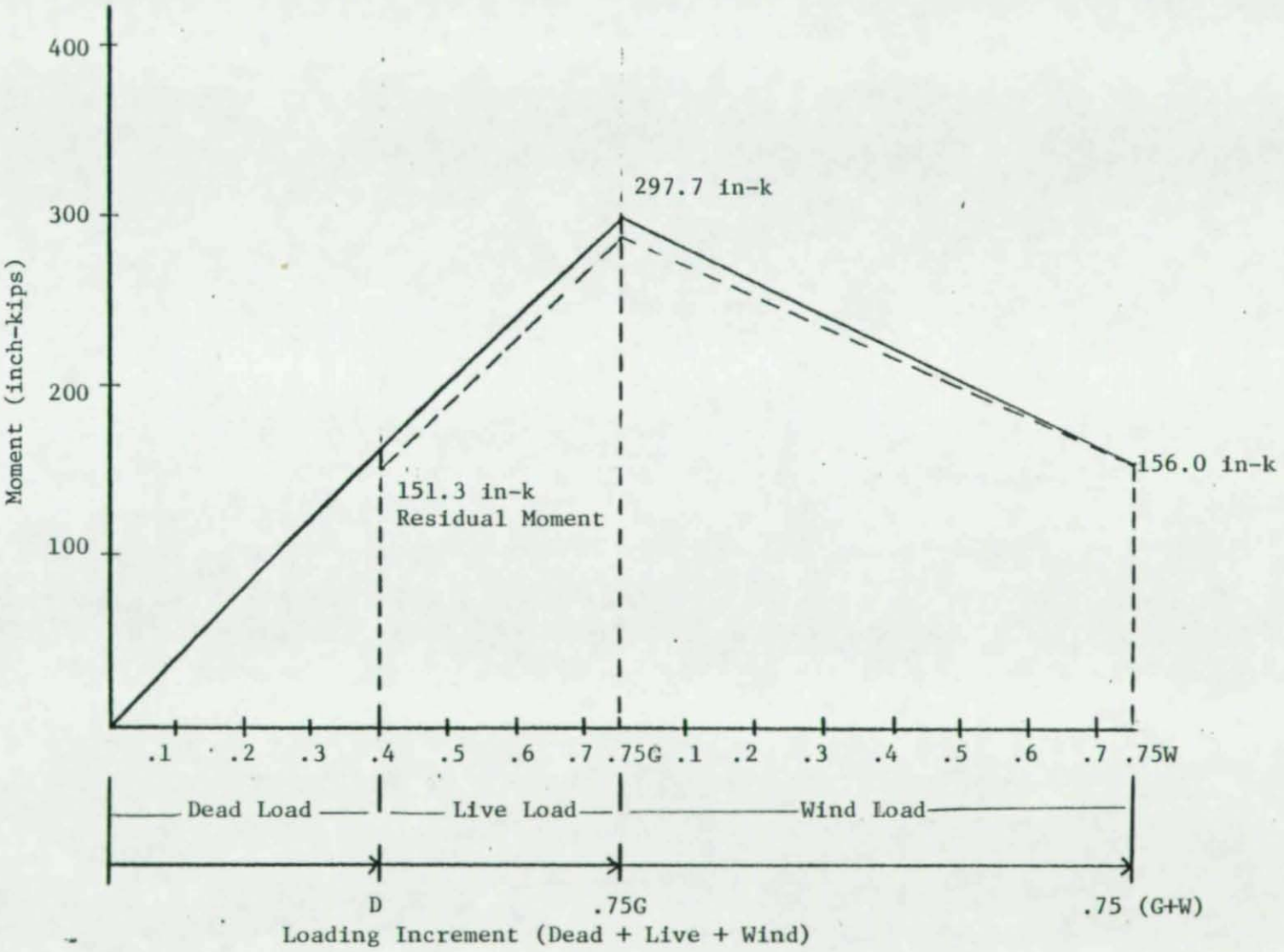

Fig. 4.13 Behavior of Windward Connection Upon Loading and Unloading - Method 2

00503

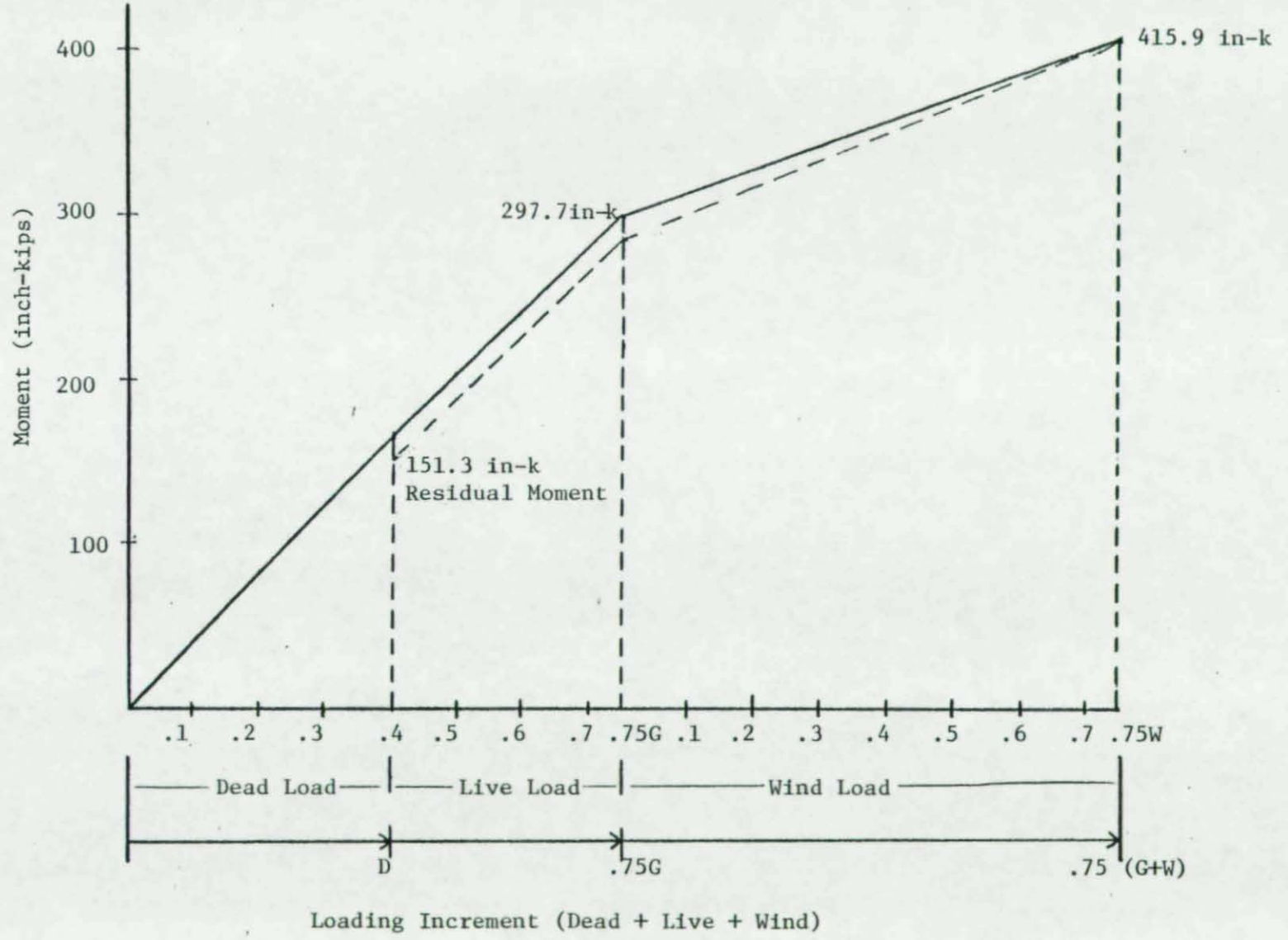

Fig. 4.14 Behavior of Leeward Connection Upon Loading And Unloading - Method 2

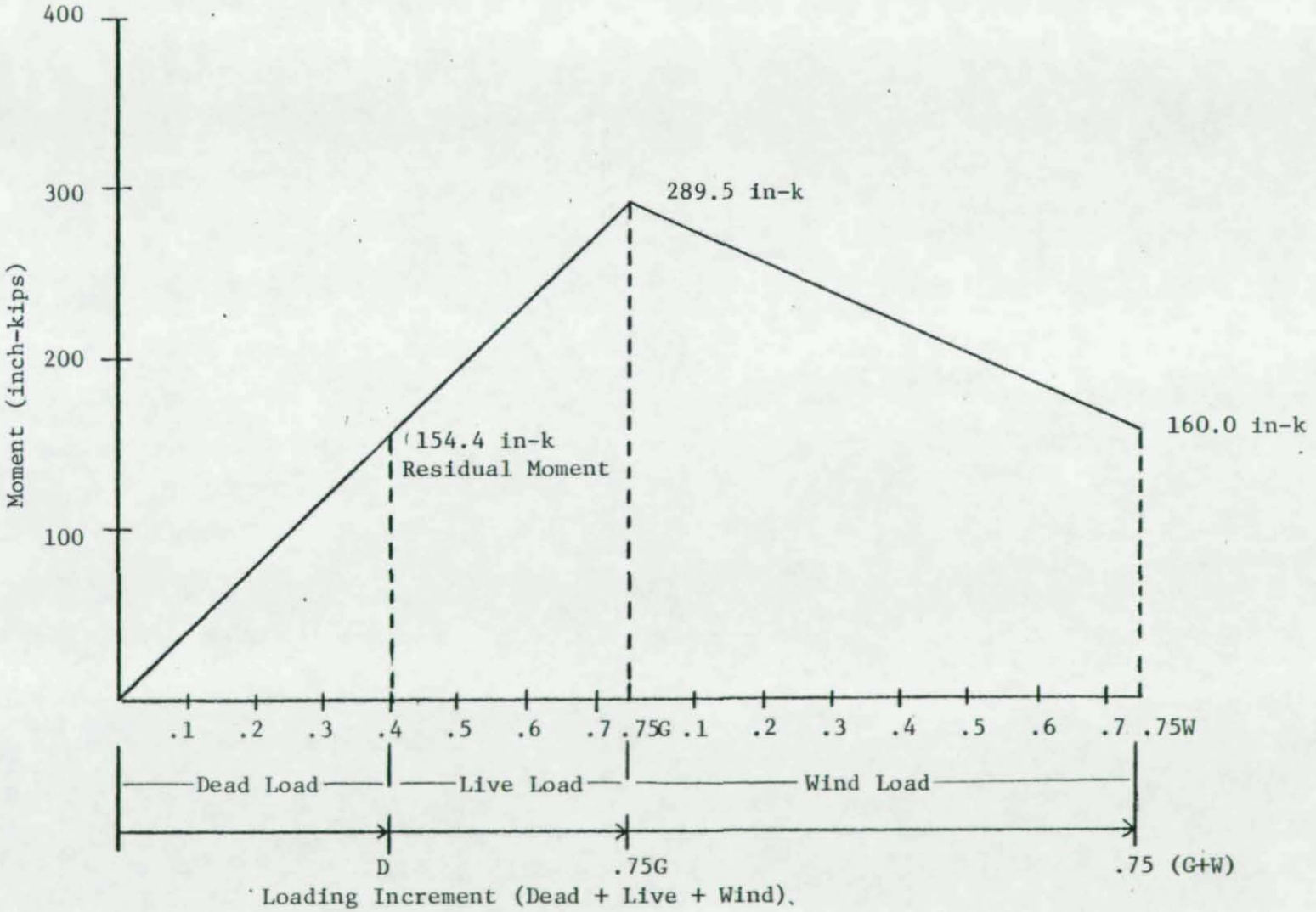

Fig. 4.15 Behavior of Windward Connection Upon Loading And Unloading - Method 3 (RIS)

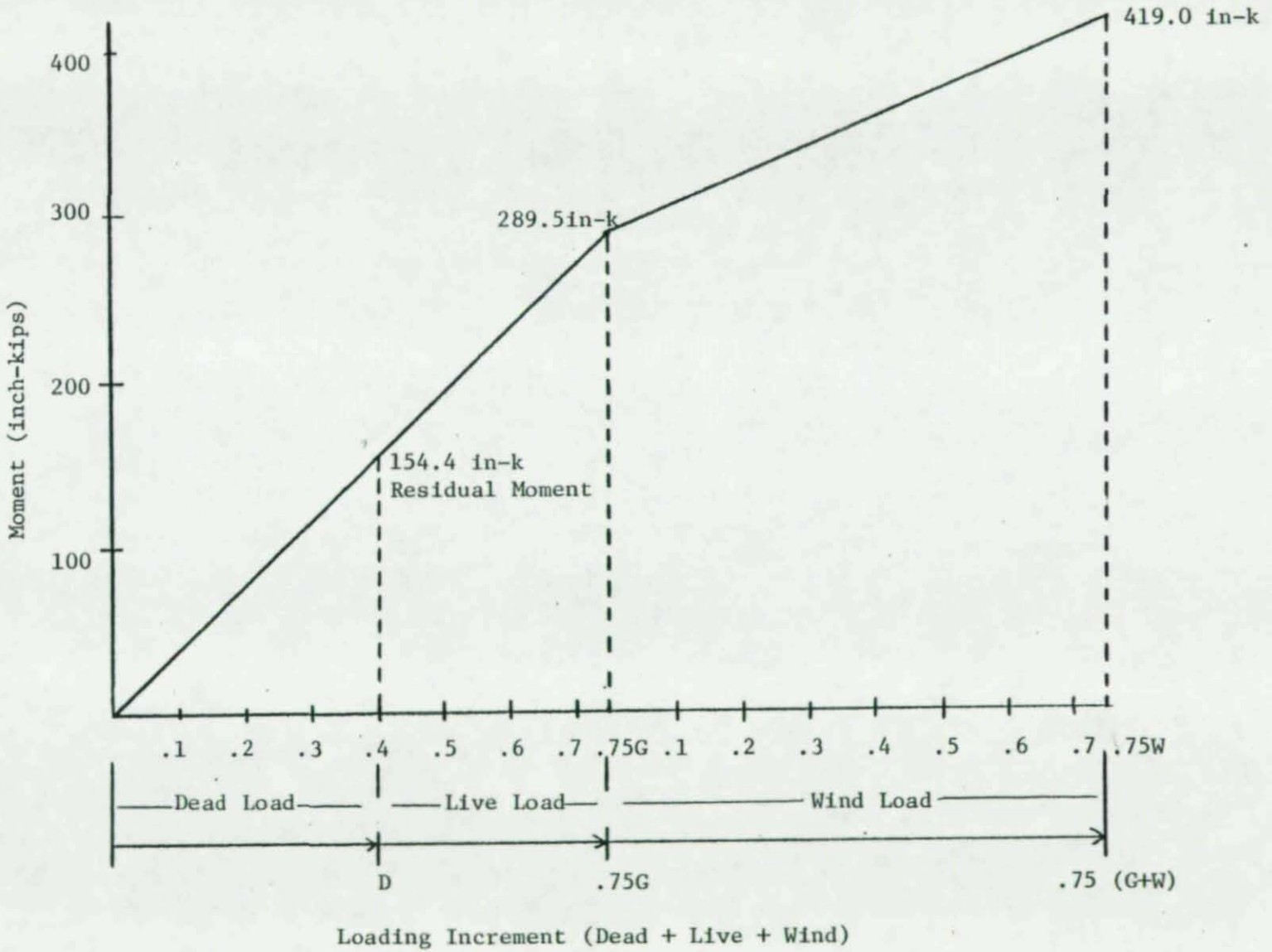

Fig. 4.16 Behavior of Leeward Connection Upon Loading and Unloading - Method 3 (RIS)

90508

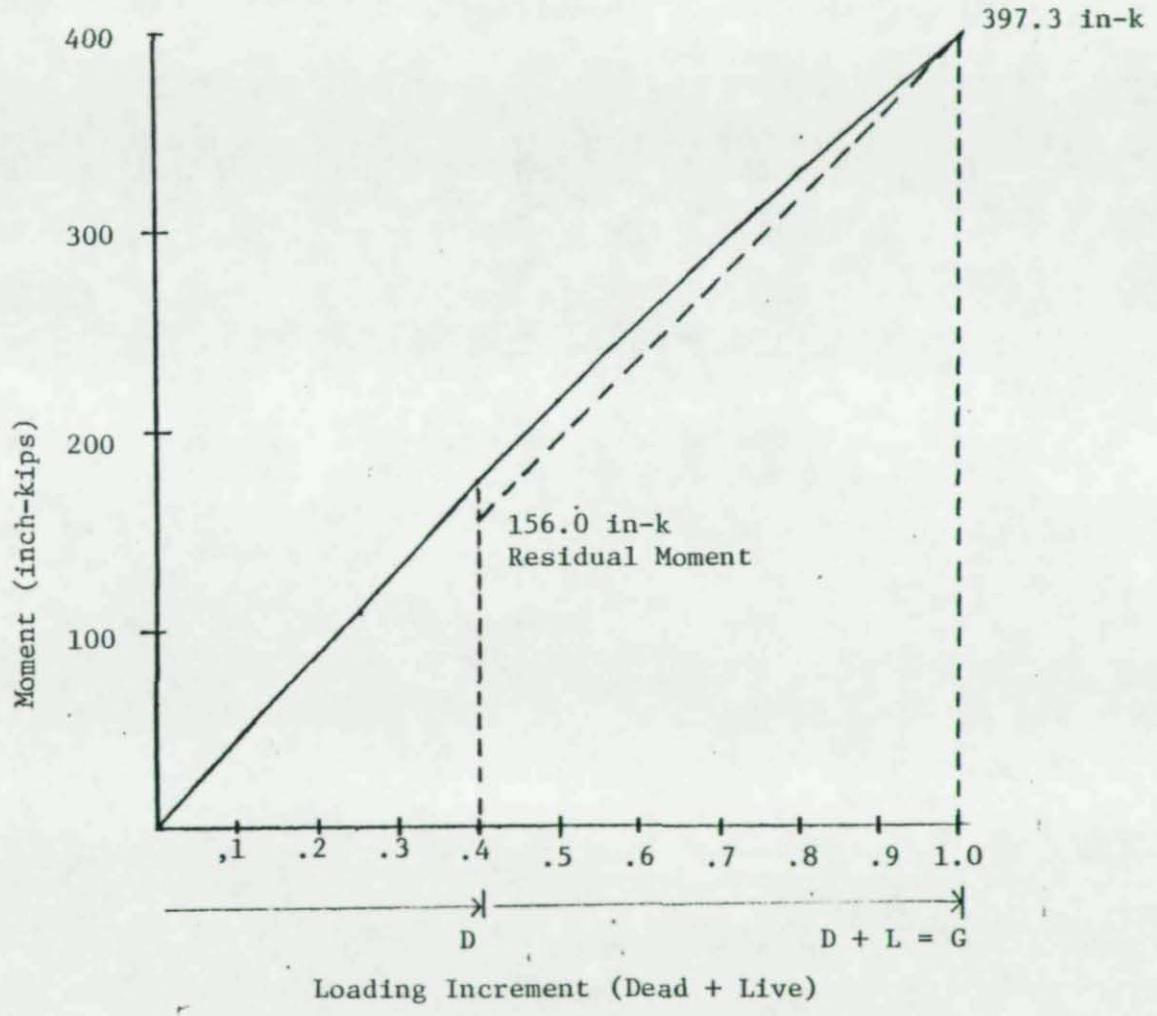

Fig. 4.17 Behavior of Connection Upon Gravity Loading and Unloading - M-Ø Loading Curve

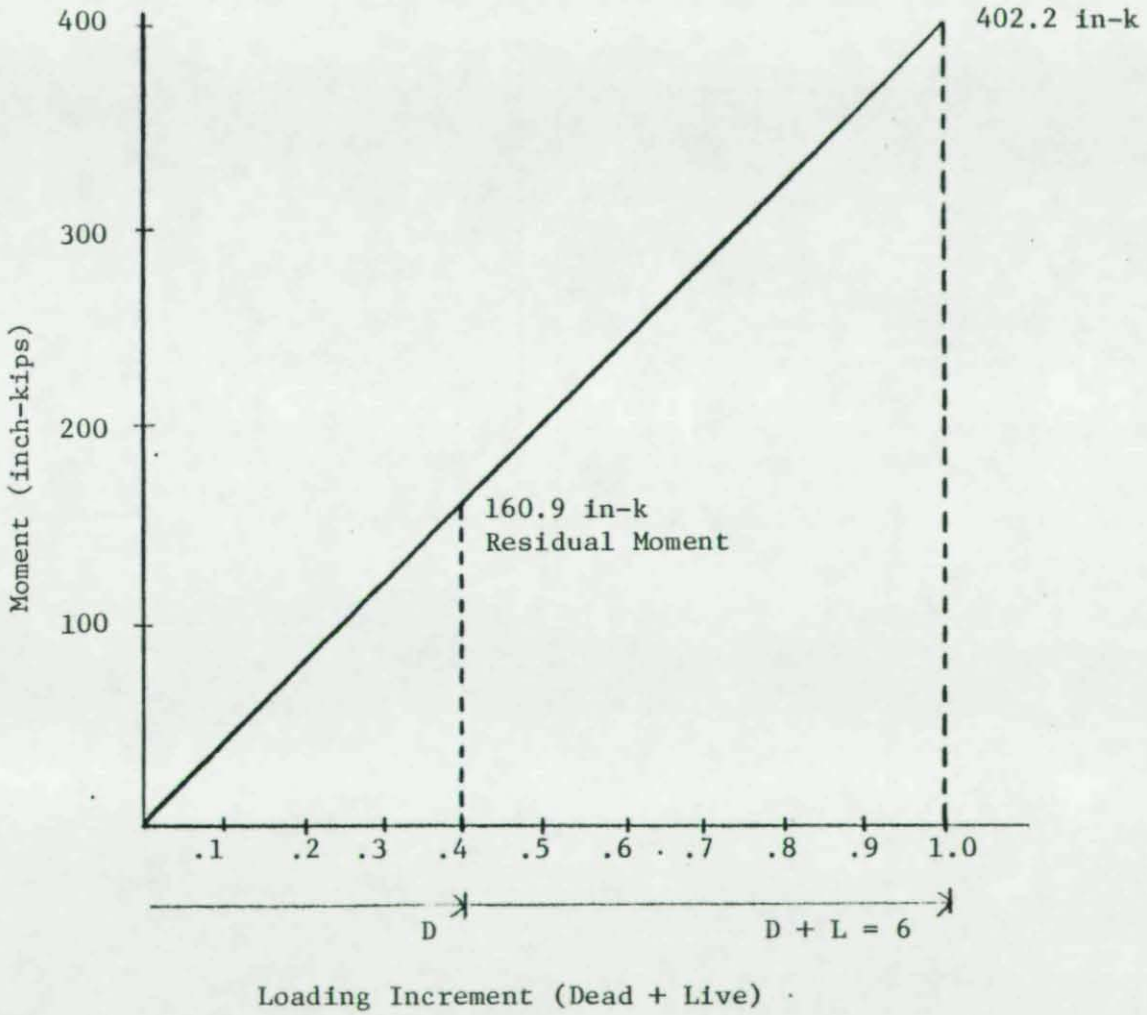

Fig. 4.18 Behavior of Connection Upon Gravity Loading and Unloading - RIS Loading Curve

00503

Acknowledgments

This project was supported under the Fellowship Awards Program of the AISC Educational Foundation. The investigation was conducted under the supervision of Dr. J. B. Radziminski, Professor of the Civil Engineering Department at the University of South Carolina. The guidance and suggestions that were given by Dr. Radziminski throughout the entire project were very helpful and were greatly appreciated by the author of this report.

Guidance in the area of computer-aided analytical procedures was provided by Dr. J. H. Bradburn, Associate Professor of the Civil Engineering Department, and by A. Azizinamini, Research Assistant in Civil Engineering. Their assistance in this area is gratefully acknowledged. Special thanks are extended to Ms. M. Butterworth for the typing of this report.